


12-2016

The influence of alkalinity of portland cement on the absorption characteristics of superabsorbent polymers (SAP) for use in internally cured concrete

Juan D. Tabares Tamayo
Purdue University

Follow this and additional works at: https://docs.lib.purdue.edu/open_access_theses

 Part of the [Civil Engineering Commons](#), and the [Materials Science and Engineering Commons](#)

Recommended Citation

Tabares Tamayo, Juan D., "The influence of alkalinity of portland cement on the absorption characteristics of superabsorbent polymers (SAP) for use in internally cured concrete" (2016). *Open Access Theses*. 902.
https://docs.lib.purdue.edu/open_access_theses/902

This document has been made available through Purdue e-Pubs, a service of the Purdue University Libraries. Please contact epubs@purdue.edu for additional information.

THE INFLUENCE OF ALKALINITY OF PORTLAND CEMENT ON THE ABSORPTION
CHARACTERISTICS OF SUPERABSORBENT POLYMERS (SAP)
FOR USE IN INTERNALLY CURED CONCRETE

A Thesis

Submitted to the Faculty

of

Purdue University

by

Juan D. Tabares Tamayo

In Partial Fulfillment of the

Requirements for the Degree

of

Master of Science in Civil Engineering

December 2016

Purdue University

West Lafayette, Indiana

**PURDUE UNIVERSITY
GRADUATE SCHOOL
Thesis/Dissertation Acceptance**

This is to certify that the thesis/dissertation prepared

By Juan David Tabares Tamayo

Entitled

The Influence of Alkalinity of Portland Cement on the Absorption Characteristics of Superabsorbent Polymers (SAP) for use in Internally Cured Concrete

For the degree of Master of Science in Civil Engineering

Is approved by the final examining committee:

Jan Olek

12/06/2016

Co-chair

W. Jason Weiss

12/06/2016

Co-chair

Kendra A. Erk

12/01/2016

John E. Haddock

12/01/2016

To the best of my knowledge and as understood by the student in the Thesis/Dissertation Agreement, Publication Delay, and Certification Disclaimer (Graduate School Form 32), this thesis/dissertation adheres to the provisions of Purdue University's "Policy of Integrity in Research" and the use of copyright material.

Approved by Major Professor(s): Jan Olek

Approved by: Duley M. Abraham

12/06/2016

Head of the Departmental Graduate Program

Date

To the people I love the most, my beautiful family:

Jorge H. Tabares and Ana María Tamayo

Jorge and Ana Cristina

For every memory and wise word, and the endless love that has taught me to dream,

love, be humble and achieve happiness in life.

ACKNOWLEDGEMENTS

First, I would like to present my sincere gratitude to Cementos Argos, the company that has continuously supported me throughout my personal and professional development.

I would like to thank my advisor and mentor, Professor Jan Olek, for sharing with me his friendship, knowledge, and experience throughout my graduate school program.

I also appreciate all the contributions and guidance received from my advisory committee, Professor Jason Weiss, Professor Kendra Erk, and Professor John Haddock.

I am grateful to Raikhan Tokpatayeva, who besides becoming such a great friend, also devoted her time to teach me about cement chemistry and characterization techniques.

I also extend my gratitude to Warda Ashraf, HyunGu Jeong, Parth Panchmatia, Ali Behnood, Santiago Ruiz, and Belayneh Desta.

I want to thank my mentor and friend, Jose Alberto Velez, for his valuable support and guidance along this journey. His trust and vision reminded me to enjoy every experience in life to the fullest.

Tori, Libby, Emily, and Marissa: There are no words to describe how thankful I am to have such a beautiful group of friends who have taught me to see life from the happy side.

Finally, I would like to thank my family for encouraging me to pursue my dreams and supporting me at each stage of my life.

TABLE OF CONTENTS

	Page
LIST OF TABLES	viii
LIST OF FIGURES.....	x
ABSTRACT.....	xv
CHAPTER 1. INTRODUCTION	1
1.1 Introduction.....	1
1.2 Justification.....	2
1.3 Main Objectives.....	4
1.3.1 Research Questions	5
1.3.2 Challenges.....	5
1.3.3 Hypotheses	6
1.4 Research Approach.....	6
1.5 Thesis Content.....	7
CHAPTER 2. LITERATURE REVIEW	10
2.1 Introduction.....	10
2.2 Ordinary Portland Cement (OPC)	13
2.3 Superabsorbent Polymer (SAP)	18
2.4 Absorption/Desorption Capacity of Superabsorbent Polymer (SAP).....	20
2.5 Superabsorbent Polymers in Cementitious Systems	26
2.5.1 Hydration in Internally Cured Systems (ICS).....	27
2.5.2 Autogenous Shrinkage of Internally Cured Systems (ICS)	30
CHAPTER 3. MATERIALS CHARACTERIZATION	33
3.1 Introduction.....	33

	Page
3.2	Materials..... 34
3.2.1	Cement..... 34
3.2.2	Superabsorbent Polymer (SAP)..... 38
3.3	Experimental methods 40
3.3.1	Cement Paste 40
3.3.2	Superabsorbent Polymers (SAP) 51
3.4	Experimental Results 54
3.4.1	Chemical composition of Pore solution..... 54
3.4.2	Image analysis of Superabsorbent polymers..... 59
CHAPTER 4.	SYNTEHTIC PORE SOLUTION AND ABSORPTION CAPACITY OF SAP..... 71
4.1	Introduction..... 71
4.2	Materials..... 71
4.3	Experimental Methods 72
4.3.1	Synthetic Pore Solution (SPS) Preparation 72
4.3.2	Absorption Capacity SAP –Tea Bag Method 73
4.4	Experimental results..... 74
4.4.1	Chemical Analysis of Synthetic Pore Solution (SPS) 74
4.4.2	Absorption Capacity of SAP 84
4.5	Discussion for Absorption Capacity 91
4.5.1	Stages of the Absorption Capacity Isotherms..... 91
4.5.2	Effect of pH and Ion Concentration 93
4.5.3	Statistical Analysis..... 98
CHAPTER 5.	INFLUENCE OF SUPERABSORBENT POLYMERS IN THE INTERNAL CURING MECHANISM IN CEMENT PASTE 102
5.1	Introduction..... 102
5.2	Experimental Methods 102
5.2.1	Cement Paste 102
5.2.2	Isothermal Calorimetry 106

	Page
5.2.3 Autogenous Strain of Cement Paste	108
5.3 Experimental Results	110
5.3.1 Isothermal Calorimetry	110
5.3.2 Autogenous Shrinkage	125
CHAPTER 6. CONCLUSIONS	130
LIST OF REFERENCES	134

LIST OF TABLES

Table	Page
Table 1 - Commercial Superabsorbent Polymers (SAP) Suppliers (TC225-SAP, 2012)	19
Table 2 - Mill certificates for Cem1, Cem2 and Cem3	35
Table 3 - Mix Designs for reference cement pastes	41
Table 4 - Sample preparation for Atomic Absorption spectroscopy (AA)	48
Table 5 - Ionic concentration of pore solution extracted from fresh cement pastes (w/c of 0.30 and 0.35) after 5 minutes of hydration	55
Table 6 - Quantiles for Particle Size Distribution of SAP "A" (BASF).....	65
Table 7 - Quantiles obtained for Particle Size Distribution of SAP B	67
Table 8 - Mean and standard deviation of the sample - SAP B	68
Table 9 - Quantiles describing values observed and estimated for Normal Distribution of SAP B	68
Table 10 - Preparation schemes and list of chemicals used to create artificial pore solution for w/c=0.3 paste from Cem3.....	76
Table 11 - Chemical compounds used in grams to prepare 1 liter of synthetic pore solution based on cement sample.....	76
Table 12 - Comparison of compositions of extracted and synthetic pore solutions.....	79
Table 13 - Absorption capacity of hydrogels based on synthetic pore solution (SPS)	87
Table 14 - Absorption capacity of SAP based on pore solution composition.....	88
Table 15 - Concentration of ions and pH values (Calculated and measured) for synthetic solutions.....	96
Table 16 - Most significant models	100
Table 17 - Determined absorption capacity of SAP based on the synthetic solutions...	101

Table	Page
Table 18 - Mix designs used for reference and internally cured cement pastes	103
Table 19 - Volumetric distribution based on DOH of a sealed cement paste of $w/c=0.30$	105
Table 20 - Mix proportions for reference samples at different w/c ratios and internally cured samples	121

LIST OF FIGURES

Figure	Page
Figure 1- Cement Manufacturing Process (Encyclopaedia Britannica, 2007)	14
Figure 2 - Concentration of ions in expressed pore solution from OPC (Diamond, 1981)	17
Figure 3 - Superabsorbent polymers - SAP at time zero, before water contact (on the left side of the figure) and SAP during swelling process (Right hand side of the figure) (Luís Pedro Esteves, 2011a)	19
Figure 4 – SAP particle based on poly-acrylic acid – Courtesy of BASF (TC225-SAP, 2012)	20
Figure 5 - Sorption Isotherm for a SAP (Absorption and desorption). The figure on the left presents the complete sorption isotherm for SAP tested in water. The figure on the right presents a close-up analysis on the absorption isotherm. A sorption isotherm for concrete is also shown in order to be compared to that of SAP (Jensen, 2013).	23
Figure 6 – Hydration heat flux of cement pastes at different w/c and 10% silica fume by mass of cement (J. Justs et al., 2015)	28
Figure 7 – Cumulative heat of hydration of cement pastes at different w/c and 10% silica fume by mass of cement (J. Justs et al., 2015).....	28
Figure 8 – Autogenous strain of an ultra-high-performance cementitious binder with a w/c of 0.30, 20% silica fume (by weight of cement) and different levels of SAP addition (by weight of cement) (Jensen, 2013).	31
Figure 9 – Autogenous Shrinkage of UHPC at various w/c and SAP levels (J. Justs et al., 2015).....	32

Figure	Page
Figure 10 – Compressive Strength development of cement paste presented in mill certificate ASTM C-109 for all the cements studied.	37
Figure 11 - Optical microscope of SAP (Masterlife IC-400)	39
Figure 12 - SAP A – Optical image taken from optical microscopy analysis done for superabsorbent polymer provided by BASF - Masterlife IC 400 - (Magnification 140x)	39
Figure 13 - Mixing of cement paste using a Hobart mixer following ASTM C305-14.....	41
Figure 14 - Vials containing different extracted pore solutions at w/c of 0.30 and 0.35. 42	
Figure 15 - Pore solution extraction from fresh cement paste by means of Millipore™ pressure filtering system.	43
Figure 16 - Setup for pH measurement of the pore solution by means of Cole-Parmer pH-meter electrode. The figure also depicts the ongoing calibration of the electrode	46
Figure 17 - On the left hand side, samples are being prepared for ICS. On the right hand side, DIONEX ICS-900 is running.....	47
Figure 18 - Sample tested for determination of cations using VARIAN SpectrAA 10/20. 49	
Figure 19 - Samples solutions prepared for inductively coupled plasma spectrometry (ICP)	50
Figure 20 - 6850 Cryomilling Freezer/Mill	52
Figure 21 - Extraction of SAP sample after milling process	52
Figure 22 - Image Analysis of SAP by means of Optical Microscopy	53
Figure 23 - Concentration of ions in pore solutions of pastes prepared with different cements at w/c of 0.30.....	56
Figure 24 - Pore solution composition in cement paste at w/c = 0.65 (Kurdowski, 2014)	57
Figure 25 - Sulfate concentrations as a function of the OH ⁻ concentration at early hydration time (presence of gypsum and Portlandite) and later hydration times (presence of ettringite and Portlandite) (Vollpracht et al., 2016)	58

Figure	Page
Figure 26 - Optical image of SAP A taken from optical microscopy analysis done for superabsorbent polymer provided by BASF (Magnification 140x)	60
Figure 27 - Optical image for superabsorbent polymer obtained after cryomilling process, SAP B (Magnification 140x)	60
Figure 28 - Optical image of SAP taken at time 0 at room conditions of 21°C and 50% RH.	61
Figure 29 - Optical image (of the same SAP presented in Figure 28) 9 days after exposition to environment - Room conditions of 21°C and 50% RH.	61
Figure 30 - Scatter Plot of the Particle Size Distribution (PSD) of SAP A	62
Figure 31 - Particle Size Distribution of SAP A in logarithmic scale	63
Figure 32 - Normal and Kernel distribution plots - SAP A.....	64
Figure 33 - Particle Size Distribution of SAP B in microns (Logarithmic scale) – SAP B is the finer SAP obtained after milling SAP A by means of Cryomilling.....	66
Figure 34 - Histogram combined with two density plots, normal density estimate and kernel density estimate	67
Figure 35 - Swelling behavior of SAP A in synthetic pore solution (SPS) resembling the extracted solution from cement paste prepared using Cem3	69
Figure 36 - Swelling behavior of SAP B in SPS resembling the system prepared with Cem3	70
Figure 37 - Evolution of the appearance of the synthetic solution during preparation ..	77
Figure 38 - SEM Image #1 for Preparation Scheme #1 - potassium, sulfur, sodium and calcium are the main peaks found in this portion of the precipitates.....	80
Figure 39 - SEM Image #2 for Preparation Scheme #1 - potassium, sulfur and calcium peaks found in the precipitates.....	81
Figure 40 - SEM Image #3 for Preparation Scheme #2 – calcium, potassium, sulfur and sodium are the elements represented by the main peaks found in this portion of the precipitates.	82

Figure	Page
Figure 41 - SEM Image #4 for Preparation Scheme #2 - calcium and potassium are the main peaks found in the precipitates.....	83
Figure 42 - Absorption Capacity Isotherm for SAP A when different synthetic solutions used	85
Figure 43 - Absorption Isotherm for SAP B when different synthetic solutions used.....	86
Figure 44 - Absorption capacity isotherm for polymers A and B in SPS1 Cem1.....	89
Figure 45 - Absorption capacity isotherm for polymers A and B in SPS2 Cem2.....	89
Figure 46 - Absorption capacity isotherm for polymers A and B in SPS3 Cem3.....	90
Figure 47 - Absorption capacity isotherm describing different swelling behavior for the same SAP sample through Stage 1 and 2.....	92
Figure 48 - Swelling behavior of SAP A for different pH and concentration of ions in synthetic pore solution. All the concentrations are in units of mMol/L.....	97
Figure 49 - Power's model for a cement paste at w/c 0.30 (cured in sealed condition)	105
Figure 50 - TAM Air Isothermal Calorimeter used for calorimetry studies of cement pastes with and without inclusion of superabsorbent polymers (SAP).....	107
Figure 52 - Comparison of Autogenous and Chemical Shrinkage (Japan Concrete Institute, 1999).....	109
Figure 53 –Autogenous shrinkage test of cement paste - ASTM C1698 – 09 (Reapproved 2014), “Standard Test Method for Autogenous Strain of Cement Paste and Mortar”.....	110
Figure 54 - Isothermal Calorimetry of reference cement pastes at w/c=0.30 (First 24 h)	112
Figure 55 - Isothermal Calorimetry of reference cement pastes prepared with Cem1, Cem2 and Cem3 at free w/c=0.30.....	114
Figure 56 - Rate of heat Flow for cement pastes prepared with Cem1 at w/c=0.30 and SAP A and B	115
Figure 57 - Isothermal Calorimetry of cement pastes with and without SAP prepared with Cem1 at free w/c=0.30.....	116

Figure	Page
Figure 58 - Rate of heat Flow for cement pastes prepared with Cem2 at $w/c=0.30$ and SAP A and B	117
Figure 59 - Isothermal Calorimetry of cement pastes with and without SAP prepared with Cem2 at free $w/c=0.30$	118
Figure 60 - Rate of heat Flow at 24 h for cement pastes prepared with Cem3 at $w/c=0.30$ with and without SAP. Samples with SAP inclusion are considered Internally Cured Systems (ICS).....	120
Figure 61 - Isothermal Calorimetry of cement pastes with and without SAP prepared with Cem3 at free $w/c=0.30$	122
Figure 62 - Rate of heat Flow at 24 h for reference cement pastes and IC-0.20SAP cement pastes	123
Figure 63 - Isothermal Calorimetry of cement pastes with and without SAP B prepared with Cem1 and Cem3	124
Figure 66 - Autogenous Shrinkage of cement Pastes with and without SAP - Following ASTM C1698 – 09 (Reapproved 2014)	127
Figure 67 - Autogenous Shrinkage of Cem1 with and without SAP - Following ASTM C1698 – 09 (Reapproved 2014).....	128
Figure 68 - Autogenous Shrinkage of Cem3 with and without SAP - Following ASTM C1698 – 09 (Reapproved 2014).....	129

ABSTRACT

Tabares, Juan D.. M.S.C.E., Purdue University, December 2016. The Influence of Alkalinity of Portland Cement on the Absorption Characteristics of Superabsorbent Polymers (SAP) for use in the Internally Cured Concrete. Major Professor: Jan Olek.

The concrete industry increasingly emphasizes advances in novel materials that promote construction of more resilient infrastructure. Due to its potential to improve concrete durability, internal curing (IC) of concrete by means of superabsorbent polymers (SAP) has been identified as one of the most promising technologies of the 21st century. The addition of superabsorbent polymers into a cementitious system promotes further hydration of cement by providing internal moisture during the hardening and strength development periods, and thus limits self-desiccation, shrinkage, and cracking.

This thesis presents the work performed on the series of cement pastes with varying alkalinity of their pore solutions to provide a better understanding of: (1) the influence of the chemistry of the pore solution (i.e. its level of alkalinity and the type of ionic species present) on the absorption capacity of SAP, and (2) the effectiveness of SAP with different absorption capacities as an internal curing agent.

This research work was divided into three stages: (a) materials characterization, (b) measurement of absorption capacity of SAP in synthetic pore solutions, and (c) evaluation of the internal curing effectiveness of SAP.

During the first stage (***Materials Characterization***), pore solutions were extracted from the fresh (5 minutes old) cement pastes prepared using cements with three different levels of alkalinity. The pH values of the extracted solutions were determined (using the pH meter) and their chemical analysis was performed by means of titration (concentration of hydroxyl), ion chromatography (sulfates and chlorides), atomic absorption (AA) and inductively coupled plasma optical emission spectrometry (ICP) (sodium, potassium and calcium).

The commercial SAP adopted for this study was used with “as-supplied” gradation and with the finer gradation obtained by grinding the original polymer in the 6850 Cryomilling Freezer/Mill. The physical properties of these SAP’s, such as the shape and size of the particles, were determined by optical microscopy combined with image analysis.

The second stage, the ***absorption capacity of SAP’s***, involved determination of the swelling behavior and the absorption capacity of polymers exposed to artificial pore solutions with different levels of alkalinity. The swelling behavior was followed using the optical microscope while the absorption capacity was characterized using the tea bag

method. It was found that changes in the chemical compositions of the pore solutions influence the adsorption kinetics and result in different absorption isotherms.

In the third stage, the *internal curing effects* of inclusion of SAP in cement pastes **were** evaluated. Mixture proportions of pastes used in this stage of the study were selected based on the absorption capacity of the SAP determined in stage two. The testing of the pastes involved determination of their set times, heat of hydration, and autogenous shrinkage.

CHAPTER 1. INTRODUCTION

1.1 Introduction

The internal curing (IC) method has been identified as the 21st century technology that provides an internal source of water for curing to maximize cement hydration and reduce self-desiccation; as a result, the potential to develop unwanted early-age cracking may be mitigated and more durable concrete may be produced (Dale P Bentz & Weiss, 2010). The 2013 edition of the American Concrete Institute (ACI) Concrete Terminology (ACI CT-13) defines internal curing as “process by which the hydration of cement continues because of the availability of internal water that is not part of the mixing water”. To date, the most common technologies that have been successfully use to produce the IC concrete include the usage of fine pre-wetted lightweight aggregate, pre-wetted recycled concrete fines, superabsorbent polymers (SAP), and pre-wetted wood fibers. The IC technology is particularly suitable for the use in high and ultra-high-performance concrete, which, due to their typically low value of w/c are particularly prone to self-desiccation and early age cracking (Janis Justs, Wyrzykowski, Winnefeld, Bajare, & Lura, 2014). Similarly to what has been obtained with the use of LWA, internally cured concrete using superabsorbent polymers (SAP) may also promote the

hydration of cement (by providing internal moisture during the hardening and strength development periods) and limit self-desiccation, shrinkage and cracking. It has been previously reported that addition of super absorbing polymers (SAP) into high performance concrete (HPC) resulted in significant reduction of the autogenous shrinkage (Craeye, Geirnaert, & Schutter, 2011). Despite the proven benefits of SAP with respect to their internal curing capabilities, especially about their contribution to reduction in autogenous shrinkage and the ability to control micro cracking, there are still several unexplored issues that need to be addressed. These include the use of SAP in frost protection applications (i.e. as “artificial” air bubbles), the use of these materials to modify the rheology of shotcrete and in other special applications (Luis Pedro Esteves, Lukosiute, & Cesniene, 2014). In addition, little information is available with respect to the robustness of SAP performance in cases involving changes in the chemistry of the cement.

1.2 Justification

Nowadays, the construction industry is facing environmental, economic and social challenges that encourage materials’ manufacturers to rethink their strategies, process and technologies with the aim of producing high-tech and long-lasting solutions that might offer good return on the investment while minimizing environmental and social impacts. Cement producers and concrete manufacturers are viewing technology innovations as the instrument to produce more durable and useful materials to allow architects and civil engineers to design and build structures that are more resilient. As

an example, the relatively novel technology of “Internally cured concrete” has been identified as one of the potential solutions that could improve concrete durability while maximizing the hydration of cement, densifying the microstructure and minimizing the effects of self-desiccation (Assmann, 2013). Various materials have been used for internal curing applications. These include pre-wetted lightweight aggregates, pre-wetted recycled concrete fines, super absorbent polymers (SAP) and pre-wetted fibers (Dale P Bentz & Weiss, 2010). Due to non-uniform availability of sources of lightweight aggregates around the globe, and due to potentially higher variability in the characteristics of the naturally derived products that can be used for internal curing, SAP may offer an attractive alternative due to their potentially higher uniformity of properties and easiness to be commercialized in different geographies and markets.

Although previous investigators (Janis Justs et al., 2014) (Craeye et al., 2011) (Luís Pedro Esteves, 2011a) reported that SAP could be quite effective in providing efficient means of internal curing, they also indicated that this effectiveness is a function of many parameters. These include physical and chemical properties of SAP themselves as well as the overall chemistry of the system, in particular cement contribution to alkalinity of the pore solution. These issues represent a knowledge gap that needs to be addressed in order to provide a more objective assessment of the utility of using SAP in the internal curing applications. To this end, the current project utilized three types of cement (each with different alkali content) and two different size of SAP in studying the effects of these parameters on the effectiveness of SAP as the internal curing material

and thus providing supporting technical data, which can help with a more widespread usage of this technology in the construction industry

The research plan involved studies of the effects of alkalinity of the cement and particle size distribution of the SAP on the kinetics of fluid absorption, degree of cement hydration, and susceptibility to volumetric changes due to the loss of water.

It would be beneficial for the science and industry to use the knowledge gained during this project for developing further research into the concrete mixtures optimization with respect to their internal curing capabilities and suitability for field production. Also, the concrete properties that might be evaluated will include strength development (both early and over time), early-age cracking susceptibility (due to loss of water bleeding water) and selected durability properties.

1.3 Main Objectives

- To assess the compatibility between the commercial super absorbent polymers and low (0.37%), medium (0.62%) and higher alkalinity (0.72%) cements
- To focus on the contribution of SAP to cement hydration and reduction of the potential for early-age cracking of pastes internally cured with SAP inclusions.

1.3.1 Research Questions

A previous review of existing literature on the use of SAP for internal curing purposes indicated that it is a viable technology yet variable. Therefore, differences in methodology, sources and purposes promote diversity in respect to science behind this technology. Here are few technical questions that need to be answered in view of the objectives of this project.

- How is the absorption capacity of SAP influenced by changes in the chemistry of the pore solution?
- When different alkalinity cements are used, different pore solution compositions are implemented; how does this influence the hydration of the paste based on the contribution of SAP as an internal curing agent?
- Is there any reduction in autogenous shrinkage of the cementitious system associated to the internal supply of water through SAP?

1.3.2 Challenges

- To identify the critical parameters related to internal curing (IC) with SAP when the cement chemistry is modified.
- To promote further cement hydration even when cement alkalinity is modified and SAP are added.
- To reduce early-age strain development of cement paste when SAP are added.

1.3.3 Hypotheses

- Absorption capacity of SAP will be influenced by chemistry of the pore solution (i.e. alkalinity and type of ionic species) and size of the polymer.
- The contribution of SAP (as an internal curing agent) to promote further cement hydration in cement pastes depends on its absorption capacity.

1.4 Research Approach

The proposed research program was envisioned to investigate the interaction between SAP and cement to develop a more in-depth understanding of the parameters that drive the effectiveness of the SAP-based internal curing mechanism. This mechanism is expected to vary when cement alkalinity and particle size distribution of SAP are modified. Therefore, variables studied in this research were separated in stages. This experimental work contains three independent research stages, characterization of the materials, absorption capacity of the polymers using synthetic solutions and evaluation of internally cured cement paste.

The first stage presents activities developed to identify the chemistry of the pore solution at early ages for three different cements and the image analysis used to define the morphology of the polymers. The second illustrates the work done to replicate the pore solution composition and study the absorption capacity of SAP. The third stage states the research activities conducted and results for the evaluation of the

contribution of SAP to improvement of the degree of hydration and shrinkage reduction at early ages in cement paste.

1.5 Thesis Content

Chapter 2 corresponds to the state of the art and literature review. In this, a literature review was developed about the variables that control (influence) the efficiency of super absorbent polymers (SAP) in providing the internal curing mechanism for Portland cement concrete. The search was limited to information such as cement chemistry associated with the pore solution and its physical and chemical interaction with SAP, particle size of the polymer, kinetics of absorption/desorption, heat liberation during hydration and after setting of cement, shrinkage control, and contribution of IC mechanism through the usage of SAP to the strength development.

In Chapter 3, the most important physical and chemical properties of the materials investigated are stated. At first, the information provided by the suppliers is presented. Later, the results of the study of the chemical composition of pore solution of fresh cement pastes and the morphology of the SAP used in this research are listed. It has been reported that the chemistry of the liquid phase in a cementitious system, represented by the concentration of ions, play an important role in the kinetics of hydration and the ability of SAP to absorb and desorb fluids such as pore solution. Due to the rapid dissolution of alkalis, high concentrations of ions are found in pore solution. The alkali content, which differs considerably among Portland cements, will drive the

ionic strength of the composites. Therefore, it was envisioned that this research program had to be carried out using three different cements and two different sizes of SAP. Based on the preliminary literature review, the alkalinity of the cement appears to have a strong influence on the performance of SAP; for this reason, chemical characterization of the pore solution extracted from fresh cement pastes prepared with low ($\sim 0.37 \text{ Na}_2\text{Oeq}$), medium ($\sim 0.62 \text{ Na}_2\text{Oeq}$) and higher ($\sim 0.72 \text{ Na}_2\text{Oeq}$) alkalinity cements was developed. In addition, it has also been reported that the size of the polymer has impact on the absorption and desorption kinetics of SAP (Luís Pedro Esteves, 2011b); thus, size and shape of two SAP samples were assessed by means of image analysis.

In Chapter 4, synthetic pore solutions were prepared and the absorption capacity of the SAP when the artificial solutions are used to hydrate the polymers was studied. With the information provided in Chapter 3 about the chemical composition of pore solution at early age, synthetic solutions were made to simulate the actual liquid phase in a cementitious system at early ages and study the interaction between the pore solution and SAP. Thus, the kinetic of absorption, swelling time and changes in size or volume of the SAP were evaluated for three different pore solutions, which were formulated based on the chemical composition of each cement. This task allowed us to determine the absorption capacity of SAP that is used for mix design of internally cured cement pastes studied in Chapter 5.

Finally, in Chapter 5, cement pastes were prepared with and without the addition of SAP to compare the evolution of the hydration process in terms of calorimetry, and volumetric change due to autogenous shrinkage. In this section, changes in fresh properties and hydration mechanism of pastes might occur when the chemistry of the cement and constituents of the paste are modified. For our purposes, the addition of SAP and the variation in the cement chemistry (and thus variation in the chemistry of the pore solution) in pastes represent obvious changes in material properties. However, we concentrated our attention on assessing any change in degree of hydration through the study of calorimetry and volumetric change.

CHAPTER 2. LITERATURE REVIEW

2.1 Introduction

An inevitable need to repair existing infrastructure and build longer-lasting infrastructure using more sustainable materials has challenged current and future professionals in global engineering.

According to the American Society of Civil Engineers (ASCE), “infrastructure is a set interrelated system that connects a nation’s businesses, communities and families, drives the country’s economy and improves quality of life” (American Society of Civil Engineers, 2013). For instance, roads and ports, rails and aviation, waste and drinking water, and energy, are part of a country’s infrastructure. Therefore, countries in the search of developing a world economy need a first-class infrastructure. In the US; for instance, there is a measured lack of investment in infrastructure that is reflected by the assessed overall average of infrastructure in poor condition. As one of the examples reported in the American Society of Civil Engineers (ASCE) 2013 Report Card for America’s infrastructure (American Society of Civil Engineers, 2013), dams; graded D due to their poor condition, require an investment of \$21 billion to repair 84,000 dams in the US.

One in nine of the bridges built in the US was rated as structurally deficient, and an overall grade of C+ (mediocre: requires attention) was assigned to 607,380 bridges in the US. To satisfy the infrastructure needs by 2028, the US needs to invest \$20.5 billion annually in bridge repair while only about \$12 billion are currently invested. Additionally, roads were graded as deficient. The Federal Highway Administration (FHWA) has estimated that \$170 billion are needed to invest on improving roads condition and performance. According to (USDOT-FHWA, US Department of Transportation - Federal Highway Administration, 2016)., there is a need to stop short-term measures and pass a long-term transportation bill due to the current condition of infrastructure. Besides the lack of investment, the advanced deterioration of the structures has also been attributed to materials' performance and properties, such as, in the case of reinforced concrete structures, poor strength development, early-age cracking and corrosion of reinforcing steel in concrete that diminish their service life.

Concrete, which is produced more than any other material on earth (CSHub, MIT Concrete Sustainability Hub, s.f.), is also the most widely used construction material, especially for infrastructure. Even though the usage of concrete in general is favorably compared to the use of other construction materials (Lemay & Lobo, 2011), its excessive production and consumption embody large amounts of carbon dioxide (CO₂). The largest contribution of CO₂ to the concrete carbon footprint comes from the cement used in concrete mixtures. Thus, an approximate of 100 to 300 kg of CO₂ is embodied per cubic meter of concrete.

The facts presented previously have moved the cement industry forward towards the development of more sustainable products such as internally cured concrete. This technology provides internal water reservoirs to promote further cement hydration, improve resistance to deterioration at early ages (Craeye et al., 2011), increase service life of structures (Hasholt & Jensen, 2015), and reduce the carbon footprint of structures.

Due to the low permeability of a cementitious system at low w/c ratios, external curing water only promotes further hydration of the cementitious material located in (or near) the outer surface of the concrete element (Lopez, Kahn, & Kurtis, 2010). As such, it is likely that cement particles located in the core of the concrete element may only be partially hydrated (or remain completely unhydrated) due to the lack of hydration water. As a result, the expected material properties may eventually not be met. Conversely, the usage of internal water reservoirs (supplied through the internal curing agents) will provide a self-curing mechanism that will facilitate further cement hydration and shrinkage reduction (Lopez et al., 2010). Although many different internal curing agents and methods have been tried in the past (e.g. superabsorbent polymers, natural fibers and recycled concrete aggregates, (Dale P Bentz & Weiss, 2010)), the method used most commonly involves substitution of part of the natural sand with fine saturated lightweight aggregates (LWA). The usage of LWA as an internal curing agent has been widely implemented due to the high ability of these aggregates to absorb water and subsequently release it as the internal curing water that reduces the effects of self-

desiccation in low water-to-cement ratio materials and promotes larger extent of hydration of cement (Castro, Keiser, Golias, & Weiss, 2011).

In this research, the internal curing of cementitious systems was studied by utilizing superabsorbent polymers (SAP) as the internal curing agent. These polymers, also known as hydrogels, are capable of absorbing the pore solution during the first few minutes of the hydration process. It is expected that the absorbed pore solution will then be released back to the hydrating system as soon as self-desiccation of the cementitious system takes place; this will promote further hydration of unhydrated cement particles by maintaining the high degree of saturation of the cementitious system. Previous research work developed in this field will be presented in the upcoming sections.

2.2 Ordinary Portland Cement (OPC)

In the book, Portland Cement (Bye, 2011), "cement is defined as a material which binds together solid bodies (aggregate) by hardening from a plastic state". For this research, Ordinary Portland Cement (OPC) will be referenced and studied. An OPC is considered a hydraulic inorganic cement that reacts with water to produce a plastic cement paste (during fresh state) and hardens over time to provide strength (Bye, 2011).

By definition, OPC is primarily composed of Tricalcium silicate (C_3S) or alite, Dicalcium silicate (C_2S) or belite, Tricalcium aluminate (C_3A) and Tetracalcium aluminoferrite (C_4AF).

However, these main compounds are contained in cement as the results of mixing, processing, heating to temperatures around 1450°C, and grinding down raw materials (see manufacturing process in Figure 1) such as:

- Limestone (as a source of calcium oxide - CaO)
- Clay (as the source of iron oxide or ferric oxide - Fe₂O₃, and silicon dioxide - Si₂O₃)
- Sand, shale or marl (as the source of silicon dioxide - Si₂O₃)
- Clay, shale, fly, ash, aluminum ore (as the source of aluminum oxide - Al₂O₃)
- Gypsum (as the source of sulfates)

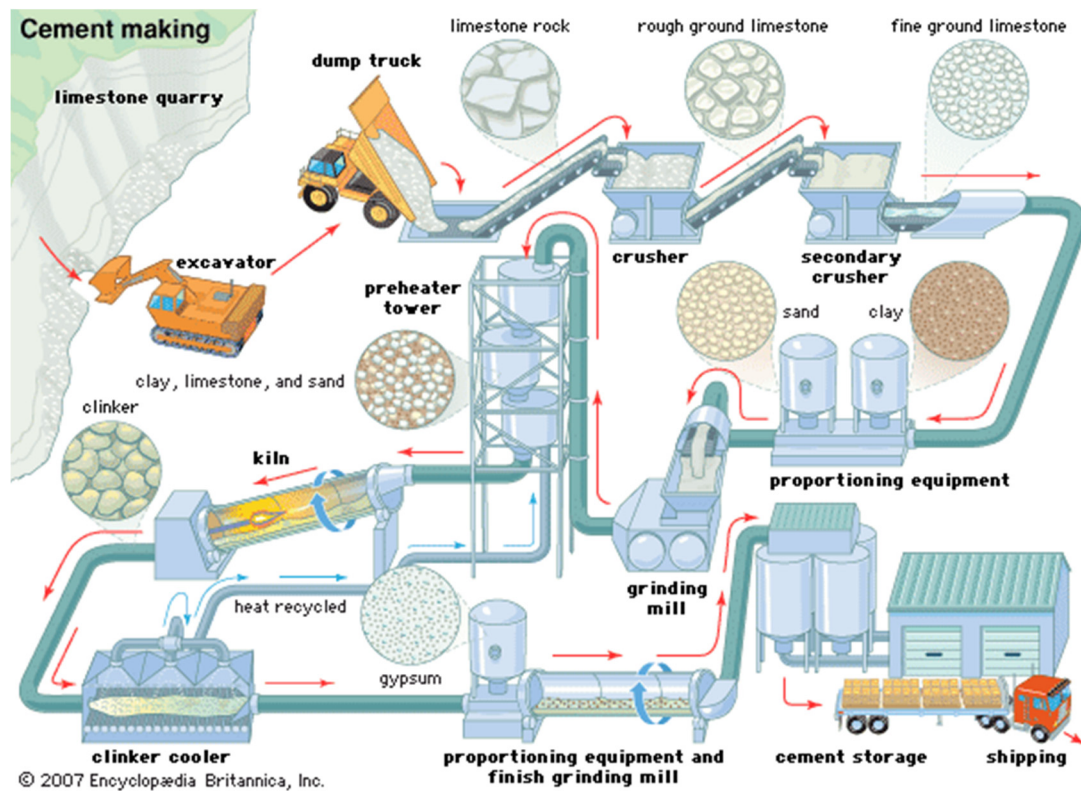


Figure 1- Cement Manufacturing Process (Encyclopædia Britannica, 2007)

Main alkalis (Na_2O and K_2O) in the cement come from clay, shale, stack dust returned to the preheating process, and high sulfur coal used to burn clinker that promotes the retention of alkalis in the clinker; for instance, potassium oxide (K_2O) (McCoy, 1978). The same author states that the alkalis sulfates are formed during the burning process when alkalis combine with sulfates available. However, there are not enough sulfates to combine with all the alkalis present. Therefore, the remaining portion of alkalis are combined with the aluminates and silicates. Na_2O mainly goes into aluminate phases whereas K_2O goes into silicate phases (McCoy, 1978).

The hydration process starts as soon as cement comes in contact with water, from which the development of a set of reactions is activated. Calcium silicate hydrate (C-S-H) and calcium hydroxide ($\text{Ca}(\text{OH})_2$) are the main hydration products. At the same time, as soon as the hydration starts, an immediate and fast dissolution of alkalis sulfates occurs. Because of this, the concentration of potassium in the liquid phase of the fresh cementitious system is higher than that of sodium (McCoy, 1978). The same author presents the concept of faster dissolution of the other sodium phases due to the earlier reaction of the aluminates when compared to that of silicates. However, not all the alkali content is water soluble. According to McCoy, “the amount of alkali in a cement that is water soluble can vary from less than 10% to over 60% of the total alkali present”.

The concentration of alkalis in the liquid phase or pore solution of a hydrating cement paste varies continuously. Experimental work presented by (Brouwers & Eijk, 2003)

stated that the only alkali-binding phase corresponds to calcium silicate hydrate or C-S-H. Therefore, the latter research work concludes that at early ages, alkalis are bound to the reaction products, which release the alkalis back to the pore solution after a few days. Similarly, (Diamond, 1981) reported a study of the effects of fly ashes on alkali content of pore solutions of cement-fly ash pastes. Figure 2 presents some results from (Diamond, 1981), in which pore solutions were expressed from plain Portland cement pastes. The concentration of potassium (K^+), sodium (Na^+), calcium (Ca^{2+}), and hydroxyl (OH^-) ions in the extracted solutions were determined by means of flame emission, atomic absorption spectroscopy, and acid titration.

Figure 2 shows that after 4 days, variation of the pore solution composition over time is due to both sulfate and calcium consumption. In addition, an increasing pH was found at early ages because of the increasing concentration of hydroxyl ions. The latter mechanism occurs due to the need of achieving electro-chemical balance between cations and anions, and it is pushed by the concentration of alkali ions in pore solution reached after 4 days of hydration. The concentration of alkalis in pore solution becomes important in internal curing-IC (when using superabsorbent polymers as the IC mechanism) because of the influence of alkali metal ions on the efficiency and absorption capacity of superabsorbent polymers.

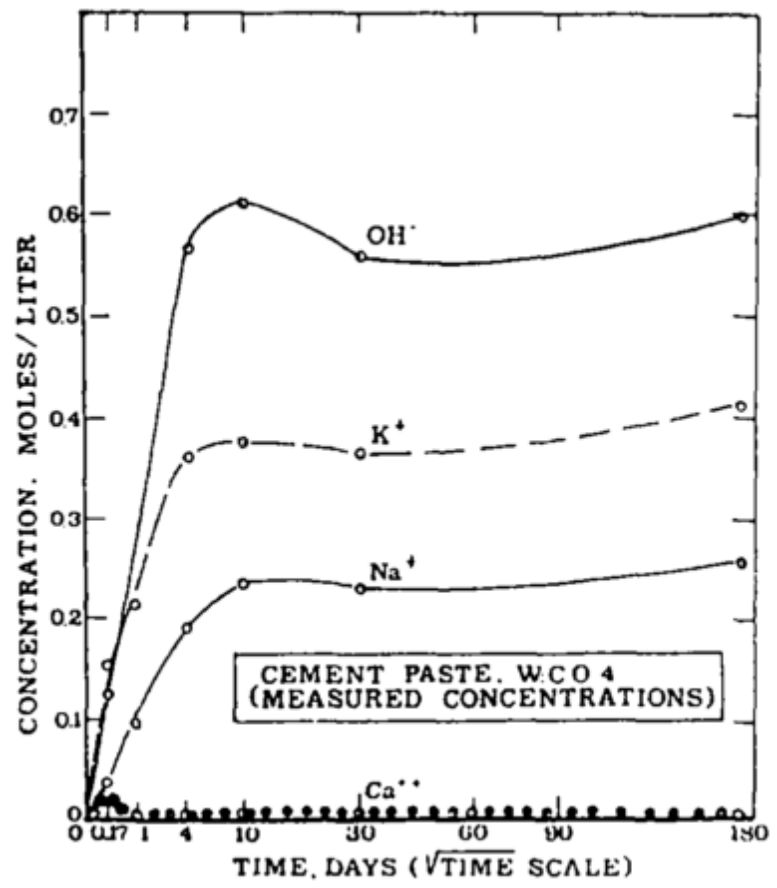


Figure 2 - Concentration of ions in expressed pore solution from OPC (Diamond, 1981)

2.3 Superabsorbent Polymer (SAP)

According to (Klemm & Sikora, 2012), superabsorbent polymers (SAP), are cross-linked polyelectrolytes characterized by their large capacity to absorb liquids (aqueous solutions). The addition of cross-linking agents during the manufacturing process drives the polymer's resistance to dissolution (Luís Pedro Esteves, 2011b). The state of the art prepared by the **RILEM Technical Committee 225-SAP** (TC225-SAP, 2012) reports that SAP are commercialized in two industries, hygiene and technical. The former includes baby diapers and adult care articles whereas the latter comprises any other application not included in hygiene (see Table 1). Hansen and Jensen introduced the use of SAP in the concrete industry as water-entrained cement-based materials (Luís Pedro Esteves, 2011b). Physical appearance of SAP and their swelling behavior when exposed to an aqueous solution is shown in Figure 3 (Luís Pedro Esteves, 2011b), which contains a set of pictures of spherical polyelectrolyte polyacrylamide super absorbent polymer particles. In this figure, a suspension polymerized covalently cross-linked acrylamide/acrylic acid copolymer is presented before and after swelling. The fast transition from dry to swollen state (see the right-column), is noticeable in Figure 3.

The SAP shown are perfect spheres; however, polymers' shape is strictly driven by the polymerization process. Irregularly shaped SAP are produced by means of solution polymerization whereas perfect SAP spheres can be obtained through suspension polymerization (Zhu, 2014). The latter author states that larger absorption capacity can be obtained for hydrogels manufactured through solution polymerization.

Among all polymer properties, swelling capacity and elastic modulus of the swollen elastic gel are considered the most important related to performance. From the polymer network standpoint, these polymer properties are influenced by the structure of the polymer network and cross-link density, respectively. For instance, when the density of the cross-link increases, the modulus also increases. In this case; however, the swelling capacity of the polymer decreases (Buchholz, 1994).

Table 1 - Commercial Superabsorbent Polymers (SAP) Suppliers (TC225-SAP, 2012)

Industry	Hygiene Industry			Technical SAP	
Supplier	BASF SE	Evonik Stockhausen GmbH	Nippon Shokubai	Arkema	SNF Floerger.

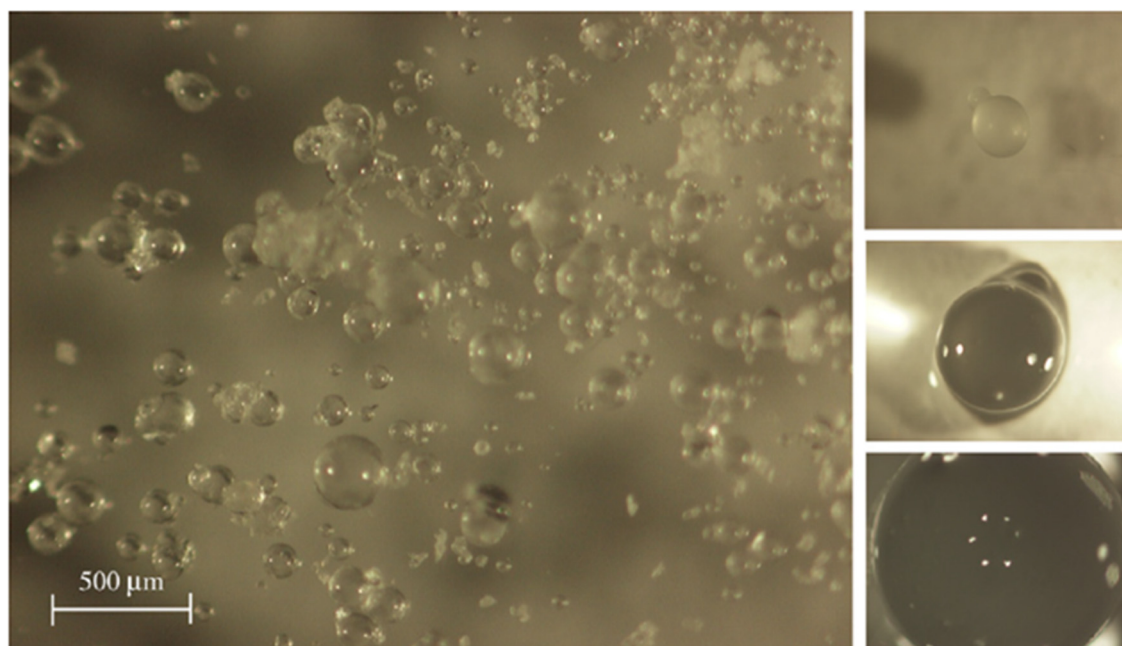


Figure 3 - Superabsorbent polymers - SAP at time zero, before water contact (on the left side of the figure) and SAP during swelling process (Right hand side of the figure) (Luís Pedro Esteves, 2011a)

2.4 Absorption/Desorption Capacity of Superabsorbent Polymer (SAP)

Absorption capacity of SAP is defined as the time that the polymer takes to reach a stable volume when exposed to an aqueous solution (Luís Pedro Esteves, 2011a). This polymer ability (to absorb and retain liquids) is driven by the presence of carboxylic acid functions and cross-links attached to the monomer structure. The *carboxyl group enables the ability to bind hard elements (metals) present in water* such as calcium (Ca^{2+}) and magnesium (Mg^{4+}). In addition, the presence of cross-linking agents between network chains establishes the resistance of the polymer chains to dissolution. Figure 4 presents a schematic of an SAP particle before and after interaction with an aqueous solution containing water molecules and metal ions (TC225-SAP, 2012). In the figure, metal ions (Na^+) from the solution are fixed to the carboxylic function while the polymer is swelling due to water absorption. The cross-linking agents avoid dissolution of SAP.

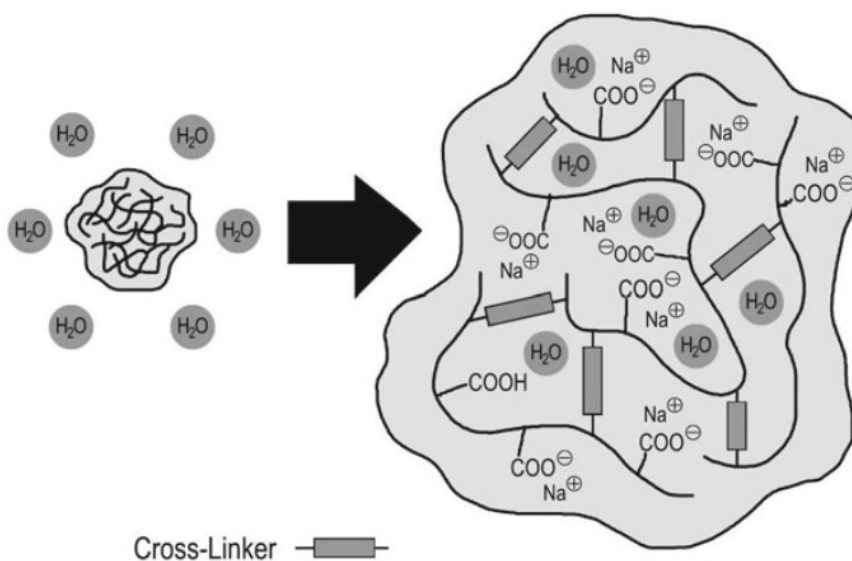


Figure 4 – SAP particle based on poly-acrylic acid – Courtesy of BASF (TC225-SAP, 2012)

The *absorption/desorption kinetic of SAP is strongly driven by the osmotic pressure*, which is proportional to the concentration of ions present in the solution. Before contact with water, ions in SAP are forced by the polymer network to stay together; therefore, the osmotic pressure is very high inside the polymer. However, once the polymer absorbs water, the osmotic pressure is diminished by diluting the charges. Thus, absorption capacity of SAP is governed by the concentration of ions in the swelling medium. Also, additional external forces may act in the system to affect the absorption capacity (TC225-SAP, 2012).

The absorption characteristic of SAP of up to 1500 grams of pure water per gram of dry polymer (TC225-SAP, 2012) enables the usage of the polymer in different applications; for instance, as an internal curing agent. An advantage of using SAP to provide an internal water reservoir in concrete is that polymer properties (size, shape, and absorption capacity, among others) can be tailored for a particular use (TC225-SAP, 2012). In cementitious systems, a tailored pore-system can be introduced to the concrete matrix based on the specifications required. On the other hand, new applications such as the inclusion of chemical substances that would be released under certain conditions to benefit the composite have also been considered (TC 260-RSC, 2014).

The absorption kinetics plot is called absorption isotherm, in which the Y-axis corresponds to the amount of solution absorbed, and the X-axis corresponds to time in

minutes. (Jensen, 2013) has shown sorption isotherms for SAP depending on the nature of the hydrogel and the solution used for the test. Not only the absorption capacity of the polymer can change when any of those parameters are modified, also the shape of the isotherm can vary. The maximum absorption capacity has been reached for pure water. The author states that SAP submerged in water can absorb from 100 to 400 grams of solution per gram of dry polymer. However, when the aqueous solution has high concentration of ions, as commonly found in extracted pore solution, the absorption capacity may drop to values as low as 10 to 30 grams of solution per gram of dry polymer. Some researchers (Miller, Barrett, & Weiss, 2013) observed that when exposed to the pore solution extracted from fresh cement paste with $w/c=0.30$, a commercially produced SAP have absorption capacity values of 1830% and 2350% for two different polymer sizes. Additionally, the isotherm presented in Figure 5 shows that 95% relative humidity (95% RH) is critical with respect to characterizing the response of SAP due to sudden changes in moisture content that occur at this point. On the other hand, (Luís Pedro Esteves, 2011a) presented a research work in which the absorption capacity of SAP (suspension polymerized covalently cross-linked acrylamide/acrylic acid copolymer) was tested for various polymer sizes using synthetic pore fluid. It was found that smaller particles swell faster because smaller particles have smaller nucleus. Synthetic pore solutions described in Chapter 4 - Table 17 were used to study changes in absorption capacity when the size of SAP is modified. SAP particles with a diameter of 50 μm achieved their absorption capacity in less than 1 min whereas for SAP with 300 μm diameter, full absorption capacity was reached after 20 min.

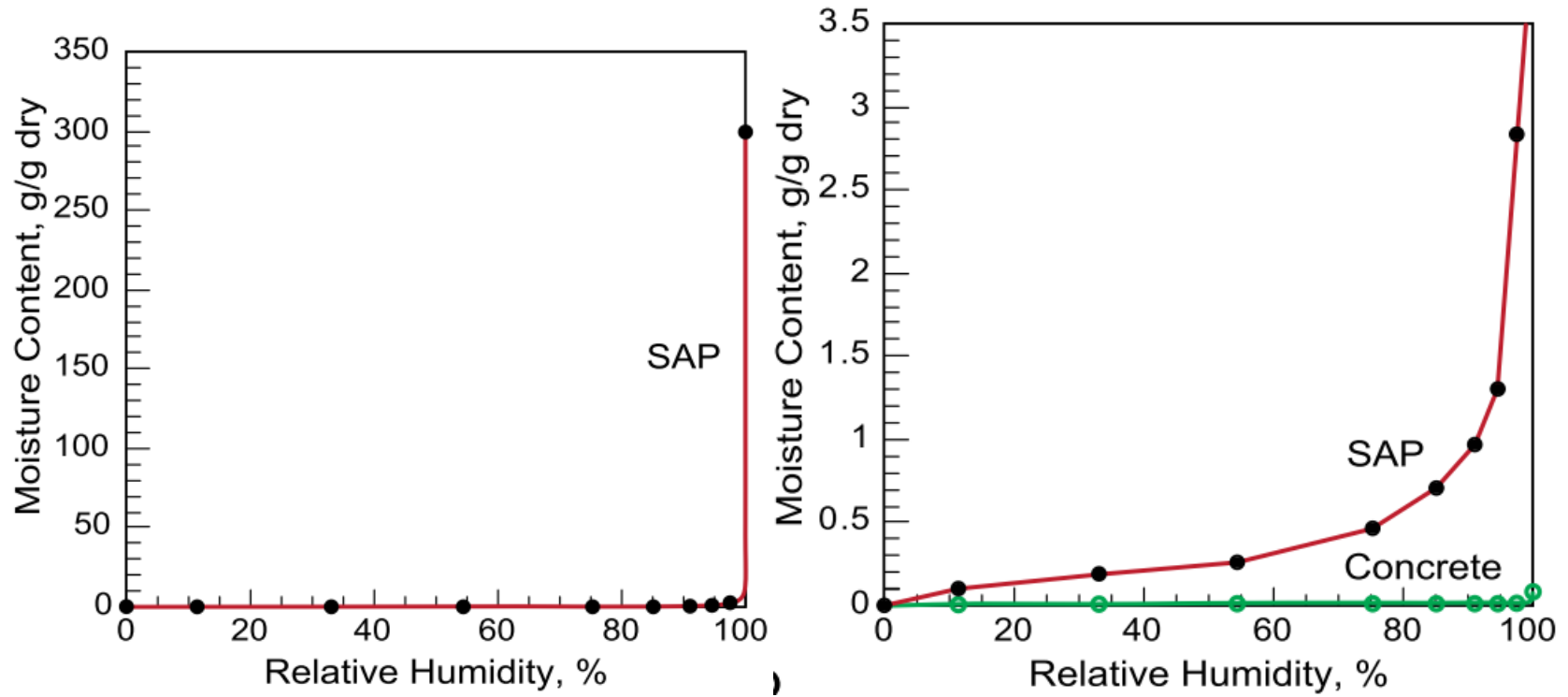


Figure 5 - Sorption Isotherm for a SAP (Absorption and desorption). The figure on the left presents the complete sorption isotherm for SAP tested in water. The figure on the right presents a close-up analysis on the absorption isotherm. A sorption isotherm for concrete is also shown in order to be compared to that of SAP (Jensen, 2013).

The absorption capacity also depends on the **pore solution composition**, which in the case of a cementitious system is the swelling media. When submerged, SAP will absorb liquids until a balance between expansive and shrinking forces is reached (TC225-SAP, 2012). According to (TC225-SAP, 2012), “both osmosis and solvation of the hydrophilic groups present will contribute to the water flow into the polymer”. In the same reference, it is stated that the presence of metals in the solution causes shielding of charges on the polymer chain, which results in limited swelling capacity. (Elliott, MacDonald, Nie, & Bowman, 2004) state that *pH and composition of the pore solution drive the equilibrium swelling of SAP* made of poly-acrylic acid. The same authors state that *salting out and reduction of the crosslinking density* may occur when high ionic strengths are reached.

On the other hand, additional external factors have shown effects on the absorption capacity, for example, the capacity of the polymer to absorb under load condition. The **Absorbency Under Load (AUL)** is a property of superabsorbent polymers that describes the material’s ability to absorb aqueous solutions while the hydrogel is subject to loading conditions. The higher the AUL, the better fluid acquisition developed by the hydrogel. This is due to a more porous gel mass during hydration and higher gel strength achieved because of higher degree of crosslinking (Herbert, 1994). During hydration of a cementitious system, the formation of hydration products associated to the strength gain may represent loading cycles that could potentially influence the absorption capacity of SAP. Similarly, while SAP particles swell, cement grains and fine aggregates

might be displaced by the polymer, which results in loading cycles that could affect the absorption kinetics of SAP (Luís Pedro Esteves, 2011a).

With respect to **desorption**, superabsorbent polymers desorb due to **self-desiccation** of the cement paste and osmotic pressure. For the former, capillary pressure is developed due to the process of emptying out of pores, and for the latter, differences in ionic concentration are detected between the absorbed pore solution and the pore solution still present in the cement paste (TC225-SAP, 2012). The same document reports that for cementitious systems with low w/c ratio, at 98% relative humidity (98% RH), most of the solution absorbed is released back to the cementitious system at very early ages (within the first days). This is due to self-desiccation of the system.

2.5 Superabsorbent Polymers in Cementitious Systems

Based on the state-of-the-art report prepared in 2010 by Bentz and Weiss (Dale P Bentz & Weiss, 2010), the objective of internal curing is to keep the capillary porosity of the cement paste saturated during the hydration process to reduce the autogenous stresses and strains. The presence of additional water will also improve the hydration of cementitious materials, which might represent higher strength development and lower permeability. Recently, superabsorbent polymers (SAP) have been actively studied as a material that can potentially provide internal water reservoirs for curing purposes of cementitious systems; then, self-desiccation and autogenous shrinkage may be mitigated by providing internal curing by means of superabsorbent polymers (J. Justs, Wyrzykowski, Bajare, & Lura, 2015). As the latter authors reported, in Ultra-High Performance Concrete (UHPC), SAP particles smaller than 63 microns in dry state can be used to cure internally the cementitious system while providing a significant reduction in autogenous shrinkage and only a slight reduction in compressive strength.

Previous research works have performed mixing process for internally cured systems in two steps. The first step corresponds to dry mixing of SAP and cement (J. Justs et al., 2015) (Janis Justs et al., 2014) (Miller et al., 2013). In the second step, dry powders are mixed with water following the corresponding standard, which may differ due to geography.

2.5.1 Hydration in Internally Cured Systems (ICS)

The application of SAP as an internal curing agent is focused on HPC and UHPC due to the low w/c used in these applications. As a result, complete hydration is seldom reached because of the lack of free water along with the deficiency in free pore space to be filled with new hydration products (Janis Justs et al., 2014). However, the inclusion of SAP also constitutes changes in chemistry, kinetics of hydration and type of hydrates that occur during cement hydration (Luis Pedro Esteves et al., 2014). In the latter study, in cement pastes with w/c=0.25 and high SAP content, up to 50% more Ca(OH)_2 was produced yet the same effect was not obtained for calcium silicate hydrate or C-S-H. Other effects such as retardation of the main peak in calorimetry and lower heat flow rate are obtained in ICS and attributed to the dilution of alkalis (Janis Justs et al., 2014).

(J. Justs et al., 2015) presented results for isothermal calorimetry of cement pastes with and without the addition of SAP (Figure 6). A delay of the main hydration peak was evidenced (w/c from 0.15 to 0.25, and different levels of SAP -up to 0.5% by mass of cement). The evidenced delayed hydration changes the time of set and strength development, which may affect the structure performance at early ages. The inclusion of SAP shortens the dormant period while the main peak occurs earlier, and the heat flow rate is lower. It was also concluded that the lower the w/c, the earlier the main peak occurs. However, after 3 days, further degree of hydration is reached due to desorption of SAP. In ICS, the porosity also increases; therefore, a drop in compressive strength and elastic modulus can be expected.

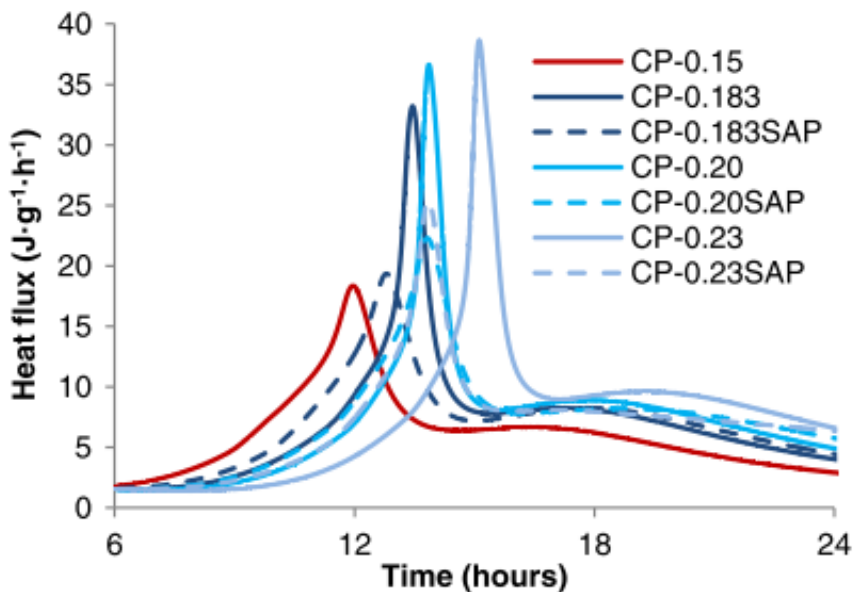


Figure 6 – Hydration heat flux of cement pastes at different w/c and 10% silica fume by mass of cement (J. Justs et al., 2015)

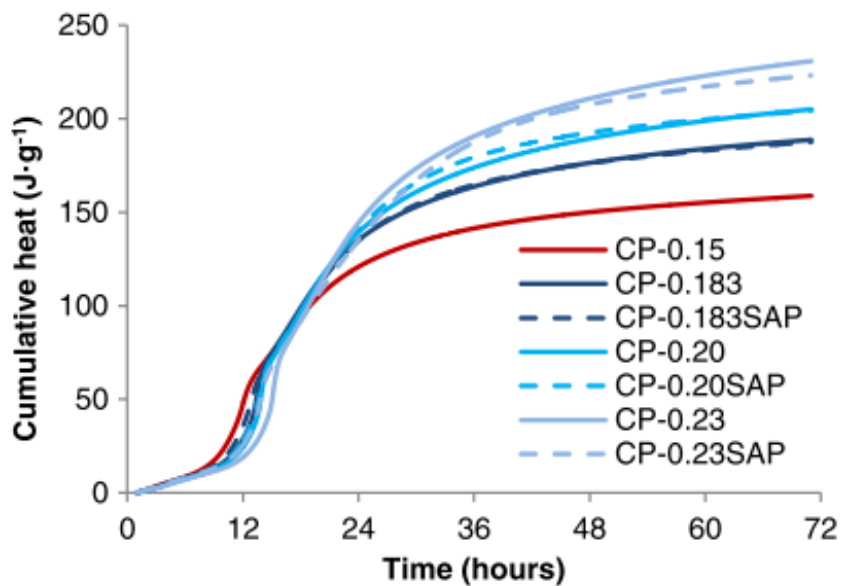


Figure 7 – Cumulative heat of hydration of cement pastes at different w/c and 10% silica fume by mass of cement (J. Justs et al., 2015)

(J. Justs et al., 2015) also presented in Figure 7 the behavior in terms of cumulative heat. As w/c increases, more cumulative heat is developed during cement hydration but most importantly, cement pastes in which SAP was added develop further hydration heat than that of the basic reference cement paste. According to (J. Justs et al., 2015), “the main hydration reaction of pastes with SAP starts earlier but then proceeds at a slightly slower rate than for the pastes without SAP”. After 3 days, similar values for cumulative heat of hydration is reached for pastes with the same total water content. In other research work, (Janis Justs et al., 2014) observed that cement pastes containing SAP develop larger cumulative heat of hydration than reference samples.

Another impact of SAP inclusion in cementitious systems is the inclusion of voids. Due to the nature of a cementitious hydrating system, polymer size changes the microstructure of the cementitious system, and thus, the transport mechanisms in the cementitious matrix. Both the effective water-to-cement ratio of the cementitious system and the porosity left behind after desorption takes place have a direct impact on mechanical and durability properties of the cementitious system. (Jensen, 2013) claims that the inclusion of hydrogels during mixing represents partial control over the liquid phase of the system due to the fashion by which the polymers can be tailored as to shape and size, which is presented by the author as an “engineered water phase distribution”. On the other hand, (Luis Pedro Esteves et al., 2014) reported that at water-to-cement ratio of 0.25, and 1% of SAP by mass of cement, the chemically bound water is not affected by the particle size distribution of the hydrogels. As a result, there are not significant

differences in the extent of hydration due to particles' size but it was proved that the finer the SAP, the more calcium hydroxide produced. In previous research work conducted by (J. Justs et al., 2015), Portlandite or calcium hydroxide was found to be formed inside the SAP particles.

The inclusion of SAP into the matrix of a cementitious material also presents benefits in terms of frost protection of concrete due to the gas-filled voids left behind when cement hydration progresses and the polymer shrinks due to the desorption mechanism. As it was presented previously, SAP not only contribute to control the water phase in concrete, they may also increase the freezing-thawing resistance by providing controlled entrained air content, along with the shape and size of the voids. In this matter, SAP are considered as "engineered air-entrainment of concrete" (Jensen, 2013).

2.5.2 Autogenous Shrinkage of Internally Cured Systems (ICS)

In addition to provide further cement hydration, internal curing is also conceived to maintain the internal relative humidity of the system, which results in lower autogenous shrinkage (Klemm & Sikora, 2012) (Wang, Zhou, Peng, Liu, & Hu, 2009) (Snoeck, Jensen, & De Belie, 2015). Figure 8 (Jensen, 2013) evidences reduction in autogenous strain developed by ultra-high-performance cementitious binders with w/c of 0.30 and SAP addition. This author investigated different mixes with variable SAP contents and 20% silica fume by mass of cement. The impact of SAP on autogenous shrinkage is driven by the amount of SAP added, showing the best results for cement pastes with SAP content

of 0.4% by mass of cement. In a research work conducted by (J. Justs et al., 2015), reduction in the stress buildup is achieved (See Figure 9). This reduction mitigates the potential for early-age cracking and increases the service life of concrete structures. The best results are achieved for the sample labeled UHPC-0.20SAP (SAP content is around 0.03% by mass of cement), in which the strain is reduced from around -550 to -50 microstrains at 7 days when compared to that of UHPC-0.20 (Reference). When SAP is added in a smaller amount, the contribution to reduce self-desiccation is only noticeable at early ages. Later, water intended for internal curing has been used up; therefore, the UHPC system continues self-desiccating.

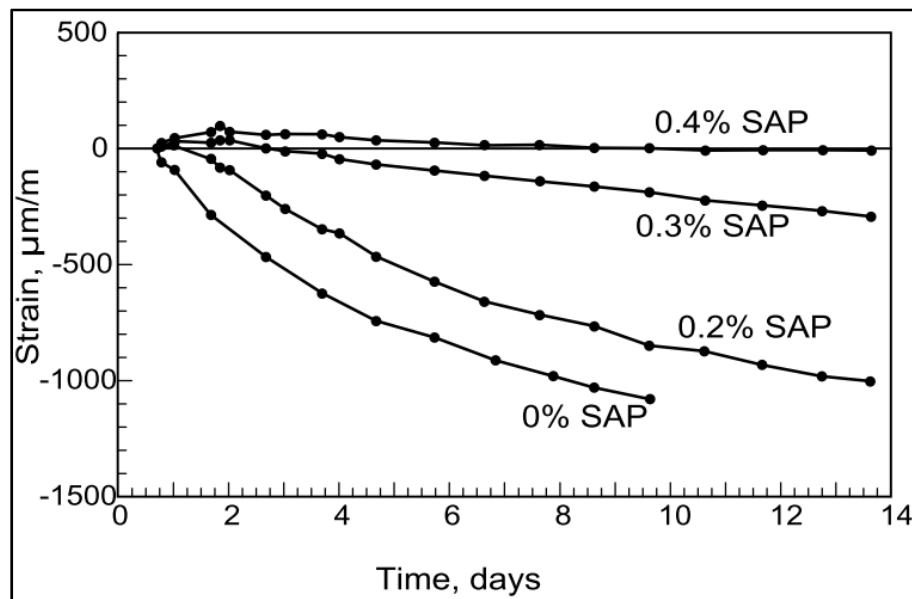


Figure 8 – Autogenous strain of an ultra-high-performance cementitious binder with a w/c of 0.30, 20% silica fume (by weight of cement) and different levels of SAP addition (by weight of cement) (Jensen, 2013).

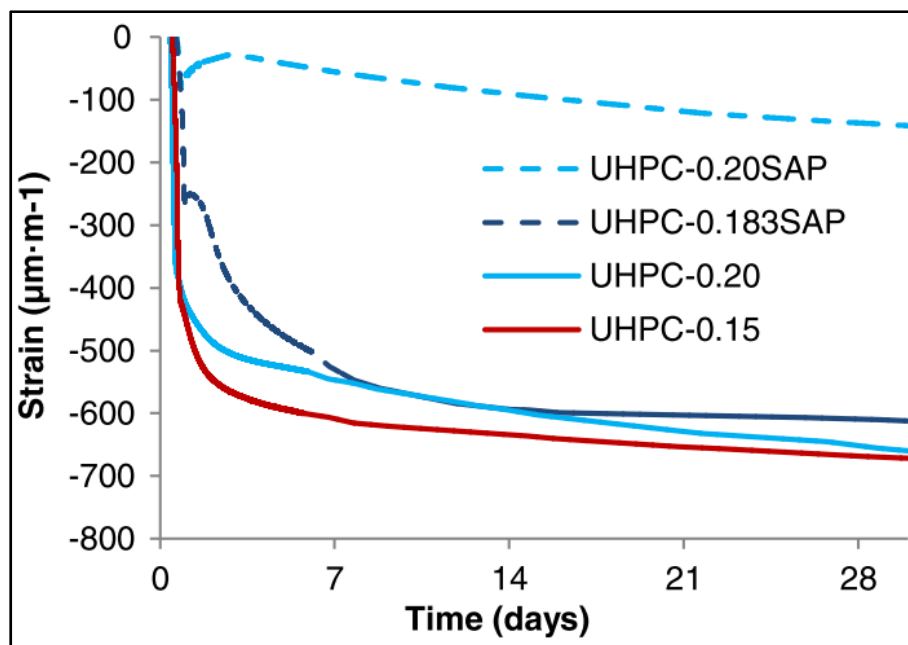


Figure 9 – Autogenous Shrinkage of UHPC at various w/c and SAP levels (J. Justs et al., 2015)

CHAPTER 3. MATERIALS CHARACTERIZATION

3.1 Introduction

The need to develop a better understanding of the variables influencing the effectiveness and consequences of superabsorbent polymer as an internal curing agent requires that properties and characteristics of the materials involved during the hydration and setting processes of a cementitious system are stated. Therefore, information provided by manufacturers along with data collected during characterization of the materials will be presented. For instance, the mill certificate of the cement and the MSDS of the polymer as well as the results of the chemical analysis of synthetic pore solution and image analysis of superabsorbent polymers.

It was observed that the contribution of superabsorbent polymers to improve the curing process of a cementitious system is truly based on the physical and chemical interaction between the polymer and the pore solution. Therefore, it is hypothesized that the success of this technology in the cement industry is driven by both the cement chemistry and properties of the superabsorbent polymers.

3.2 Materials

In this research, two different materials were studied, cement and superabsorbent polymers (SAP). The former included the study of three commercially available Type I ordinary Portland cements labeled by the manufacturers as Cem1, Cem2 and Cem3. All of them differ in chemical composition and specifically in alkalinity, which varies from 0.37% to 0.72%. On the other hand, commercially available superabsorbent polymer (SAP) supplied by BASF was the internal curing agent investigated.

3.2.1 Cement

Since the presence of alkalis in cement has several impacts on the cement hydration process and most importantly, the absorption capacity of the polymers studied, three different cement samples that differ in alkalinity were analyzed. Table 2 provides a summary of the oxide composition of the cement along with physical characteristics of the cements used in this study. The mill certificates provided by manufacturers of the three cements used in the study, Cem1, Cem2 and Cem3, supply the information needed for chemical composition of the cement samples, which will be commented in the upcoming paragraphs.

The first important variable to point out in the mill certificate is the tricalcium silicate (C_3S) content. It is important to highlight that Cem2 has the highest C_3S content, followed by Cem3 and Cem1, respectively. Alternatively, Cem1 presents the highest C_2S content, followed by Cem3 and Cem2. Figure 10 plots the results for compressive

strength presented in the mill certificates. When comparing all the values presented in the mill certificates, it is noted that even though Cem1 developed lower compressive strength at early ages, 1 and 3 days, its compressive strength at 28 days is higher than the other two cements.

Table 2 - Mill certificates for Cem1, Cem2 and Cem3

Mill certification	Cem1	Cem2	Cem3
Cement type	Type I/II (MH)	Type I/II	Type I
SiO ₂	19.6%	20.0%	20.04%
Al ₂ O ₃	4.8%	4.88%	4.85%
Fe ₂ O ₃	3.1%	3.44%	3.35%
CaO	63.0%	63.5%	63.5%
MgO	3.1%	2.47%	1.99%
SO ₃	3.1%	2.65%	3.26%
LOI	2.5%	2.02%	1.34%
CO ₂ in Cement	1.6%	1.08%	0.92%
Limestone	3.6%	3.1%	2.14%
CaCO ₃ in Limestone	98.0%	92.61%	99.5%
C ₃ S	54.0%	59.3%	58.2%
C ₂ S	15.0%	12.2%	12.3%
C ₃ A	7.0%	6.9%	7.0%
C ₄ AF	9.0%	10.1%	10.0%
C ₃ S+4.75C ₃ A	89.0%	92.0%	91.6%
Na ₂ O Equivalent	0.37%	0.62%	0.72%
Blaine (m ² /kg)	388	393.6	377
#325 Sieve passing	97.8%	99.1%	94.4%
Autoclave Expansion	0.07%	0.09%	0.03%
Initial Time of set Vicat (Min)	98	105	102
Air content	6.0%	8.4%	8.2%
f _c 1-day (MPa)	14.5	15.0	17.6
f _c 3-day (MPa)	24.7	25.4	26.5
f _c 7-day (MPa)	32.1	32.1	31.5
f _c 28-day (MPa)	43.9	42.8	34.8

With respect to setting time, it is stated that it may be attributed to the reaction between C_3A and Gypsum (Mindess & Young, 1981). According to Odler (2003), “the setting of Portland cement is due to a recrystallization of primary microcrystalline ettringite into well-developed crystals” (Odler, 2003) (p.272). Therefore, it is crucial to highlight that the C_3A content is the same for Cem1 and Cem3 and slightly lower for Cem2. The sulfur trioxide (SO_3) content is higher for Cem3 and Cem1 than that of Cem2. In Chapter 5, setting time studies conducted are compared with the values reported as the initial time of set in the mill certificates. In the information provided by the manufacturers, Cem1 has the shortest initial setting time of 98 min whereas Cem3 reaches its initial time of set at 102 min. Cem2; however, has the longest initial setting time reported of 105 min.

In cement hydration, the rate of hydration has also been related to fineness of the cement, which is represented by the Blaine parameter. The finer the cement, the higher the hydration rate and heat evolution (Mindess & Young, 1981). In this research; consequently, different hydration rates due to fineness along with phase composition of the cements studied were expected. Cem2 has the largest Blaine value, which may be understood as having the finest particles, followed by Cem1 and Cem3, respectively. It has also been stated that higher concentration of alkalis is achieved when water-to-cement ratio is reduced that leads to higher pH values, which is known for accelerating cement hydration (Janis Justs et al., 2014).

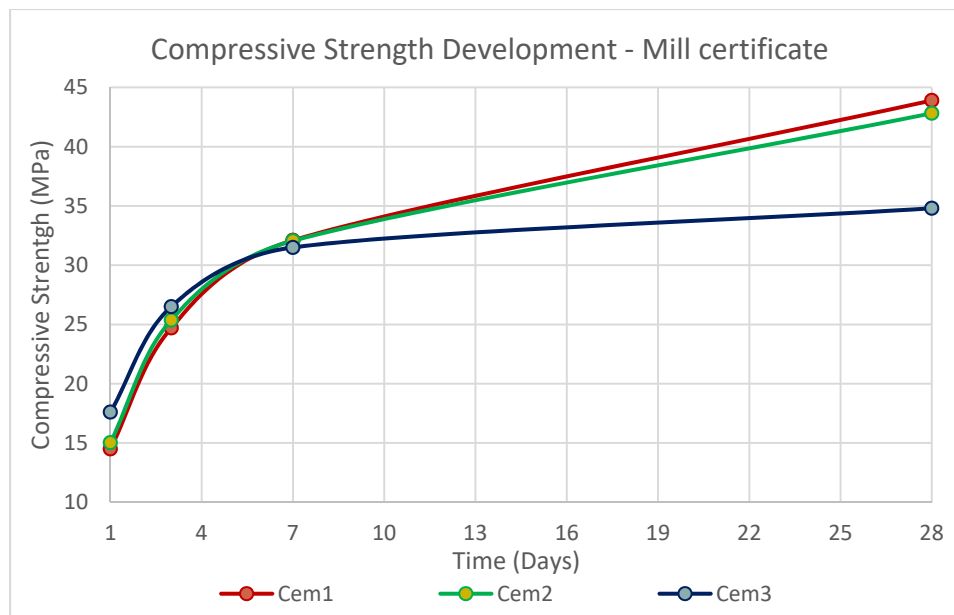


Figure 10 – Compressive Strength development of cement paste presented in mill certificate ASTM C-109 for all the cements studied.

In Ordinary Portland Cement (OPC), alkalis come from raw materials such as clay and impurities contained in the air circulated throughout the closed-circuit kiln-preheaters. The alkalis content is listed in the mill certificate as potassium oxide (K_2O) and sodium oxide (Na_2O), which can also be presented as sodium equivalent (Na_2O_{eq}) and calculated as $0.658 * (\%K_2O) + \%Na_2O$ (Jackson, 2003). During hydration of Ordinary Portland Cement (OPC), rapid dissolution of alkali ions occurs. A considerable amount of alkali ions is released into the liquid phase of the hydrated cementitious system, often called pore solution. The ionic composition of the solution drives the equilibrium between cations and anions in the system. Therefore, it may be expected that at later ages (after 10 days of hydration), the cement paste with higher concentration of alkali ions and more calcium hydroxide, as a product of the hydration reaction of calcium silicates, will reach

higher pH values (Diamond, 1981) (Moreno, 2006). Cem3, which has the highest sodium equivalent value ($\text{Na}_2\text{O}_{\text{eq}} = 0.72\%$), should have higher concentration of alkalis per liter of solution, followed by Cem2 and Cem1, respectively.

3.2.2 Superabsorbent Polymer (SAP)

A commercially available sample of superabsorbent polymer (SAP) was provided by BASF. The sample, labeled as Masterlife IC 400, is a polymer derived from acrylic acid. The material was supplied in the form of white, irregularly shaped granules as shown in Figure 11. These granules were investigated using optical microscopy to quantify their shape, aspect ratio and particle size distribution. Figure 12 shows a general appearance of a random assemblage of SAP particles as viewed under the optical microscope. As seen in the picture, the dimensions of majority of the larger particles are in the range from 300 to 700 micrometers.

For the purposes of this study, the samples of SAP were divided into two categories: "A" and "B". The SAP A category included "as-supplied" commercial polymer provided by BASF whereas SAP B was obtained by milling SAP A. As such, SAP B has a finer particle size distribution (PSD) compared to SAP A. The milling process utilized for size reduction of polymer A is described in 3.3.2.1 *Cryomilling of SAP*. Since the polymer was only treated to reduce its size, it is expected that none of its properties, other than size, will be modified.

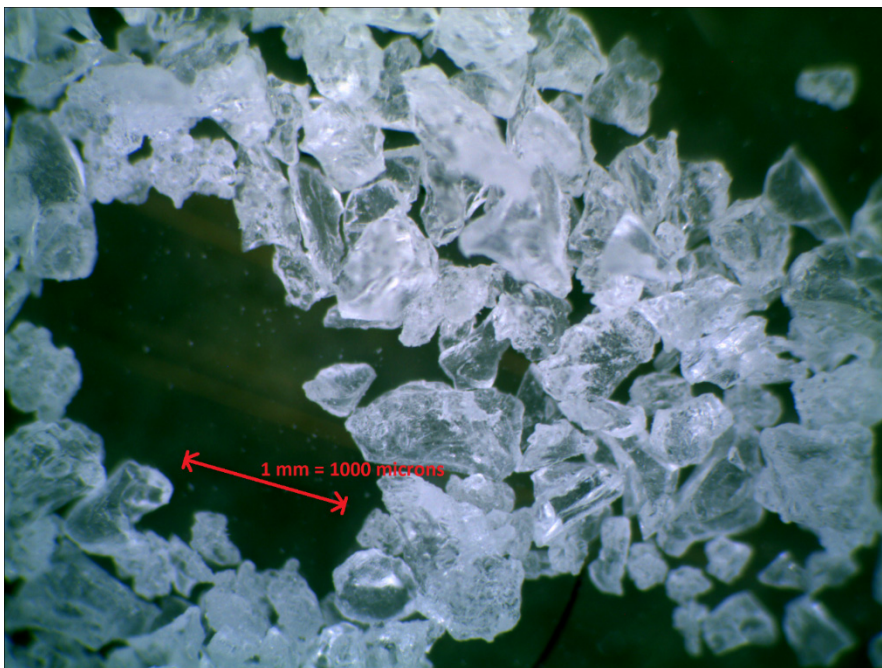


Figure 11 - Optical microscope of SAP (Masterlife IC-400)

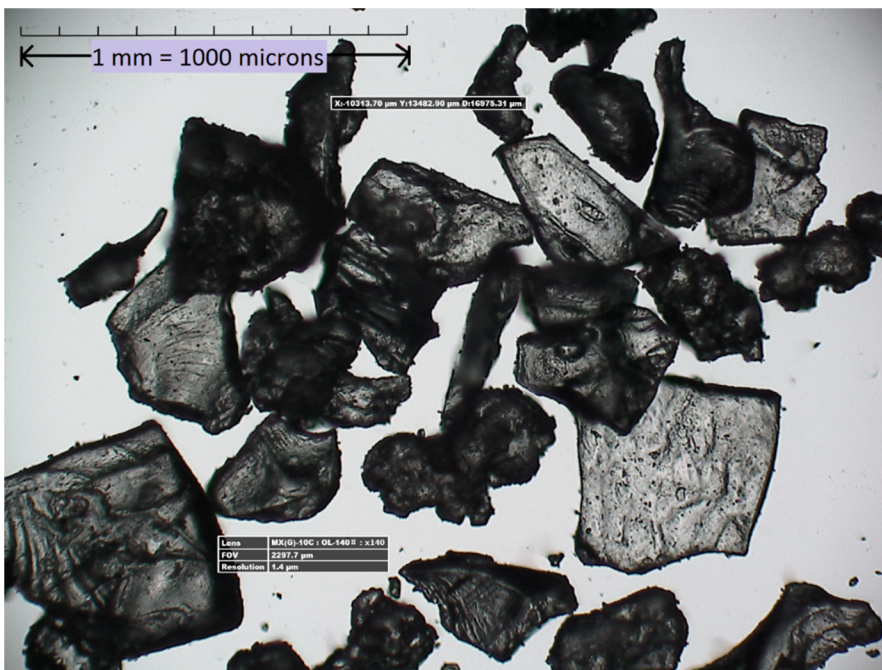


Figure 12 - SAP A – Optical image taken from optical microscopy analysis done for superabsorbent polymer provided by BASF - Masterlife IC 400 - (Magnification 140x)

3.3 Experimental methods

The upcoming sections present the experimental methods used for the study of the factors and variables that influence the interaction between SAP and the cementitious system for the development of internal curing mechanism. The study of the chemical composition of pore solution at early ages (At 5 minutes after hydration) and findings obtained about the shape and particle size of SAP by means of image analysis are reported.

3.3.1 Cement Paste

Cement pastes at water-to-cement ratio of 0.30 and 0.35 were prepared for Cem1, Cem2 and Cem3 to study the chemical composition of their pore solution at the interval of time between 5 minutes and 20 minutes after hydration. For some mixes, pore solution extraction was also conducted at the interval of time between 120 and 140 minutes as an alternative source of information about the variation of the pore solution composition over time.

3.3.1.1 Cement Paste Preparation

As recently mentioned, cement pastes were designed at water-to-cement ratios of 0.30 and 0.35 and prepared following ASTM C305-14 – “Standard Practice for Mechanical Mixing of Hydraulic Cement Pastes and Mortars of Plastic Consistency” (see Figure 13). Table 3 shows the mix designs used to produce the reference (i.e. prepared without

superabsorbent polymers) paste mixtures to assess the chemical composition of pore solution at early ages (5 and 120 minutes after cement hydration started). In all mixes prepared in this research, deionized water was used as the mixing water. All cement paste batches were prepared keeping the same room conditions, temperature of 23°C and 50+/- 1% relative humidity (50% RH).

Table 3 - Mix Designs for reference cement pastes

Mix Design	w/c	Cement (kg/m ³)	Water (kg/m ³)
Reference cement paste #1	0.3	1618	485
Reference cement paste #2	0.35	1498	524



Figure 13 - Mixing of cement paste using a Hobart mixer following ASTM C305-14

3.3.1.2 Pore solution extraction

The preparation of the cement paste for the pore solution extraction starts immediately after mixing when fresh cement paste is placed in tightly sealed plastic containers to avoid carbonation. Subsequently, at ages of 5 and 120 minutes after mixing, the liquid phase (pore solution) of the cement paste is extracted by means of Millipore™ pressure filtering system and it stored in sealed glass vials. The pressure filtering system uses nitrogen gas to provide high pressure, not higher than 40 psi must be applied, and squeezes out the fresh cement paste until the pore solution is obtained. The Millipore™ filtering system setup also includes an 8-microns filter membrane to filter out the solution and avoid the contamination of the solution extracted with solids coming from the cement paste.

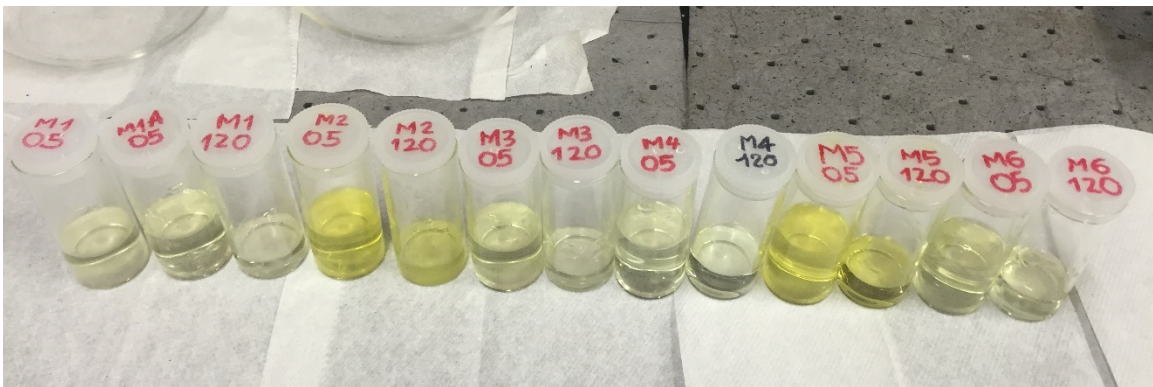


Figure 14 - Vials containing different extracted pore solutions at w/c of 0.30 and 0.35

Figure 14 shows vials with different pore solutions extracted from pastes with, respectively, w/c of 0.30 (labeled M1 through M3) and 0.35 (labeled M4 through M6). It

can be noted differences in the color of extracted pore solutions, which may be attributed to the nature of the iron oxide used and the oxidation of the ferrite phase during cement manufacturing, which has been stated to drive the Portland cement clinker color (Ichikawa, M.; Komukai, 1993) (Macphee & Lachowski, 2003). The solution extracted from Cem1 is the clearest of all, which might be related to the ferric oxide (Fe_2O_3) content it has. Contrary to this, the other two solutions obtained from Cem2 and Cem3 pastes have darker colors, which might be related to the higher Fe_2O_3 and C_4AF content than that of Cem1. Figure 15 represents the setup of the filtering system is shown on the left-hand side of the figure and an ongoing extraction of pore solution on the right-hand side.



Figure 15 - Pore solution extraction from fresh cement paste by means of Millipore™ pressure filtering system.

3.3.1.3 Pore solution characterization

In concrete pore solution, both anions and cations are studied for several purposes; for instance, to investigate the durability of concrete since it does depend on the alkalinity of the concrete pore solution. It is generally accepted that the most common ions in concrete pore solutions are the hydroxyl (OH^-), sulfate (SO_4^{2-}) and chloride (Cl^-) ions, which are the anions and potassium (K^+), sodium (Na^+) and calcium (Ca^{2+}) ions as the cations. In this section, the techniques used for the study of the ions contained in pore solution is presented. On the other hand, to evaluate the efficiency of SAP in low water-to-cement ratio system and to contribute to previous studies (Miller, 2014) developed at Purdue University, a constant water-to-cement ratio of 0.30 was set for all the mixes. However, the dilution effect of water was proven when a reference cement paste of 0.35 was tested only for chemical composition of its pore solution.

The elemental analysis of the pore solution composition was developed using different techniques. Titration and pH-meter were used to determine the concentration of OH ions and pH of the pore solution. In addition, the concentration of sulfate and chloride ions was determined by means of ion chromatography. With respect to the cations, Atomic Absorption (AA) was used to determine sodium, potassium and calcium concentrations, which were confirmed by means of inductively coupled plasma optical emission spectrometry (ICP-OES).

3.3.1.3.1 Methods for Determination of Anion Concentration [OH^- , SO_4^{2-} , Cl^-]

3.3.1.3.1.1 Determination of hydroxyl ions by titration

Titration involves a titrant, a solution with known concentration, and an analyte, a solution with unknown concentration. In this study, the titrant used was hydrochloric acid (HCl) with a concentration of 0.1N. The analyte was the extracted pore solution, to which three replicates were tested pursuing a more accurate result. For the solution preparation, one hundred microliters of pore solution were mixed with deionized water until reaching a solution volume of 20ml. Phenolphthalein was used as the indicator in the solution. The titrant was added to the solution until the endpoint was reached, represented by the solution's change in color from pink to colorless. The amount of hydrochloric acid added was used to calculate the concentration of OH^- ions and the pH of the pore solution.

3.3.1.3.1.2 Measurement of the pH using a Cole-Parmer pH-meter electrode

A Cole-Parmer pH meter electrode was used to quickly determine the pH of a solution. The pH determines the relative amount of free hydrogen and hydroxyl ions in the solution. A solution with larger hydrogen ions (H^+) represents an acidic solution. In contrast, when more free hydroxyl (OH^-) ions are present, the solution is referred to as a basic solution.

To ensure the accuracy of the measurements, the electrode was always calibrated before the measurements using buffer solutions, ranging in pH from 1.00 to 12.00. Then, the pH of the solutions was measured and an average of three measurements was reported. In Figure 16, the calibration of the pH-meter using the buffer solutions is underway. For the pH measurement of the solutions, the setup is the same. In the figure, the other buffer solutions used for calibration are in the lower part whereas all the pore solutions tested are located next to the equipment.

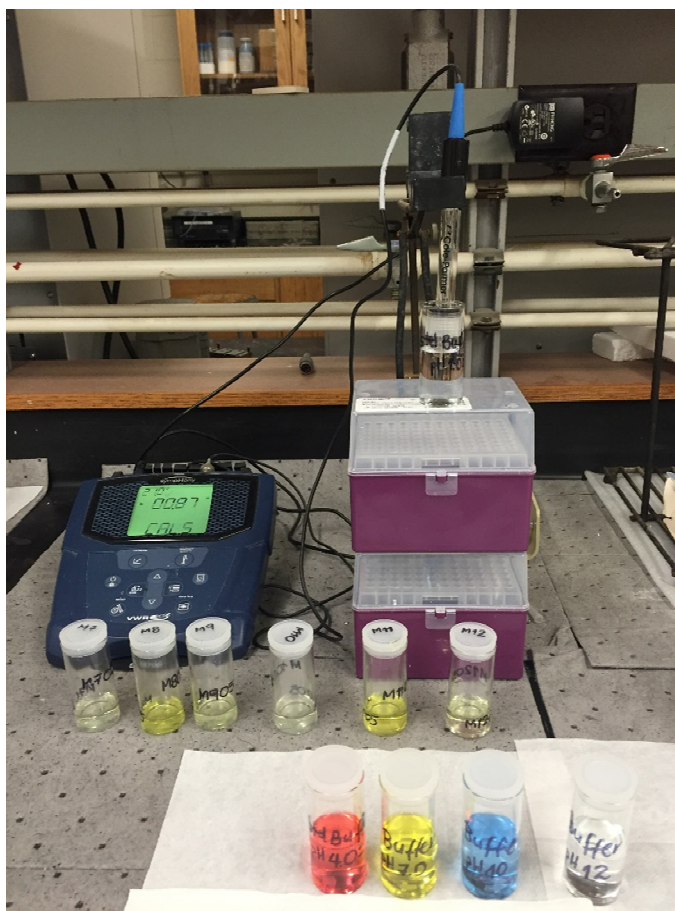


Figure 16 - Setup for pH measurement of the pore solution by means of Cole-Parmer pH-meter electrode. The figure also depicts the ongoing calibration of the electrode

3.3.1.3.1.3 Determination of the concentration of chlorides and sulfates by integrated single channel ion chromatography system (ICS-900)

The DIONEX ICS-900 is an integrated single-channel ion chromatography system that uses a hydrocarbonate solution as the eluent or carrier of ions in order to determine the concentration of sulfates and chlorides, which along with hydroxyl ions are the most predominant anions present in concrete pore solution. The sample was diluted 200 times by dissolving 0.5ml of pore solution with deionized water to a final volume of 100ml. Figure 17 depicts sample preparation and the equipment used, DIONEX ICS-900 integrated single channel ion chromatography system.

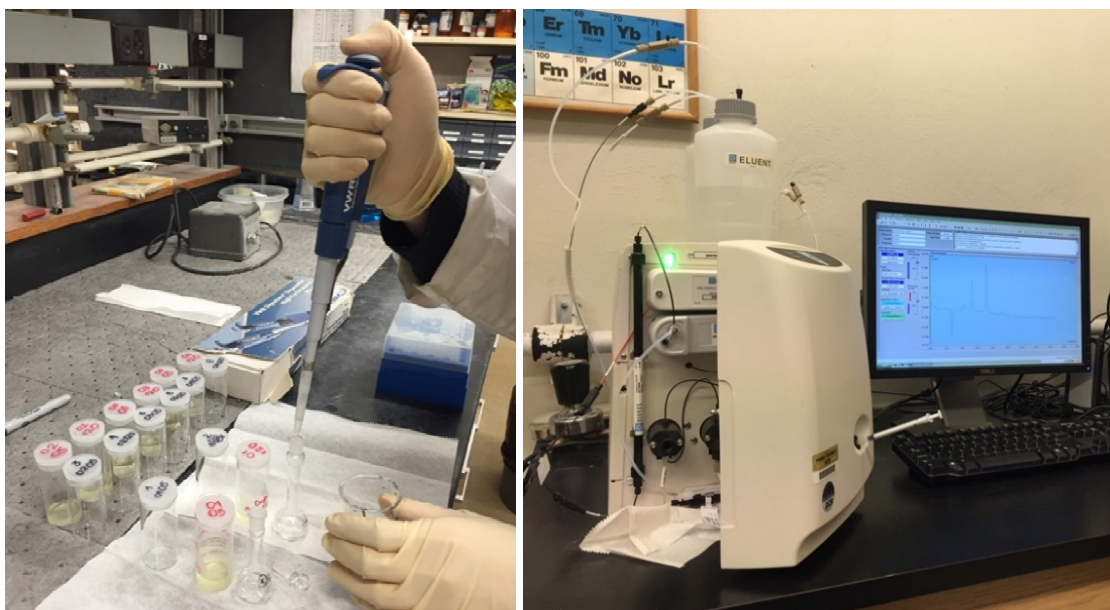


Figure 17 - On the left-hand side, samples are being prepared for ICS. On the right-hand side, DIONEX ICS-900 is running.

3.3.1.3.2 Methods for Determination of Cation Concentration [Na^+ , K^+ , Ca^{2+}]

Sodium (Na^+), potassium (K^+), and calcium (Ca^{2+}) are considered the most abundant cations in concrete pore solution. Their concentration in the extracted pore solution was determined using both Atomic Absorption spectroscopy (AA) and inductively coupled plasma spectrometry (ICP). Both techniques, which will be explained below, were used to validate the accuracy of the results.

3.3.1.3.2.1 Atomic Absorption Spectroscopy (AA) - VARIAN SpectrAA 10/20

Proper use of the atomic absorption spectrometer requires the usage of a specific lamp for the quantification of each metal. Air-acetylene flame was used as the atomizer to determine potassium (K^+) and sodium (Na^+) content. On the other hand, nitrous oxide-acetylene flame was used to measure the calcium (Ca^{2+}) concentration. The flames are used to atomize the sample; therefore, the amount of energy detected may be related to the quantity of a certain metal present in the solution.

Table 4 - Sample preparation for Atomic Absorption spectroscopy (AA)

SAMPLE PREPARATION FOR AA	ION TO MEASURE		
	K^+	Na^+	Ca^{2+}
Volume of vial	25 mL	25 mL	25 mL
Pore solution	0.5 mL	0.5 mL	125 μL
Suppressor to avoid ionization	Cesium _{10.000ppm} = 2.5 mL	Potassium _{10.000ppm} = 5 mL	Potassium _{10.000ppm} = 5 mL
Deionized water	Up to complete 25 mL	Up to complete 25 mL	Up to complete 25 mL

Table 4 specifies amounts needed for sample preparation for each of the ions studied whereas Figure 10 depicts the measurement of the concentration of cations in pore solution by means of atomic absorption, VARIAN SpectrAA 10/20.



Figure 18 - Sample tested for determination of cations using VARIAN SpectrAA 10/20

3.3.1.3.2.2 ICP-Optima 8300 Parkin-elmer optical emission spectrometer - Inductively coupled plasma (ICP)

To verify the concentration of cations found using Atomic Absorption (AA), an ICP-Optima 8300 PerkinElmer Optical Emission Spectrometer was also used to determine the alkali metal content in the sample, such as potassium (K^+), sodium (Na^+) and calcium (Ca^{2+}).

Samples were prepared by diluting pore solution 200 times. To do so, 0.5 mL of pore solution were mixed with 5 mL of 5% nitric acid (5% HNO_3), and diluted with deionized water until reaching a volume of 100 mL. The equipment was calibrated using calibration solutions prepared with Nano pure water mixed with 5% nitric acid (5% HNO_3). Figure 19 depicts a set of sample solutions prepared for the determination of alkali metals concentration in extracted pore solution.

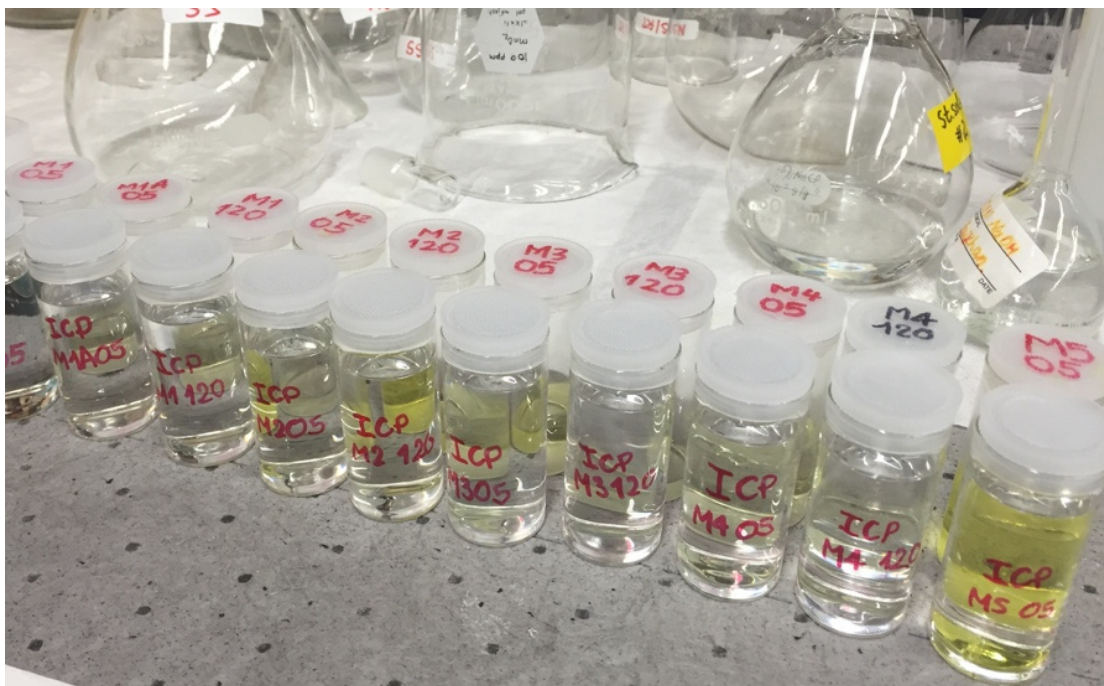


Figure 19 - Samples solutions prepared for inductively coupled plasma spectrometry (ICP)

3.3.2 Superabsorbent Polymers (SAP)

The following two sections will present the techniques used for the size reduction and analysis of particle size distribution of the polymer.

3.3.2.1 Cryomilling of Superabsorbent Polymers (SAP)

The SAP used in this study was separated into two categories based on particle size. The polymer with larger particle size was labeled "SAP A" while the polymer with a finer particle size was named "SAP B". The latter was obtained after milling the polymer SAP A using a 6850 Cryomilling Freezer/Mill, shown in Figure 20. Liquid nitrogen (LN₂) is used in the Cryomilling chamber to cause rapid freezing of the sample's environment. The low temperature in the chamber makes the SAP more brittle, which helps break down the polymer particles while avoiding melting of the polymer.

Twenty-five grams (25 g) of SAP were milled per batch in a three-step process: precooling, milling and cooling. For each run, the chamber was precooled for 10 minutes prior to milling. After that, 9 milling cycles were run, each lasting 1 minute, with a 1-minute cooling cycle between them. Both SAP samples, A and B, were stored in a desiccator at 0% relative humidity, which guarantees the polymer will not have access to any source of moisture in the environment. Figure 21 shows sample extraction after milling.



Figure 20 - 6850 Cryomilling Freezer/Mill



Figure 21 - Extraction of SAP sample after milling process

3.3.2.2 Image analysis for determination of Particle Size Distribution of Superabsorbent Polymers (SAP)

An optical microscope and an OptixCam OCVView software were used to perform image analysis of the polymers' shape and size. Additionally, the tendency of the polymer to absorb moisture from the environment was evaluated. Random samples from SAP A and B were taken to determine their morphology. Samples were placed onto a microscope glass slide and examined under the microscope. Pictures were taken at different magnifications to allow the discernment of particles of all sizes. Once collected, the images were edited using Adobe Photoshop and processed using two different software, Image J and AutoCAD, to quantify and identify particle size and shape. The resulting data was processed using SAS, an advanced statistical analysis software.

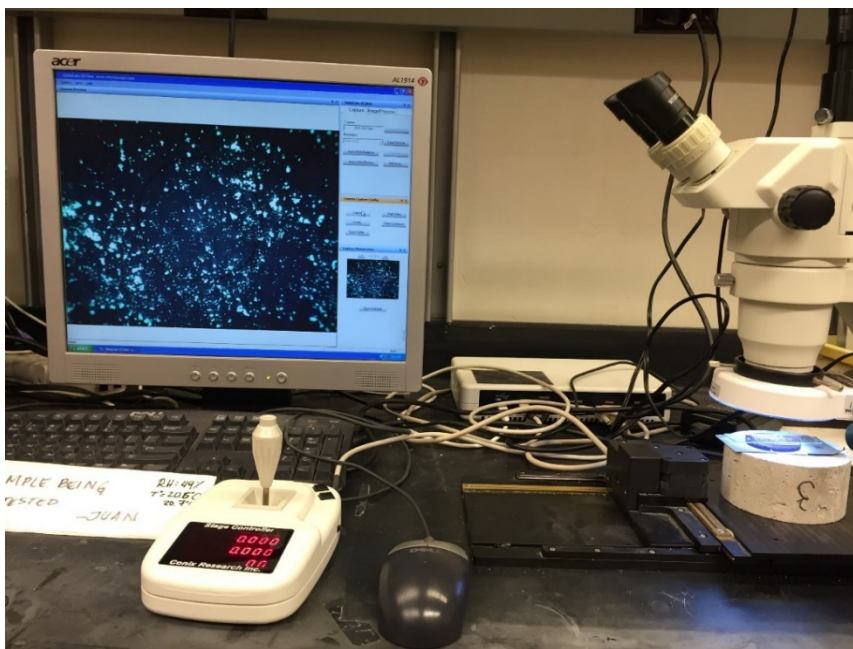


Figure 22 - Image Analysis of SAP by means of Optical Microscopy

In Figure 22, a setup for image analysis is presented. On the right-hand side of the figure, the microscope assembly is shown with the resulting image for a sample SAP B projected on the monitor. In some cases, an external source of light was used to video record the swelling behavior of the polymer while interacting with synthetic pore solution.

3.4 Experimental Results

The following sections summarize the results obtained for the chemical characterization of extracted pore solution and the image analysis of SAP. The chemical composition of pore solution is vital for the preparation of synthetic pore solution. Therefore, it is an important input for the experimental work developed in Chapter 4. On the other hand, determination of the physical properties of the polymers defined the range of sizes the cementitious systems will be dealing with, which will be further explained in Chapter 5.

3.4.1 Chemical composition of Pore solution

As stated previously, Pore Solution Characterization, different analytical techniques, including titration, atomic absorption (AA), inductively coupled plasma optical emission spectrometry (ICP-OES) and ion chromatography (IC) were used to determine the ionic (elemental) composition of the extracted pore solutions. In addition, the alkalinity of these solutions was determined using the pH-meter. The information obtained through these techniques was used to select the type and quantity of chemicals needed to reproduce synthetically the extracted pore solution of a cement paste with water-to-

cement ratio of 0.30; work that will be presented in Chapter 4. The solutions reproduced were also used in Chapter 4 to evaluate the absorption capacity of SAP.

Table 5 compiles the results of chemical analysis of the pore solution extracted after 5 minutes of hydration from pastes with w/c of 0.30 and 0.35 prepared with various cements. The concentrations of selected ions (Na^+ , K^+ , Ca^{2+} , Cl^- , SO_4^{2-} and OH^-) present in the pore solution of paste with w/c=0.30 are shown in Figure 23. At this early age, the composition of the pore solution is dominated by cations (i.e. potassium ions (K^+) and sodium (Na^+) ions). Furthermore, in all cases, the concentration of potassium ions was greater than that of the sodium ions. This is not unexpected as Portland cements typically contain higher amounts of potassium (compared to sodium) (Macphee & Lachowski, 2003) as evident from the chemical analysis of Cem2 shown in Table 2.

Table 5 - Ionic concentration of pore solution extracted from fresh cement pastes (w/c of 0.30 and 0.35) after 5 minutes of hydration

Cement	w/c	Na^+ (mmol/L)	K^+ (mmol/L)	Ca^{2+} (mmol/L)	SO_4^{2-} (mmol/L)	Cl^- (mmol/L)	OH^- Titration (mmol/L)	Calculated pH
Cem1	0.30	47	217	15	108	5	94	12.98
	0.35	43	198	19	85	5	77	12.89
Cem2	0.30	75	341	16	161	12	103	13.01
	0.35	63	291	18	137	10	92	12.96
Cem3	0.30	221	330	19	217	19	80	12.90
	0.35	198	305	18	207	17	89	12.95

In addition, data presented in Table 5 indicates that, as expected, the increase in the w/c value will lead to reduction in the concentration of Na^+ , K^+ and SO_4^{2-} ions due to the dilution effect. However, the concentration of calcium was not significantly affected by the change in the w/c values since it depends on the solubility of other phases present in the pore solution (Vollpracht, Lothenbach, Snellings, & Haufe, 2016).

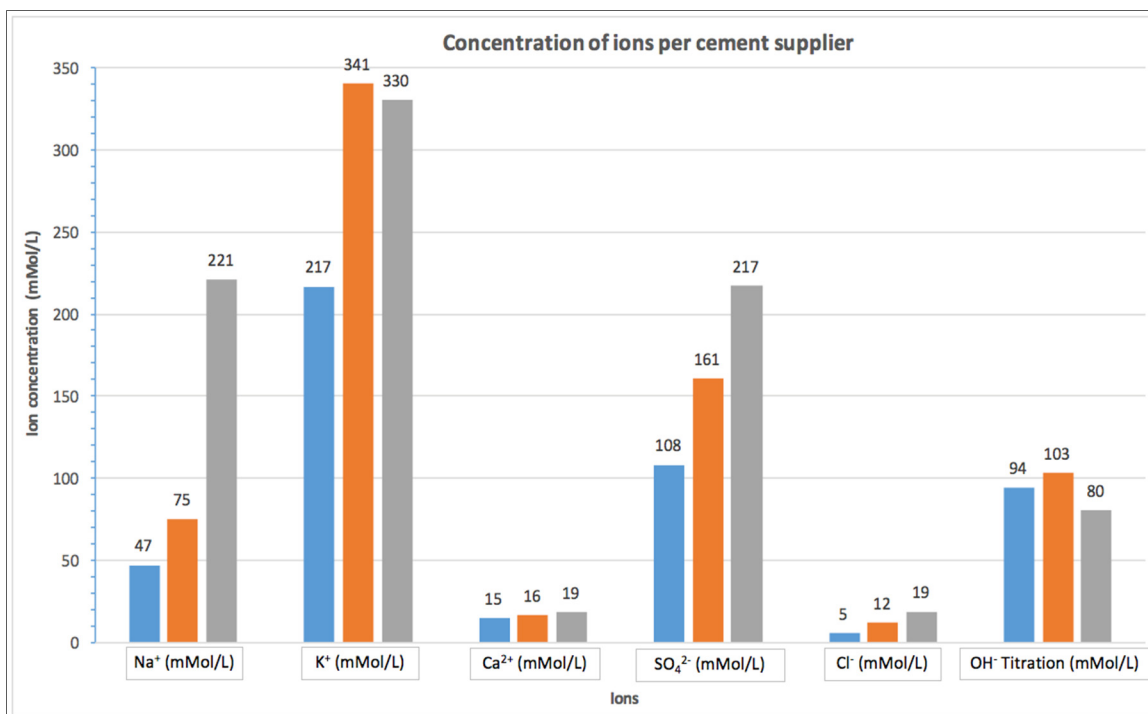


Figure 23 - Concentration of ions in pore solutions of pastes prepared with different cements at w/c of 0.30.

With respect to anions, the composition of the pore solution at this early age is dominated by sulfates (SO_4^{2-}). As the hydration process progresses, sulfates are consumed by reactions with aluminates, which leads to their depletion. To preserve the

electro-neutrality of the pore solution the concentration of the OH^- increases with time (Kurdowski, 2014). For instance, Figure 24 presents a plot presented by Kurdowski, in which for a water-to-cement ratio of 0.65, the sulfate depletion and the increasing concentration of hydroxyl ions are evidenced. It can also be noted that there is a slight increase in ionic concentration of sodium after 4 hours. For potassium; however, since its concentration is almost doubled after 180 days, the rate at which the concentration increases is more noticeable than that of sodium.

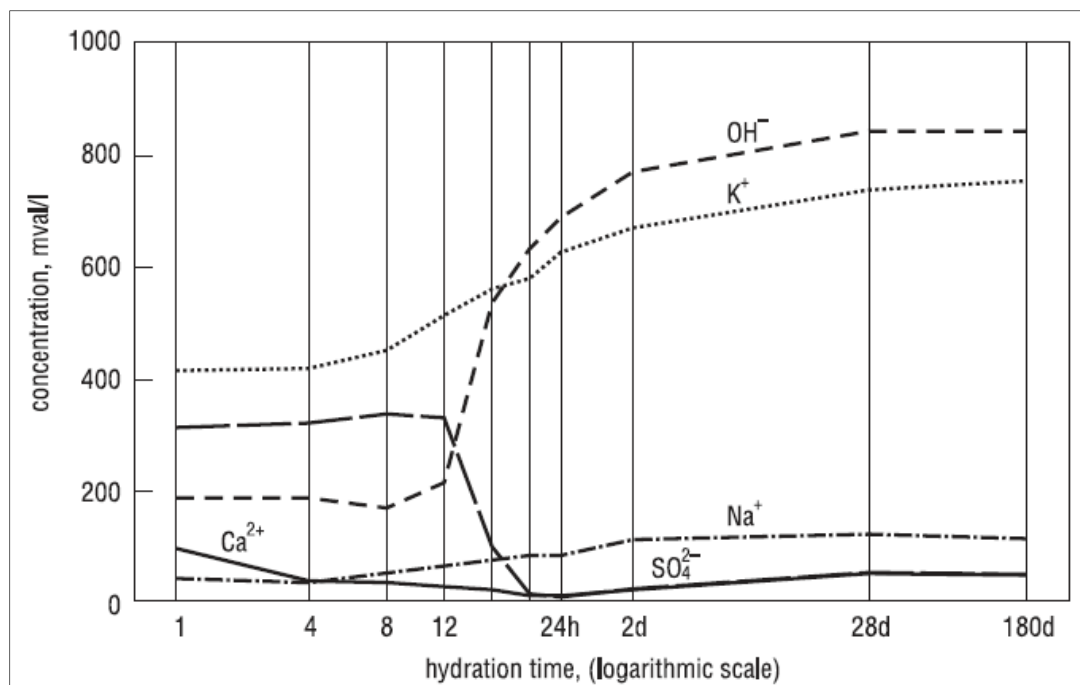


Figure 24 - Pore solution composition in cement paste at $w/c = 0.65$ (Kurdowski, 2014)

The general trends in the data obtained during this research are also well aligned with the previously reported variations in concentration of ions present in concrete pore

solution over time shown in Figure 24 and Figure 25, (Kurdowski, 2014) and (Vollpracht et al., 2016), respectively. As seen in both figures, there is a sudden reduction in the concentration of sulfates between 8 and 24 hours (due to the formation of ettringite). Both figures show that the reduction in sulfate concentration is accompanied by an increase in the concentration of potassium and hydroxyl ions.

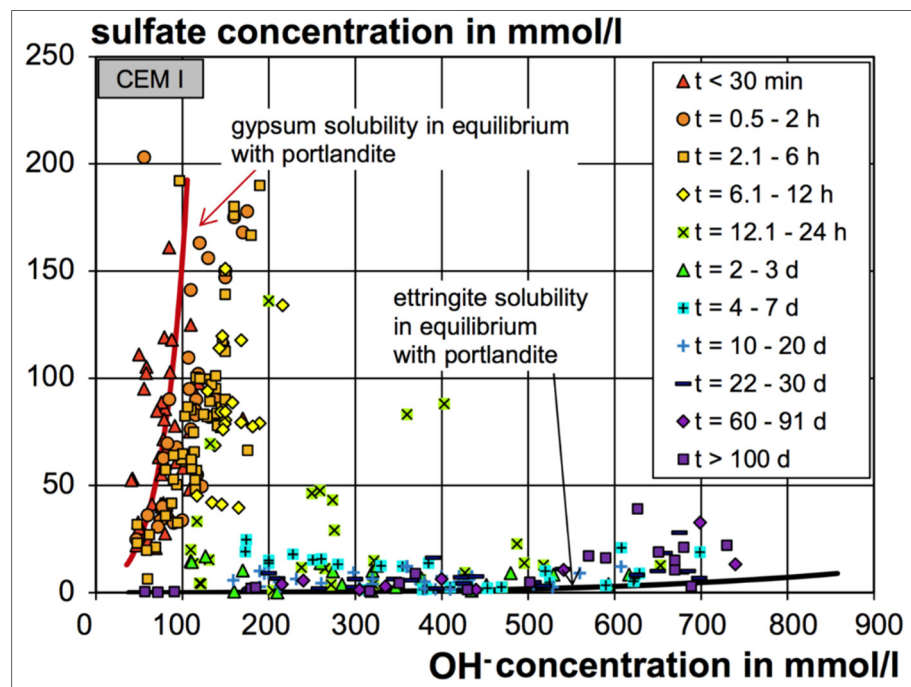


Figure 25 - Sulfate concentrations as a function of the OH⁻ concentration at early hydration time (presence of gypsum and Portlandite) and later hydration times (presence of ettringite and Portlandite) (Vollpracht et al., 2016)

3.4.2 Image analysis of Superabsorbent polymers

ASTM F1877-05 – “Standard Practice for Characterization of Particles” was used to define the morphology of the polymers. Figure 26 and Figure 27 show polymer samples A and B, respectively. It is apparent that the particle size of polymer sample A is much larger than that of polymer sample B. Therefore, polymer shape can also be seen more easily for SAP A than SAP B. Irregularly-shaped particles can be observed for both categories. It is also visible in the figures that SAP B is represented by a more uniform size distribution whereas SAP A has a considerable gap in size between particles. Both polymers can easily be identified due to their apparent difference in size while an important similarity is that their color is white.

It was common for both categories that particles clump. To avoid this in the hydrating cementitious system and provide a better distribution of the internal curing agent throughout the volume of the system, the method of mixing the polymer and cement as dry powders was developed using a FlackTek speed mixer.

Image analysis was also useful for understanding whether there is variation in polymer size (swelling) when exposed to room temperature of 21°C and relative humidity of 50%, which were the conditions for handling the material in the laboratory. In Figure 28 and Figure 29, no evidence of swelling was registered. Therefore, it was proven that handling the material under these conditions did not have any effect on polymer properties.

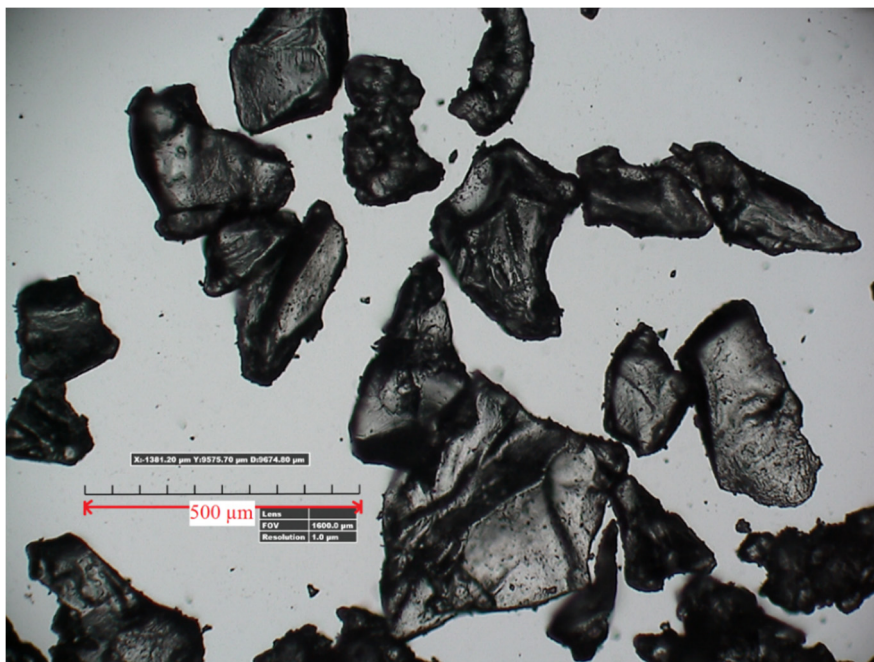


Figure 26 - Optical image of SAP A taken from optical microscopy analysis done for superabsorbent polymer provided by BASF (Magnification 140x)

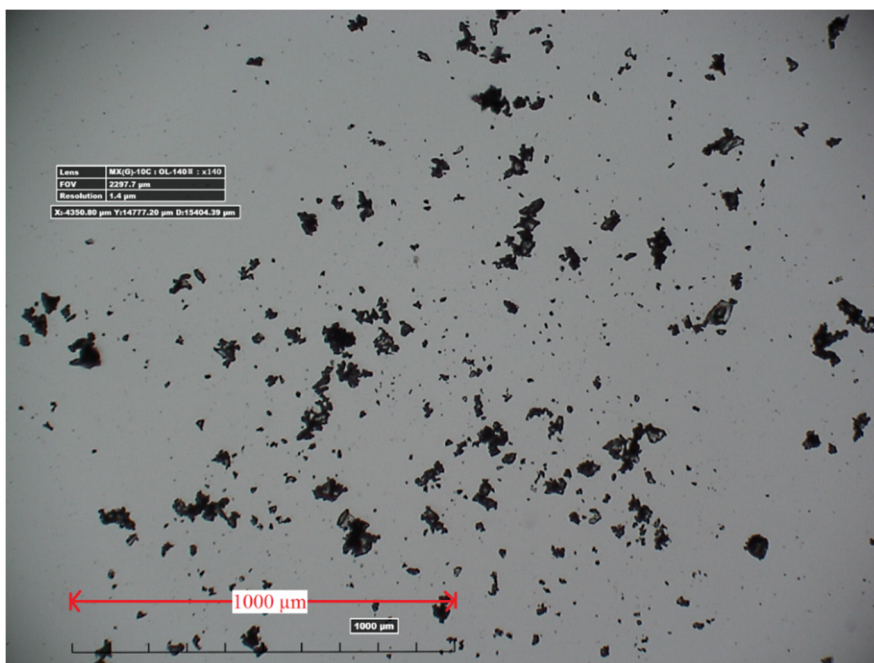


Figure 27 - Optical image for superabsorbent polymer obtained after cryomilling process, SAP B (Magnification 140x)

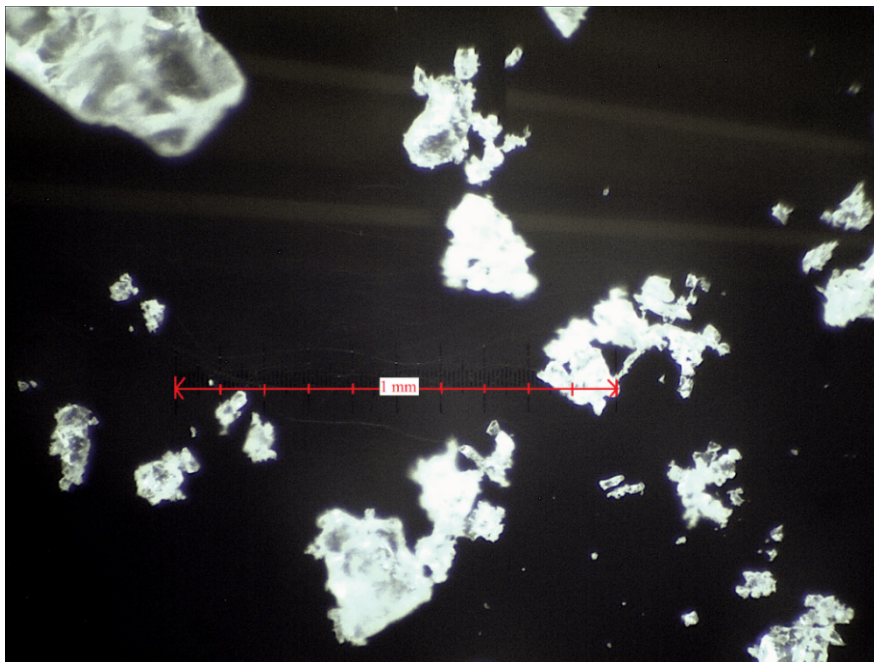


Figure 28 - Optical image of SAP taken at time 0 at room conditions of 21°C and 50% RH.

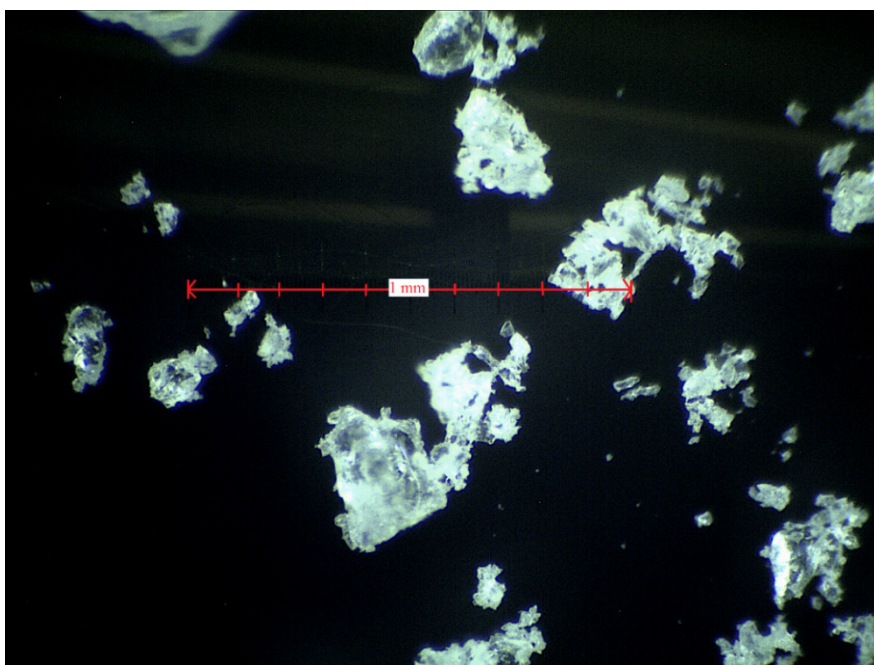


Figure 29 - Optical image (of the same SAP presented in Figure 28) 9 days after exposition to environment - Room conditions of 21°C and 50% RH.

3.4.2.1 Particle Size Distribution of SAP A

Figure 30 Figure 31 show the particle size distribution of the SAP A granules determined by image analysis. A scatter plot of the size distribution of the material obtained from SAS (Statistical Software) is presented in Figure 30. The same distribution is presented in Figure 31 but in this case, it is plotted in logarithmic scale. Two different ranges of particle size can be identified: the finer one (between 20 and 70 microns), and the coarser one (between 200 and 700 microns). Particles in the range between 200 and 700 microns are more abundant than those between 20 and 70 microns. It can also be noticed that there is a visible gap in size distribution between 90 μm and 200 μm .

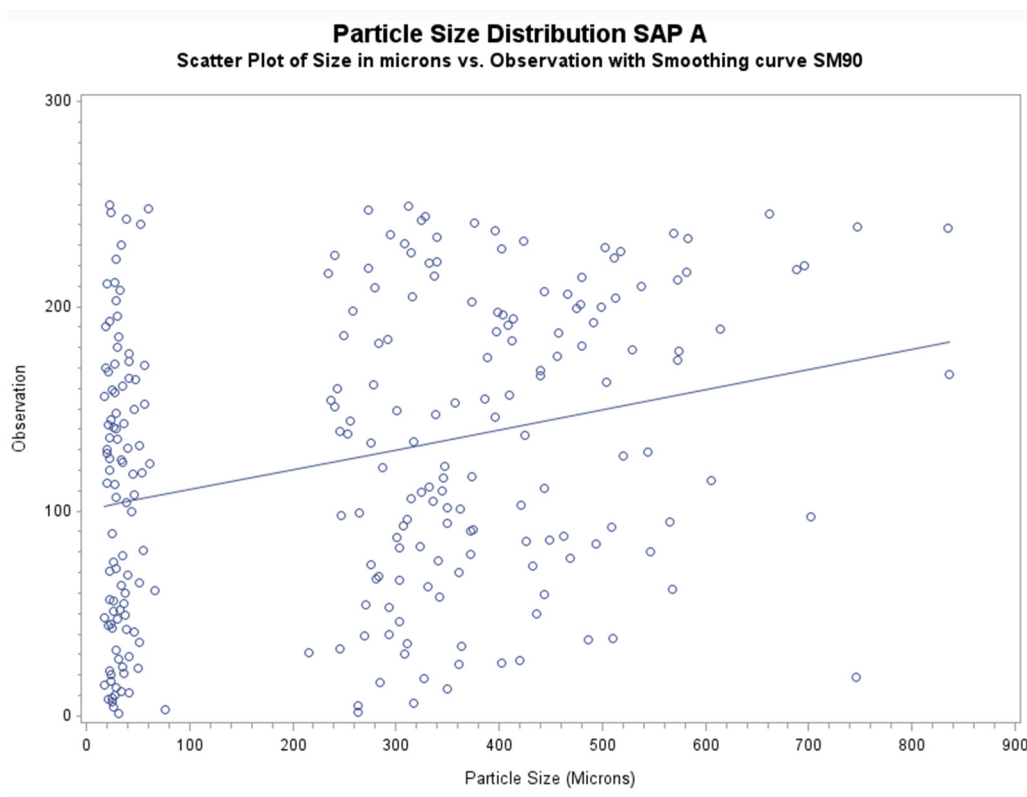


Figure 30 - Scatter Plot of the Particle Size Distribution (PSD) of SAP A

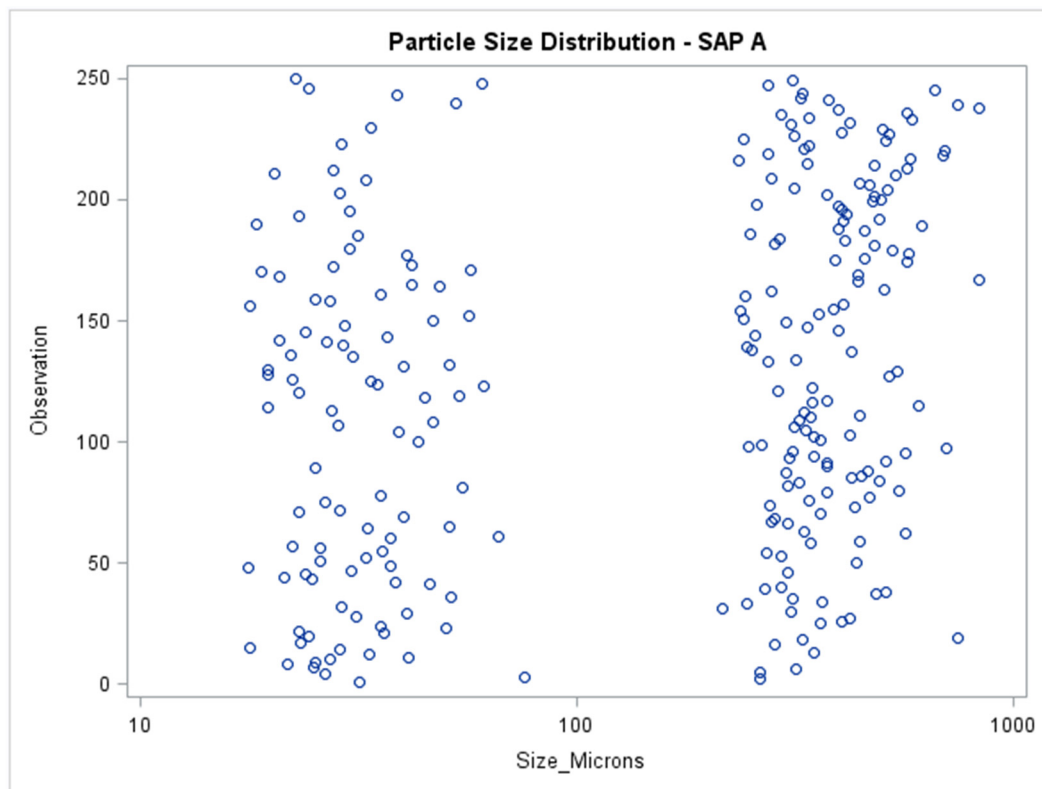


Figure 31 - Particle Size Distribution of SAP A in logarithmic scale

Figure 32 presents a histogram of the size distribution of SAP A combined with the normal density plot and the kernel density estimate. Due to the gap in size stated previously, it is not valid to comment on the normal distribution of the sample particle size because it does not have a continuous distribution. On the other hand, the kernel density estimate helps smooth out the effects of the data distribution. Therefore, two different peaks can be noticed in Figure 32. Both peaks are related to the density of the distribution of particles observed; for instance, the first peak corresponds to the density distribution for finer particles contained in SAP A according to the kernel distribution. Likewise, the second peak is related to the coarser size range obtained for SAP A.

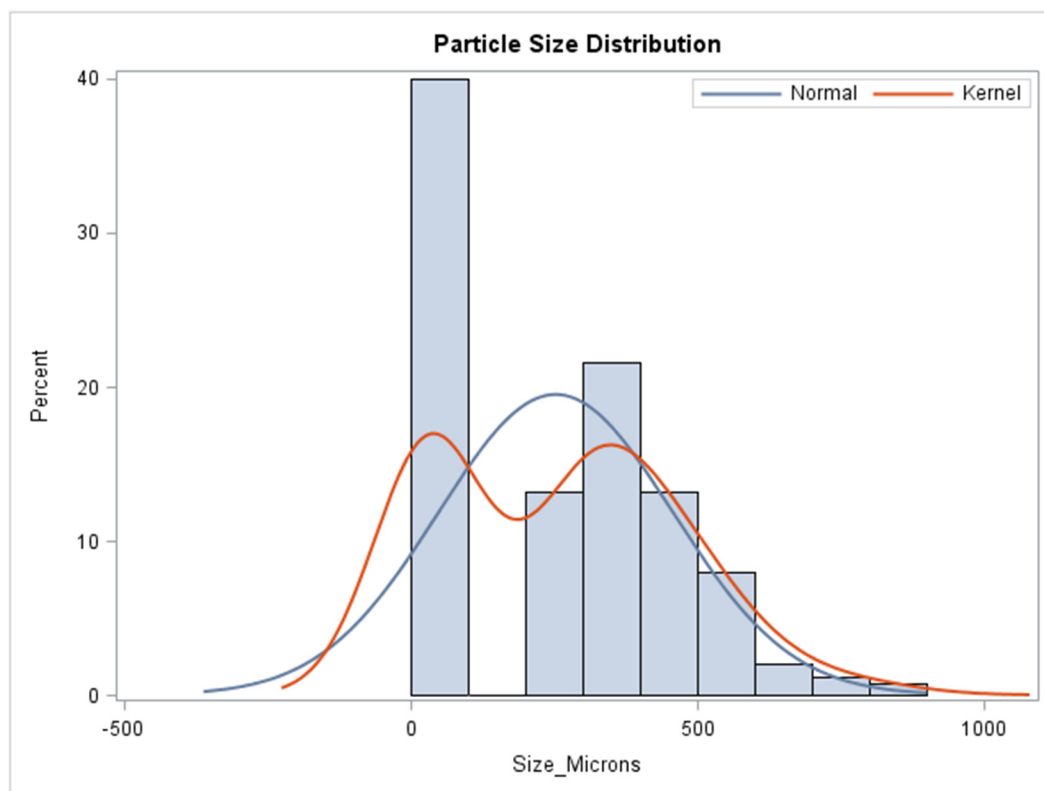


Figure 32 - Normal and Kernel distribution plots - SAP A

Table 6 contains the output of the SAS statistical software analysis, which includes the values of the quantiles as well as the lowest and highest observations in terms of particle size measured in microns. As listed in Table 6, 95% of the polymer sample supplied was composed of particles smaller than 573 microns, whereas 50% of the particles were smaller than 282 microns. Twenty-five percent of the sample was composed of particles smaller than 35 microns. The largest particle was approximately 836 microns in size while the smallest one was 17.7 microns in size.

Table 6 - Quantiles for Particle Size Distribution of SAP "A" (BASF)

Quantiles	
Level	Quantile (μm)
100% Max	836.1
99%	747.4
95%	573.8
90%	511.9
75% Q3	402.9
50% Median	281.9
25% Q1	35.0
10%	24.3
5%	21.7
1%	17.9
0% Min	17.7

3.4.2.2 Particle Size Distribution of SAP B

As expected after the polymer refinement, the particle size of the resulting material, SAP B, is finer than that of SAP A. The texture of the material is as fine and soft as cement grains; therefore, special care must be taken to avoid either clumping of the particles inside the cementitious system or wetting of the material during handling operations. In contrast, the refinement of the polymer by means of Cryomilling did not affect its white color, which makes its appearance similar to white cement. In Figure 33, the scatter plot of the size distribution of a random sample taken from the polymer is presented, which illustrates the homogeneity of the material.

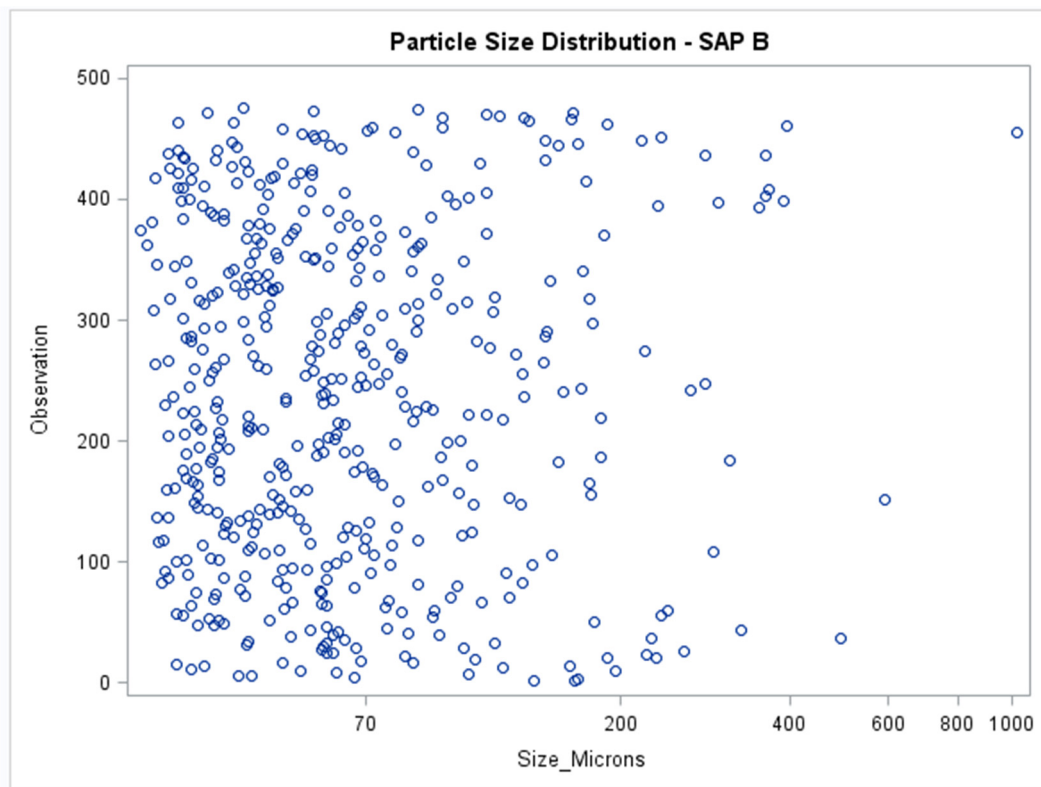


Figure 33 - Particle Size Distribution of SAP B in microns (Logarithmic scale) – SAP B is the finer SAP obtained after milling SAP A by means of Cryomilling.

The size of the material after milling is presented in Table 7, which specifies the size range of the sample to be between 27 and 1019 microns. However, 95% of the sample was smaller than 222 microns while 75% was smaller than 87 microns, which confirms that SAP B is much finer than SAP A. The median size of the SAP B was less than 58 microns whereas for SAP A it was approximately 282 microns. Additionally, the first quantile, which corresponds to 25% of the sample, had a particle size less than 41 microns.

Table 7 - Quantiles obtained for Particle Size Distribution of SAP B

Quantiles	
Level	Quantile (μm)
100% Max	1018.7
99%	390.4
95%	221.6
90%	155.0
75% Q3	87.0
50% Median	57.8
25% Q1	40.6
10%	33.9
5%	32.1
1%	29.5
0% Min	27.8

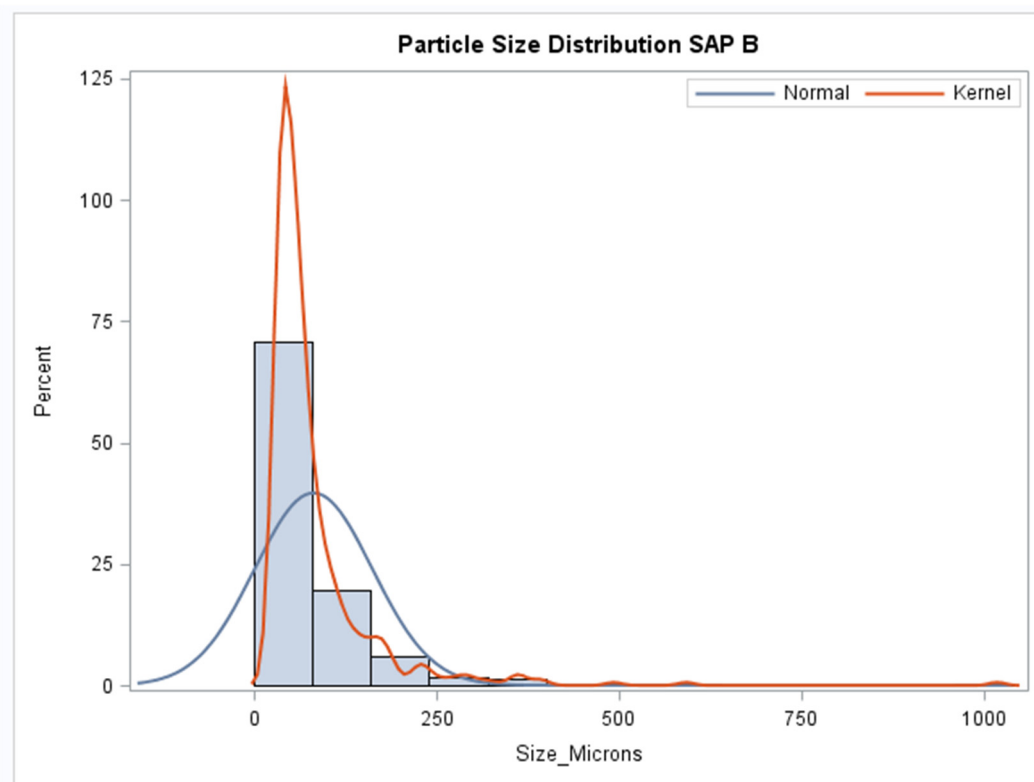


Figure 34 - Histogram combined with two density plots, normal density estimate and kernel density estimate

Figure 34 presents a histogram for the normal density estimate and kernel density estimate. Table 8 presents statistical information about the size of the sample size (n), mean of the sample and its standard deviation. The sample means corresponds to 81.5 microns. Table 9 shows a comparison between the observed and predicted values based on the normal distribution.

Table 8 - Mean and standard deviation of the sample - SAP B

Quantiles	
n	475
Mean, μ	81.5 microns
Standard Deviation, σ	80.5 microns

Table 9 - Quantiles describing values observed and estimated for Normal Distribution of SAP B

Quantiles for Normal Distribution		
Percent	Quantile	
	Observed	Estimated
1.0	29.4680	-105.8354
5.0	32.0810	-50.9643
10.0	33.8690	-21.7127
25.0	40.5760	27.1654
50.0	57.7960	81.4725
75.0	86.9730	135.7797
90.0	154.9670	184.6578
95.0	221.5530	213.9094
99.0	390.3550	268.7805

3.4.2.3 Swelling Behavior of SAP

In Figure 35 and Figure 36, the swelling behavior of SAP A and SAP B during their interaction with synthetic solution is evidenced in the set of pictures taken using an optical microscope, which proceeds from left to right and top-down. The synthetic solution used corresponds to the one prepared to mimic Cem3. The swelling behavior of SAP A is easier to observe due to the initial particle size and spread of the particles. It is also noticeable that after swelling of particles A and B, the particles become gelatinous.

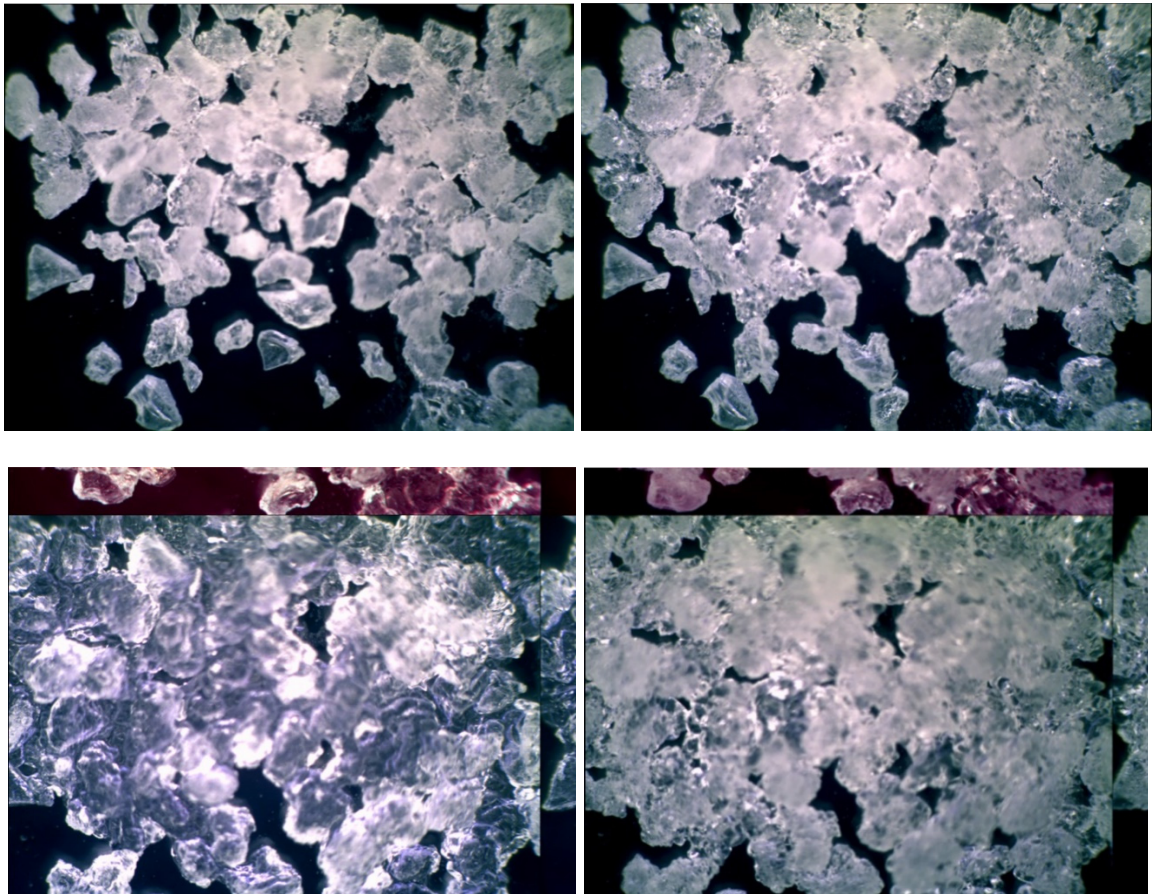


Figure 35 - Swelling behavior of SAP A in synthetic pore solution (SPS) resembling the extracted solution from cement paste prepared using Cem3

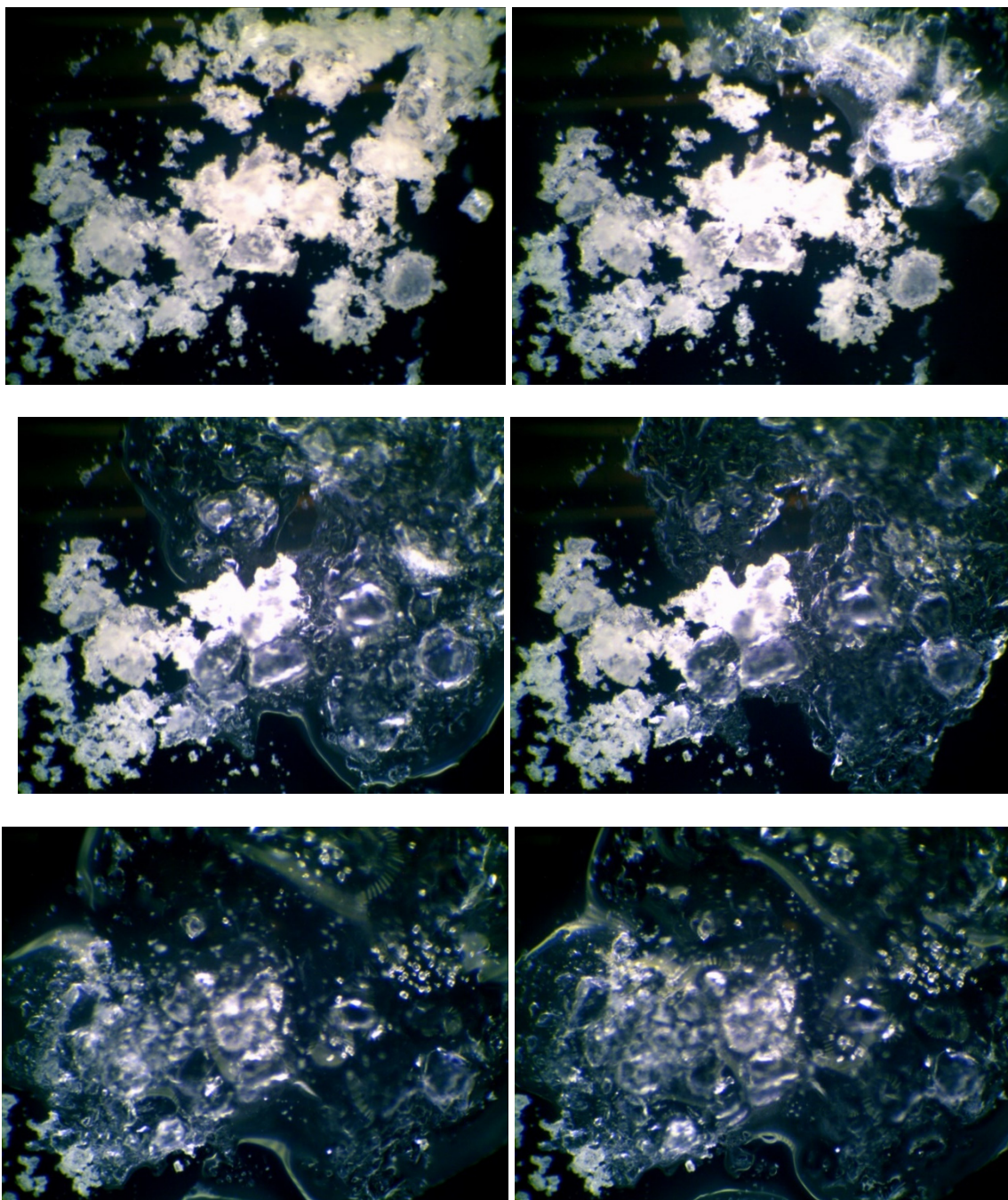


Figure 36 - Swelling behavior of SAP B in SPS resembling the system prepared with Cem3

Figure 36 evidences the clumping behavior of SAP B at dry state and illustrates how the solution is pulled in by the polymer clumps as the swelling behavior proceeds.

CHAPTER 4. SYNTEHTIC PORE SOLUTION AND ABSORPTION CAPACITY OF SAP

4.1 Introduction

Synthetic pore solution, also called artificial pore solution, has historically been used to investigate durability of cementitious systems that may impact the service life of reinforced concrete elements. For example, meaningful information about the kinetics of ion migration over time throughout a cementitious system may be obtained from the chemical analysis of pore solution composition. For the purpose of this research, synthetic pore solutions (SPS) were used to reproduce the chemistry of the liquid phase of the fresh cement pastes prepared and studied in Chapter 3. Additionally, these artificial solutions were used to determine the absorption capacity of superabsorbent polymers.

4.2 Materials

The extracted pore solution of fresh cement paste was reproduced by the dissolution of potassium sulfate (K_2SO_4), sodium hydroxide (NaOH), calcium hydroxide ($Ca(OH)_2$) and sodium chloride (NaCl) in deionized water. Sodium sulfate (Na_2SO_4) and potassium hydroxide (KOH) were also tested but not used in the final solution.

After testing different mixing schemes, only one was selected to replicate the actual extracted solution, which was later used to investigate the absorption capacity of the polymer by exposing a polymer sample to the synthetic solution in a tea bag.

4.3 Experimental Methods

In this section, the synthetic pore solution preparation and the tea bag method implemented for the study of the absorption capacity of SAP are presented.

4.3.1 Synthetic Pore Solution (SPS) Preparation

In order to replicate the composition of the extracted pore solution, selected chemical compounds, presented in Table 11, were dissolved in deionized water. However, while attempting to prepare the artificial solutions it was discovered that the order in which the chemicals were dissolved in deionized water influenced the final concentration of ions in the solution. As a result, four different solution preparation schemes were investigated (Table 10) with the aim of producing the artificial pore solution most closely resembling that extracted from the actual paste. After this, the most appropriate mixing scheme was implemented to synthetically reproduce the extracted solutions using the different compounds presented in Table 11. The prepared solutions were used to test the capacity of the polymers to absorb solutions rich in alkali ions similar to the liquid phase developed during cement hydration.

4.3.2 Absorption Capacity SAP –Tea Bag Method

As stated previously, the chemical composition of the cement drives the concentration of ions in the liquid phase resulting from cement hydration. It is expected that differences in pore solution composition, resulting from using cement samples that differ in alkalinity, will also lead to variability in the absorption capacity for superabsorbent polymers. The previous statement implies that different mix designs may be possible and that these designs will capitalize on the differences in cement chemistry and in the properties of the particular polymer. The absorption capacity of the SAP was measured by performing tea bag method, which was also used in previous research in this field (Miller, 2014).

Tea Bags Number 3 containing approximately 0.20 g of SAP were submerged in the artificial pore solution. To determine the absorption capacity of the polymer, the gain in weight of the polymer due to absorption was monitored over time. Measurements of the mass of the hydrogel after submersion in the synthetic solution at times of 0.5, 1, 3, 5, 10, 15, 30, 60, 120 and 240 minutes were conducted for SAP A. In contrast, due to the smaller size of polymer B and the associated difficulties in handling the samples, the mass change measurements were only taken at times of 10, 15, 30, 60, 120 and 240 minutes for polymer B. The absorption capacity of superabsorbent polymers was determined to be the mass in grams of fluid absorbed per gram of dry polymer after submerging the polymer in the solution for four hours.

4.4 Experimental results

4.4.1 Chemical Analysis of Synthetic Pore Solution (SPS)

While preparing the synthetic pore solutions, it was noticed that solutions with higher ion concentrations were more difficult to replicate. It is suspected that this was due to chemical interactions between the reactants; a saturation level may have been reached due to the high ion concentration, which resulted in the formation of precipitates. The first trials showed that the amount of precipitates formed in the synthetic solution replicating the pore solution extracted from fresh cement paste prepared with Cem1 cement was considerably lower than that obtained from paste prepared with Cem3, which contains the highest amount of precipitates. Therefore, the Cem3 solution was selected as the trial solution to develop the most appropriate scheme for pore solution preparation.

Values reported in Table 10 represent the artificial pore solutions created to replicate the one extracted from Cem3 paste at $w/c=0.30$ using different preparation schemes. The compositions of solutions prepared using Schemes #1 and #2 were very close to that of the extracted pore solution. However, these schemes did not yield the desired concentration of potassium ions, and formation of precipitates was also observed. Even when the attempt was made to increase the solubility of chemicals in the solution by increasing the temperature to 30°C, Schemes #1 and #2 did not produce the desired concentration of potassium ions. As a result, Schemes #3 and #4 were also developed in an attempt to increase the concentration of K^+ ions. This was achieved by adding KOH in

a higher amount than that used in Schemes #1 and #2. While increasing the amount of KOH resulted in higher concentration of K^+ ions, the resulting solutions were more clouded (i.e. they contained more precipitates than the solutions prepared using Schemes #1 and #2).

During solution preparation, visual changes are detected for synthetic solutions. Figure 37; for example, presents changes in appearance of the solution as the mixing Scheme #3 progresses. The first two pictures show a clearer solution due to the lower presence of suspended precipitates, whereas the third picture shows that the same solution became more clouded immediately after the addition of calcium hydroxide. Changes in pH, saturation of the solution and the usage of $Ca(OH)_2$ may have caused the formation of precipitates. Because of the experience gained preparing solutions using different mixing schemes and the concentration of ions measured for each synthetic solution, Scheme #1 was adopted as a reasonable compromise with respect to concentration of potassium ions and the amount of precipitates formed.

Table 11 states the mass of each compound used to prepare the three artificial solutions representing the extracted pore solutions for Cem1, Cem2, and Cem3. These solutions were then used to study the absorption capacities of superabsorbent polymers A and B.

Table 10 - Preparation schemes and list of chemicals used to create artificial pore solution for w/c=0.3 paste from Cem3

Chemicals used and Mixing Order implemented	Preparation Scheme #1	Preparation Scheme #2	Preparation Scheme #3	Preparation Scheme #4
1	K ₂ SO ₄	NaCl	NaCl	NaCl
2	NaOH	Na ₂ SO ₄	KOH	Ca(OH) ₂
3	Ca(OH) ₂	K ₂ SO ₄	Na ₂ SO ₄	Na ₂ SO ₄
4	NaCl	KOH	K ₂ SO ₄	K ₂ SO ₄
5	-	Ca(OH) ₂	Ca(OH) ₂	KOH
Average [K ⁺] (mmol/L) ¹	373	273	435	435
Average [Na ⁺] (mmol/L) ¹	217	217	221	213
Average [Ca ²⁺] (mmol/L) ¹	13	13	14	21
pH Measured	13.01	12.88	13.41	13.25
Notes (Observed)	Formation of precipitates after addition of CH	Formation of precipitates after addition of CH	Formation of precipitates after addition of CH	Formation of precipitates after addition of KOH

Note¹: average concentration of a given ion in the artificial (synthetic) pore solutions.

Table 11 - Chemical compounds used in grams to prepare 1 liter of synthetic pore solution based on cement sample

Mass of compound (grams) / L _{solution}	Cem1	Cem2	Cem3
K ₂ SO ₄	18.8225	28.0250	37.8900
NaOH	1.6755	2.5160	8.1050
Ca(OH) ₂	1.1093	1.2200	1.3720
NaCl	0.2930	0.7100	1.0870

Table 12 compares the concentrations of various ions in the actual (extracted) and synthetic pore solutions prepared using the procedure described previously. As presented, three different synthetic pore solutions, SPS-1 (Cem1), SPS-2 (Cem2) and

SPS-3 (Cem3), were prepared to reflect the variations in the alkalinity of the pore solutions extracted from pastes prepared with three different cements. Their chemical composition was determined following the same techniques presented in Chapter 3.

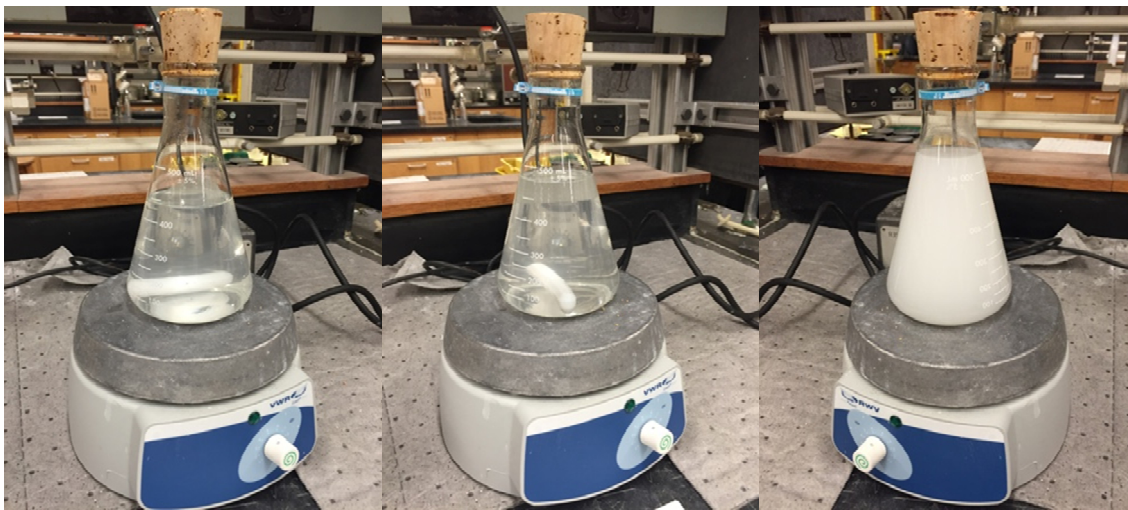


Figure 37 - Evolution of the appearance of the synthetic solution during preparation

Analysis of the data presented in Table 12 indicates that in all cases, except for the potassium (K^+) ions, the composition of the synthetic pore solutions was close to that of the actual (extracted) pore solutions. In the case of K^+ ions, their concentration in the synthetic pore solution was always lower than that in the extracted pore solution. The observed shortage of the K^+ ions in the synthetic solutions is, at this point, hypothesized to be attributable to the internal reaction that is evidenced by the formation of precipitates once all the chemicals are combined with deionized water.

The precipitates formed were filtered out from the solution, oven-dried, and analyzed using a scanning electron microscope (SEM) equipped with energy-dispersive X-ray spectrometer (EDS) to identify their potential chemical compositions. The results of these analyses showed that most of the precipitates were composed of potassium, sulfur and calcium, thus indicating a possible chemical reaction resulting in the possible formation of syngenite ($K_2Ca(SO_4)_2 \cdot H_2O$). The SEM-EDS results are presented in Figure 38, Figure 39, Figure 40, and Figure 41, in which the presence of those chemical compounds are noted at the bottom of each figure.

Table 12 - Comparison of compositions of extracted and synthetic pore solutions

Ionic concentration of the solution	Extracted Pore solution (EPS-1)	Synthetic Pore solution (SPS-1)	Extracted Pore solution (EPS-2)	Synthetic Pore solution (SPS-2)	Extracted Pore solution (EPS-3)	Synthetic Pore solution (SPS-3)
w/c=0,3	Cem1	Cem1	Cem2	Cem2	Cem3	Cem3
Na ⁺ [mmol/L]	47	46	75	74	221	217
K ⁺ [mmol/L]	217	196	341	279	330	373
Ca ⁺ [mmol/L]	15	11	16	11	19	13
Cl ⁻ [mmol/L]	5	5	12	12	19	18
SO ₄ ⁽²⁻⁾ [mmol/L]	108	108	161	159	217	216
Measured OH ⁻ [mmol/L]	94	Not determined	103	Not determined	80	Not determined
Calculated ph	12.98	Not determined	13.01	Not determined	12.90	Not determined
Measured pH	13.04*	12.73	13.08*	12.67	12.96	13.01

* pH measured after 7 days

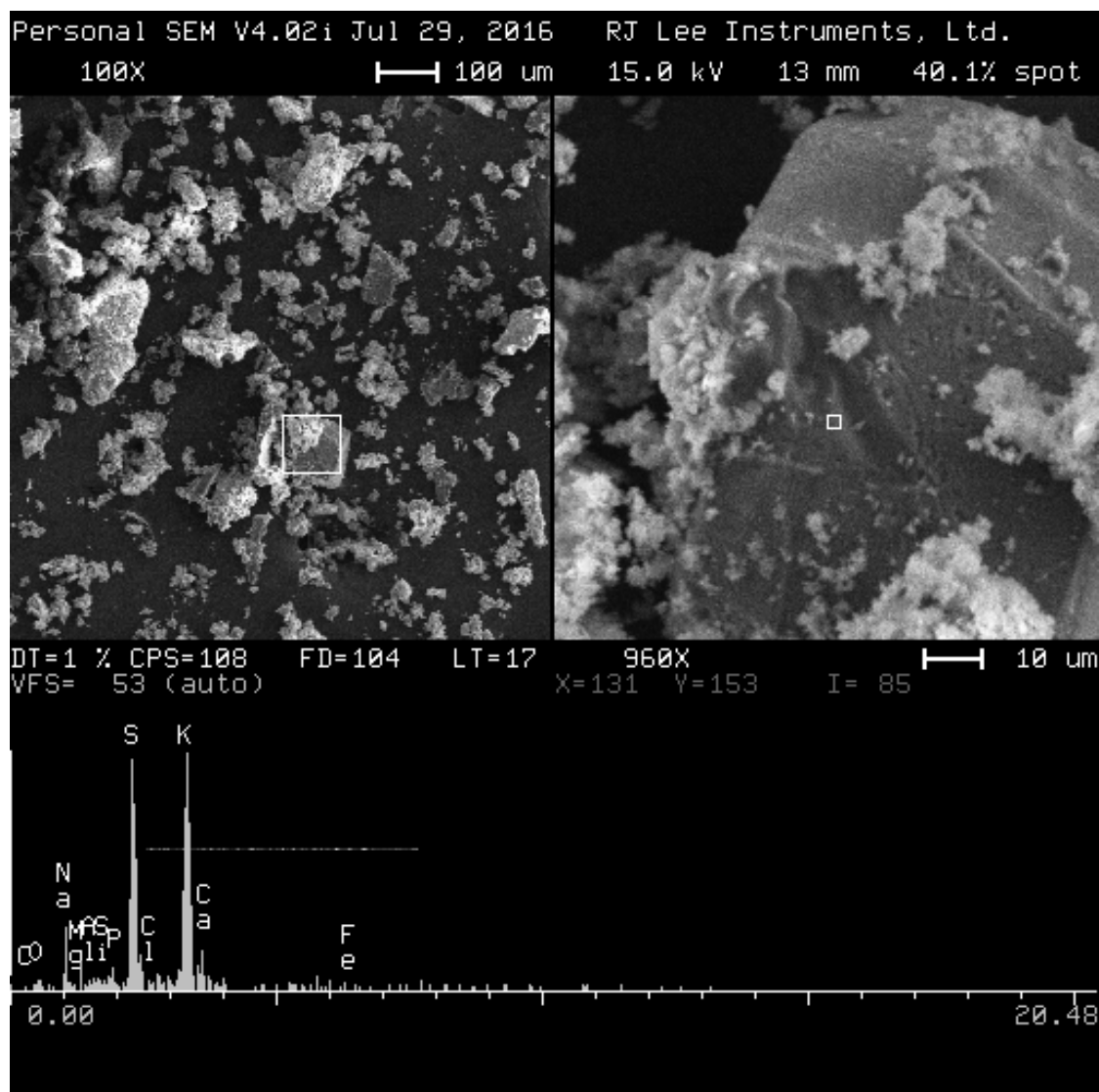


Figure 38 - SEM Image #1 for Preparation Scheme #1 - potassium, sulfur, sodium and calcium are the main peaks found in this portion of the precipitates.

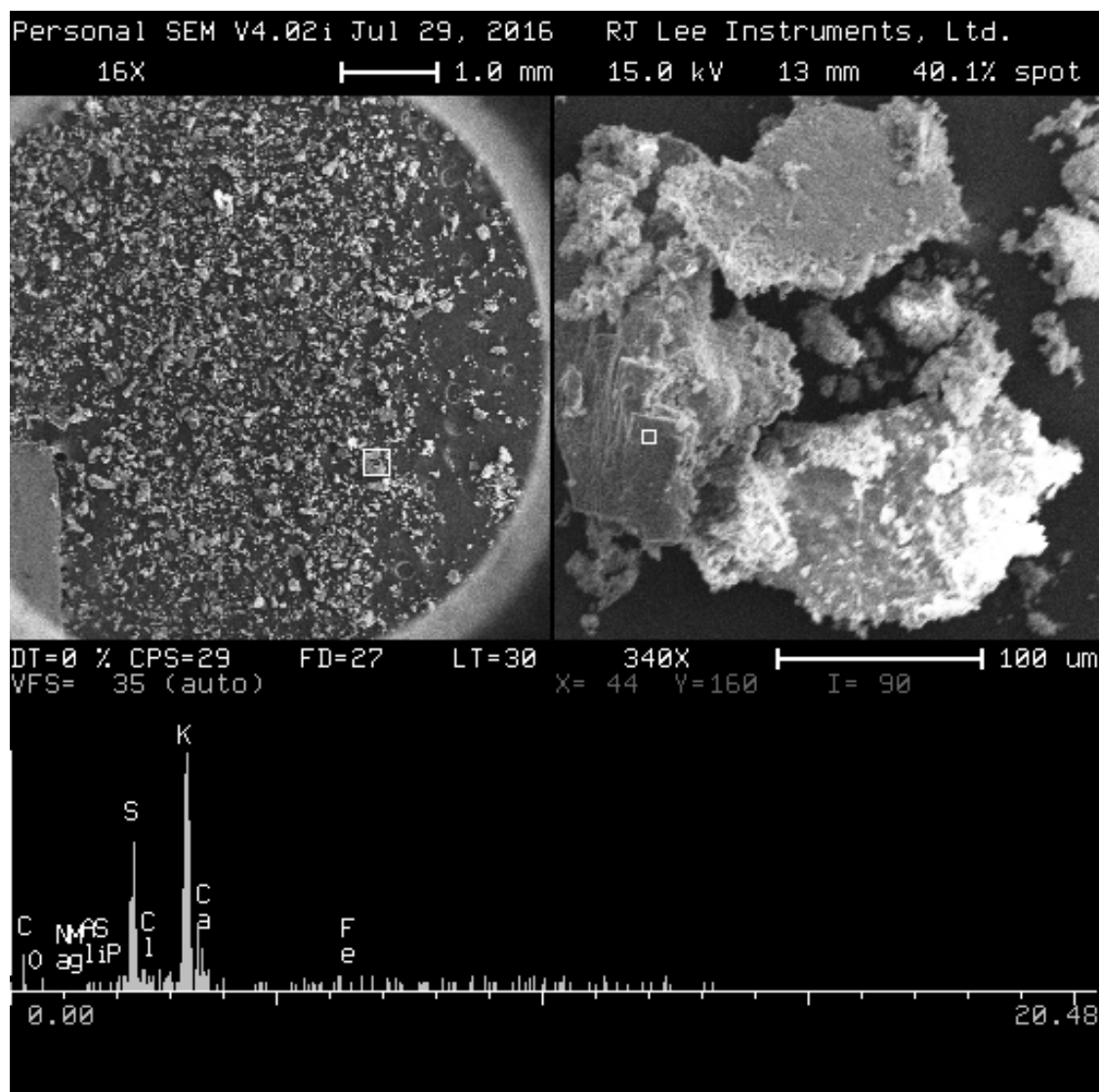


Figure 39 - SEM Image #2 for Preparation Scheme #1 - potassium, sulfur and calcium peaks found in the precipitates

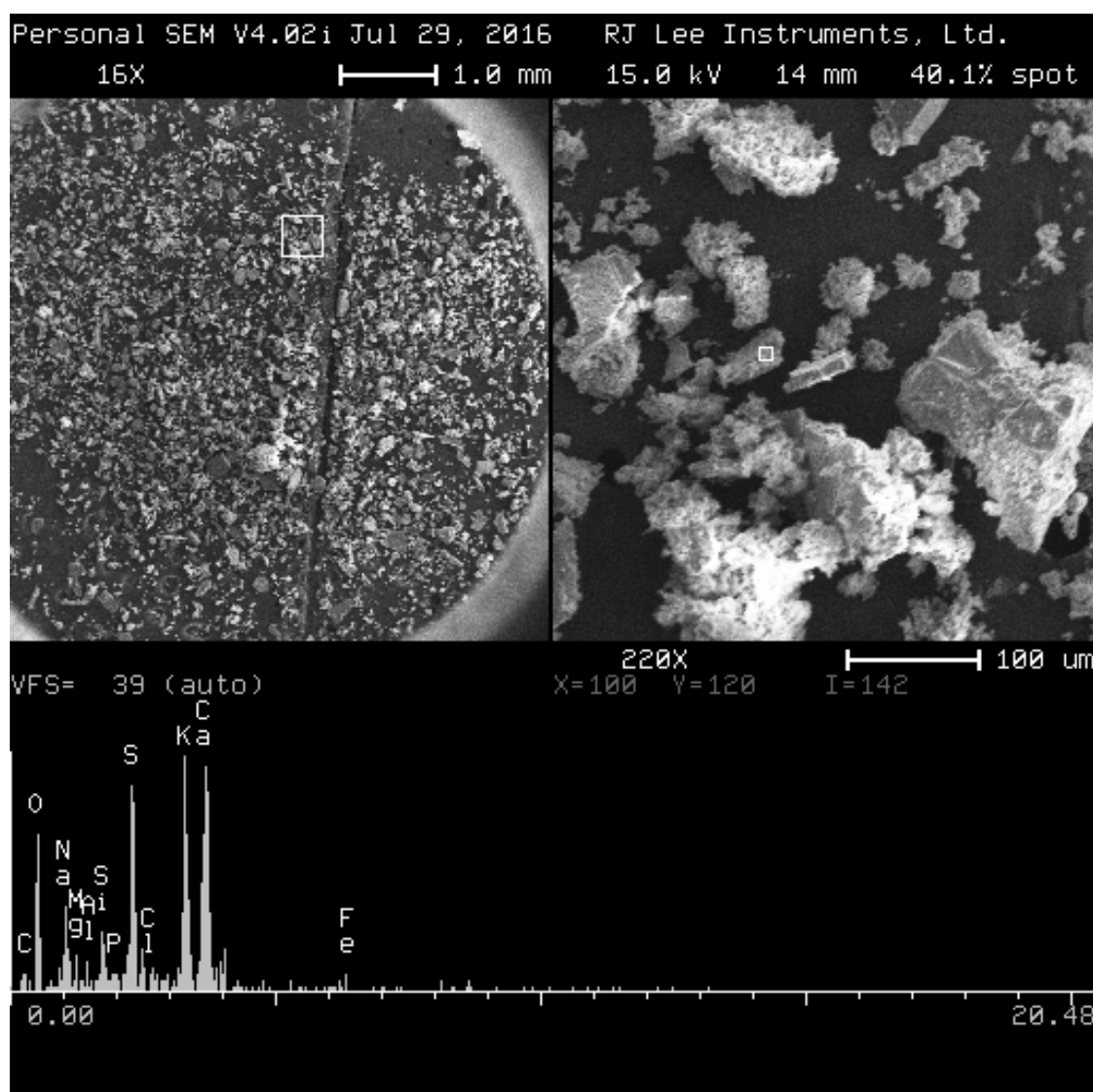


Figure 40 - SEM Image #3 for Preparation Scheme #2 – calcium, potassium, sulfur and sodium are the elements represented by the main peaks found in this portion of the precipitates.

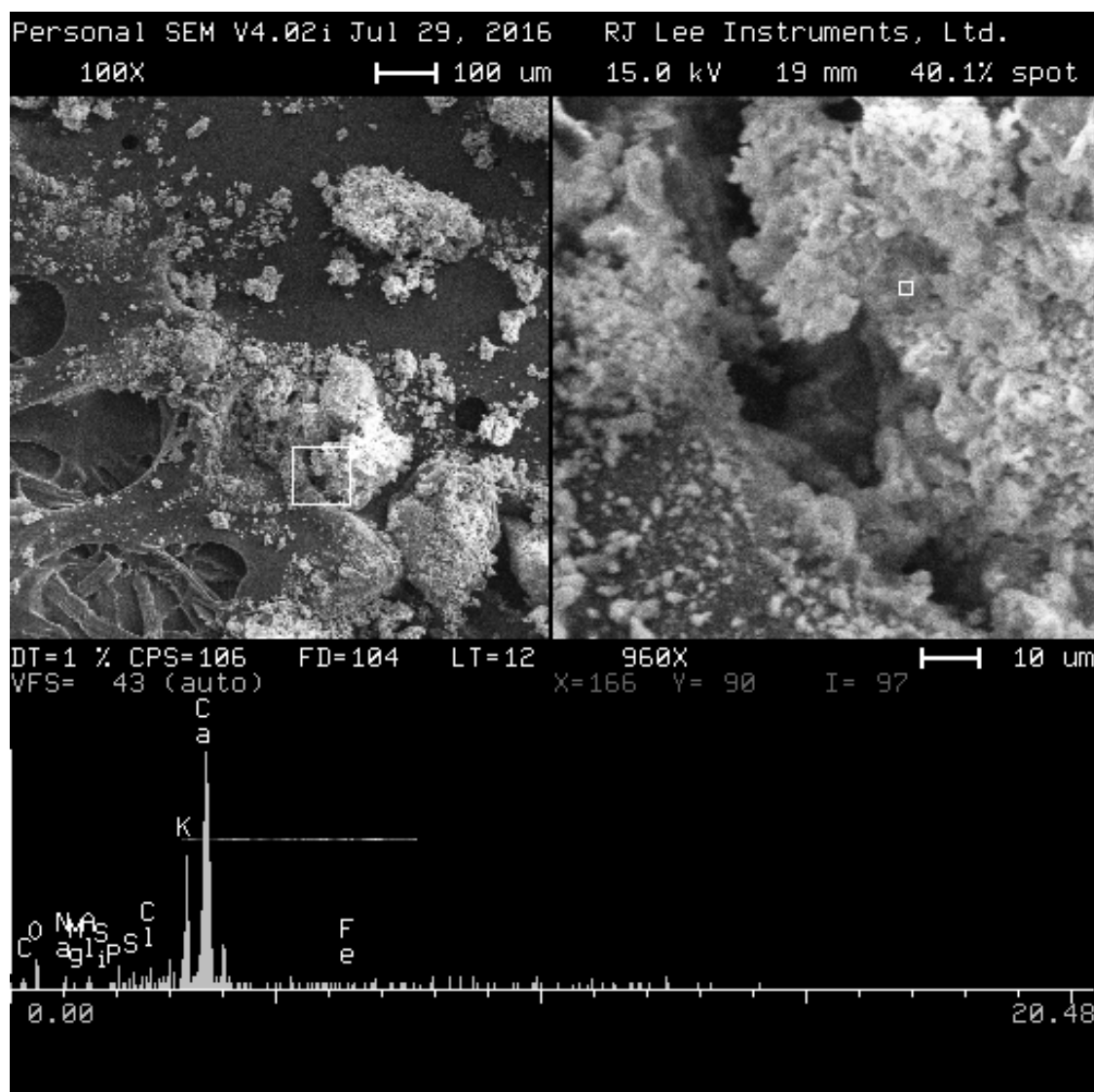


Figure 41 - SEM Image #4 for Preparation Scheme #2 - calcium and potassium are the main peaks found in the precipitates.

4.4.2 Absorption Capacity of SAP

As presented previously, the tea bag method was used to determine the absorption capacity of the commercially available superabsorbent polymer studied. This polymer property varies depending on the nature of the polymer that is comprised of composition of the polymer chain and type of cross-linking agent (Zhu, 2014), and the chemistry of the solution (TC225-SAP, 2012), which for the purpose of this research varies according to the chemistry of the cements from low to medium alkalinity. SAP A and B, with only differences in size, were tested in various synthetic solutions. It was found that pH and concentration of alkali ions in the solution play a role in determining the swelling behavior of the polymer, represented by absorption capacity of the hydrogel and shape of the isotherm. Additionally, there is a reduction in absorption capacity due to the polymer size.

Figure 42 illustrates the variation of absorption capacity of polymer A over time for three synthetic solutions. It is expected that when SAP A is exposed to a cementitious system with an alkalinity equivalent to that of Cem1 ($\text{Na}_2\text{O}_{\text{Eq}}=0.37\%$), the polymer may be able to absorb approximately 26.9 grams of pore solution per gram of dry SAP in 4 hours. On the other hand, for cementitious systems similar to that of Cem2 ($\text{Na}_2\text{O}_{\text{Eq}}=0.62\%$), the polymer capacity slightly increases to values of about 27.3 $\frac{\text{g}_{\text{pore solution}}}{\text{g}_{\text{dry SAP}}}$. When the SAP was exposed to the third and most alkaline solution, which represents Cem3 ($\text{Na}_2\text{O}_{\text{Eq}}=0.72\%$), the absorption capacity of the hydrogel was 32.7 grams of pore solution per gram of dry SAP. As evidenced, increases in alkalinity lead to

changes in absorption capacity of the polymer that are graphically represented by two absorption stages discussed in section 4.5.

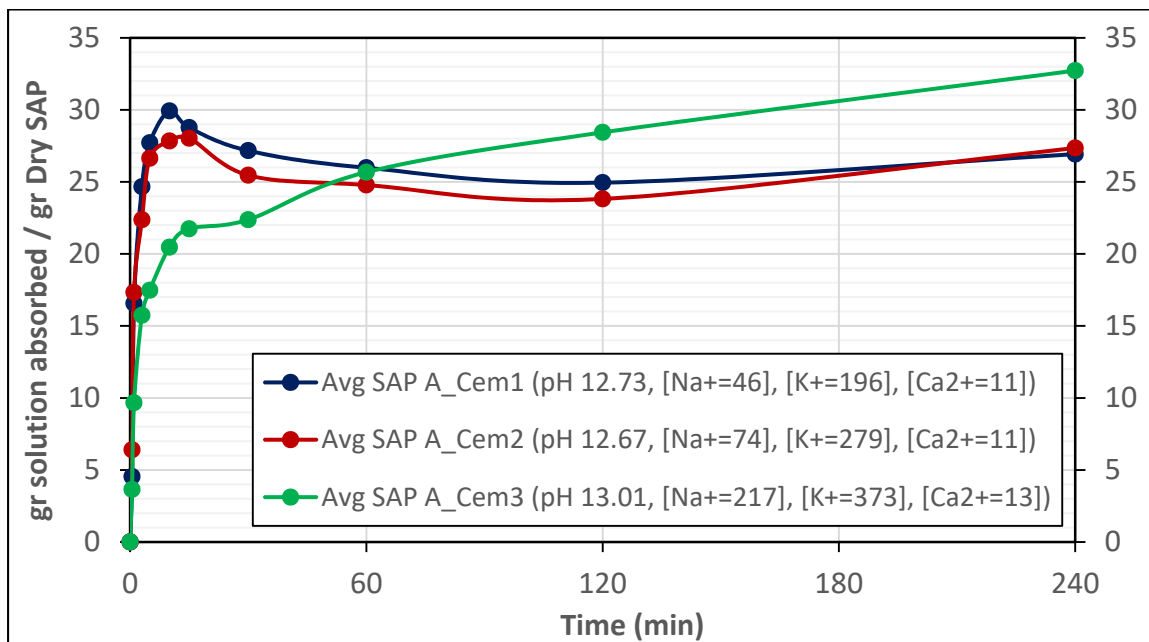


Figure 42 - Absorption Capacity Isotherm for SAP A when different synthetic solutions used

Figure 43 presents the absorption capacity for SAP B and confirms similarities between the shape of the isotherms for polymers A and B. An observed slower swelling rate for SAP B is attributed to polymer particles clumping that delays the interaction polymer-solution; therefore, the actual swelling rate of polymer particles in the range of size of SAP B should not be determined under this methodology. This effect, called *gel blocking*, is a property of fine SAP particles (smaller than 100 microns) in which the polymer forms an outer layer of hydrated SAP and an inner core of unhydrated SAP. The outer layer

acts as a barrier for the solution, and does not allow the solution to pass through it to hydrate the polymers contained in the inner core. Applications such as sealing materials have been developed (TC225-SAP, 2012). From the concrete production standpoint, particles clumping is not expected in a cementitious system since proper mixing of cement and polymer in a dry state will guarantee better distribution of the polymer throughout the volume of material. As a recommendation, mixing protocols should be adjusted in order to find the proper mixing procedure that allows the development of the fullest absorption capacity of the hydrogels in cementitious systems.

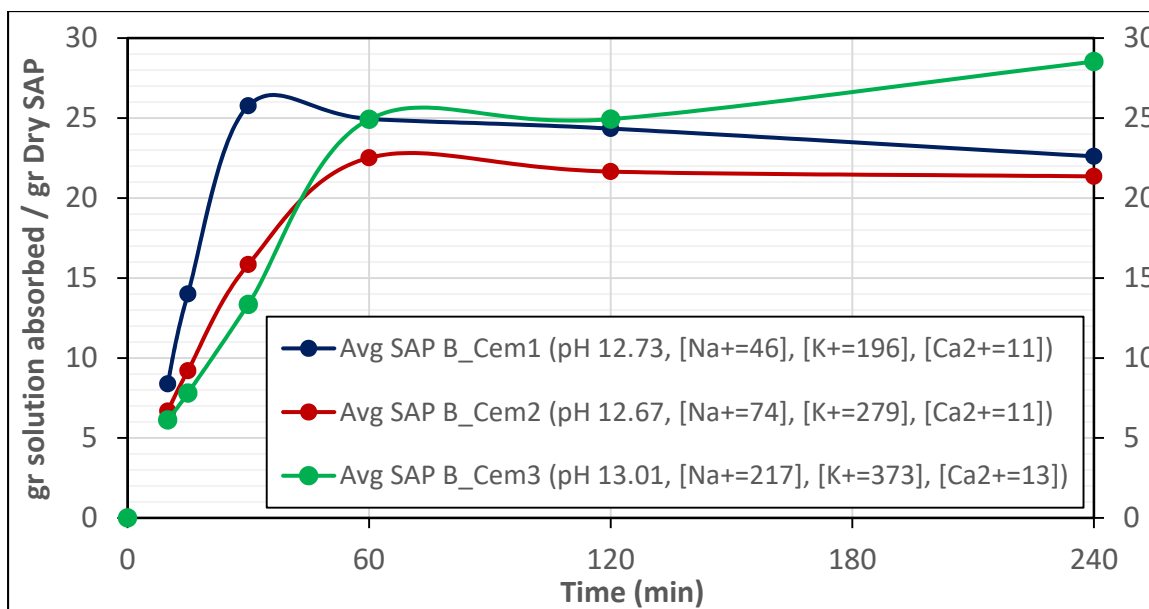


Figure 43 - Absorption Isotherm for SAP B when different synthetic solutions used

According to the results of the tea bag tests, changes in absorption capacity related to polymer size is presented in Table 13, in which lowered values are reported for SAP B

(Finer hydrogels). The largest reduction in this property was found for the polymer tested under the SPS2-Cem2, followed by SPS 1-Cem1 and SPS-3 Cem3, respectively.

Table 13 - Absorption capacity of hydrogels based on synthetic pore solution (SPS)

Absorption Capacity of SAP	SPS1 - Cem1	SPS2 - Cem2	SPS3 - Cem3
g Pore solution absorbed/g Dry SAP A	26.9	27.4	32.7
g Pore solution absorbed/g Dry SAP B	22.6	21.4	28.5
Δ in absorption capacity ($g_{\text{pore soln}}/g_{\text{dry SAP}}$)	4.3	6.0	4.2

Even though different absorption capacities were obtained, only the results for SAP A were defined to be used in the mix design whatsoever the polymer picked to use is. There are two reasons to support this assumption. First, both polymers come from the same nature; therefore, if used in the same amount, the real effect of size may be evaluated in isothermal calorimetry of internally cured cement pastes. Secondly, as stated previously, there are uncertainties about the accuracy of the tea bag method for testing the absorption capacity of SAP B due to the gel blocking effect. Then, using the absorption capacity obtained for SAP A in the overall mix design would be a reasonable approach.

Table 14 summarizes the absorption capacity established to be used for mix design purposes and all the parameters that best describe the chemistry of the prepared artificial solutions that were used to find the absorption capacity values.

Table 14 - Absorption capacity of SAP based on pore solution composition

Absorption Capacity of SAP under interaction with SPS	SPS1 - Cem1	SPS2 - Cem2	SPS3 - Cem3
g Pore solution absorbed/g Dry SAP	26.9	27.4	32.7
pH of the solution	12.73	12.67	13.01
K ⁺ (mmol/L)	196	279	373
Na ⁺ (mmol/L)	46	74	217
Ca ²⁺ (mmol/L)	11	11	13
Sum of K ⁺ and Na ⁺ (mmol/L)	242	353	590

In Figure 44, Figure 45, and Figure 46, unified plots represent the interaction of the different hydrogel samples with a specific synthetic solution. Three different plots present the isotherms for polymer A and B interacting with synthetic solutions that replicate the liquid phase of cement pastes prepared using cement from Cem1, Cem2 and Cem3. Even though lower absorption capacity was determined for all the finer SAP samples regardless of the synthetic solution tested, their isotherms show a general tendency to follow the same pattern or shape developed by those of SAP A. The absorption capacity plot for polymer B that best resembles that of SAP A was obtained for the solution that follows the chemistry of the cement paste prepared using cement from Cem1.

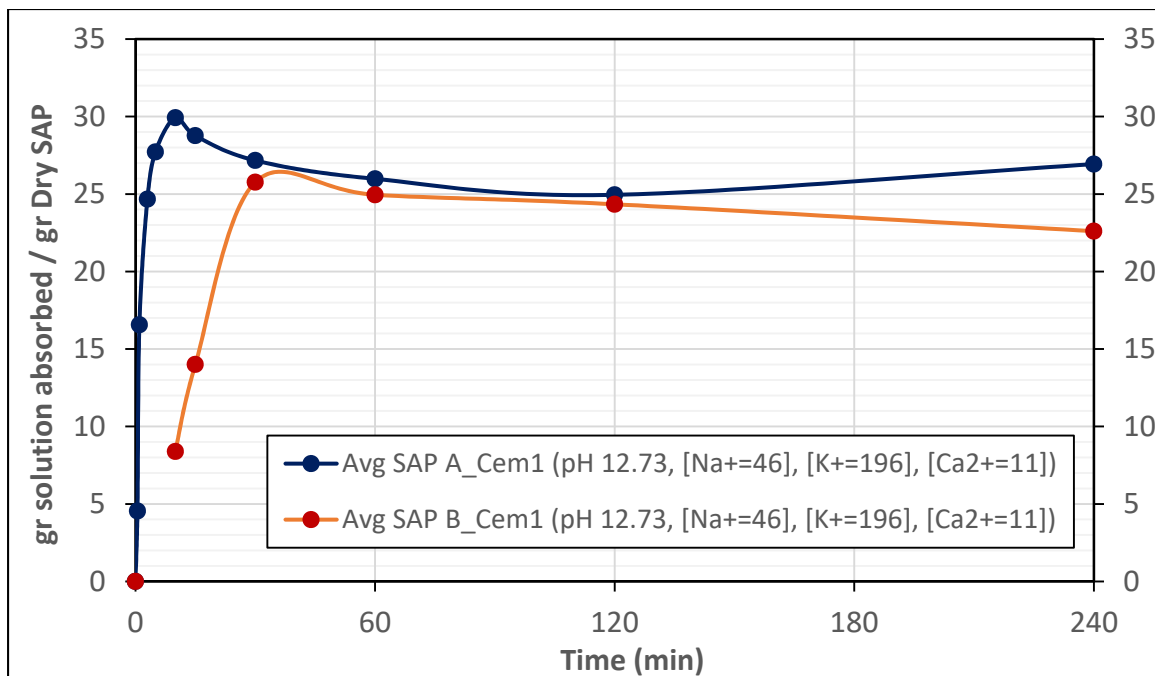


Figure 44 - Absorption capacity isotherm for polymers A and B in SPS1 Cem1

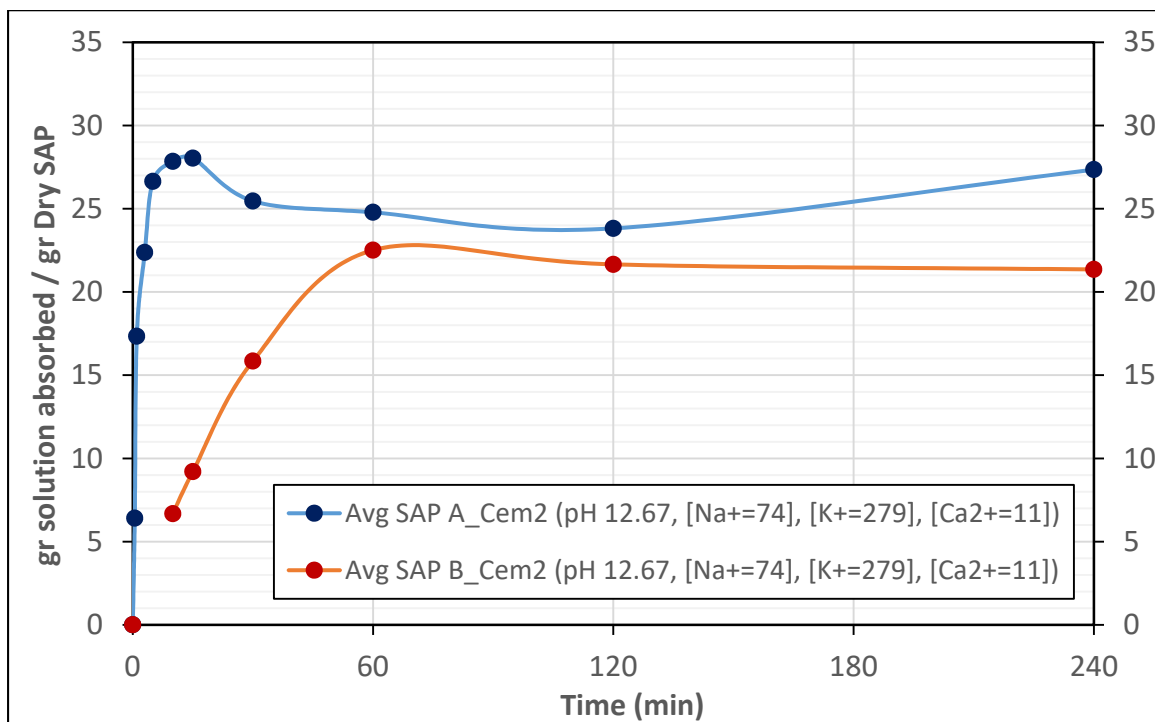


Figure 45 - Absorption capacity isotherm for polymers A and B in SPS2 Cem2

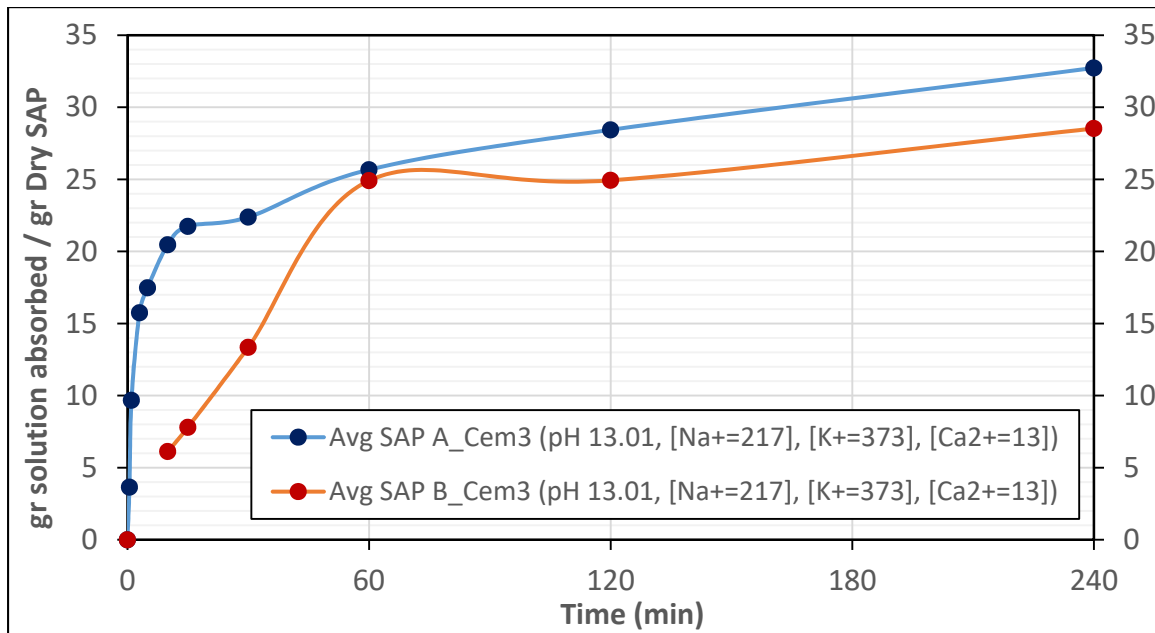


Figure 46 - Absorption capacity isotherm for polymers A and B in SPS3 Cem3

4.5 Discussion for Absorption Capacity

4.5.1 Stages of the Absorption Capacity Isotherms

As stated previously, the chemistry involved in the process of interaction hydrogel-solution along with the nature of the polymer define the shape of the absorption isotherm. In this research, during the swelling behavior of the superabsorbent polymers investigated, two stages were identified in the isotherm. In Figure 47, both stages are defined in the isotherm obtained after exposition of the polymers to the solution presented in Table 14. In terms of duration, Stage 1 goes from 0 to 30 minutes of hydration while Stage 2 goes from 30 to 240 minutes. With respect to the impact of polymer size on absorption capacity, slight differences were found. The hypothesis is these differences are attributed to smaller particles that do not have the same capacity to swell and absorb due to gel blocking effect. Figure 47 and Figure 48 prove that most of the absorption capacity of SAP may be developed during the first 10 minutes of polymer-solution interaction, as stated by (Mönnig, 2005).

Stage 1 represents the fast capacity of the studied SAP for water uptake as well as the impact of the concentration of ions on the initial absorption capacity of the polymers. SAP tested in low-alkalinity solution (Cem1) experienced a steeper swelling rate, and as concentration of ions and pH of the solution increase, absorption rate decreases. In Stage 2, it is hypothesized that either the stable or increasing absorption behavior is attributed to the combined effect of pH, potassium, and calcium over time on the polymer chains.

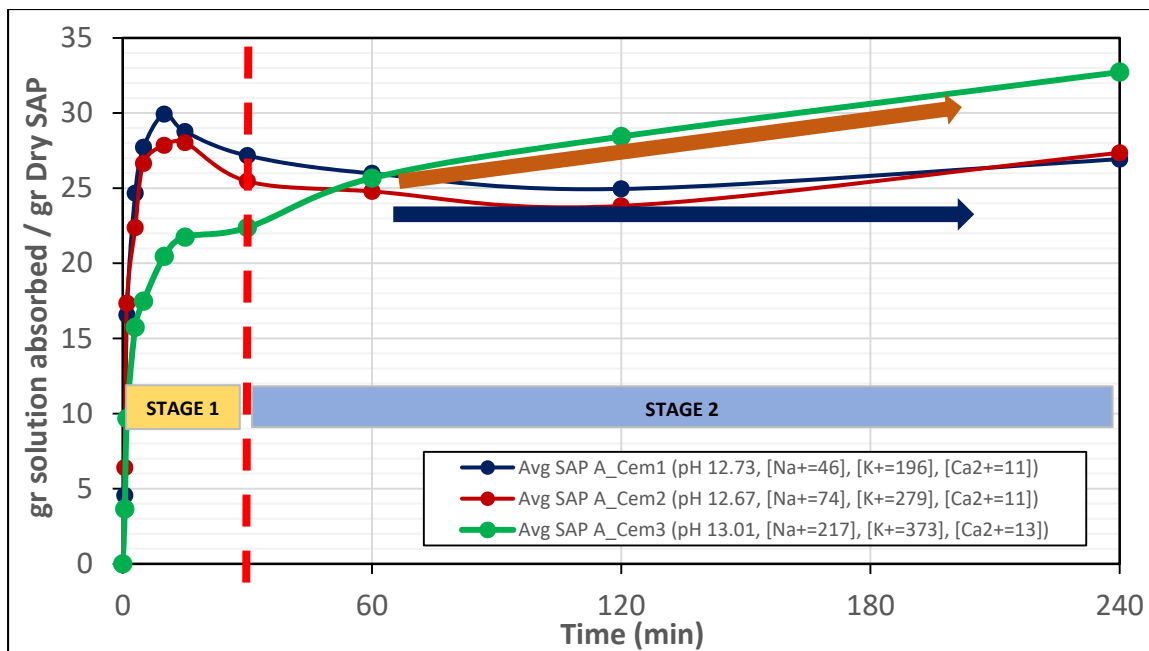


Figure 47 - Absorption capacity isotherm describing different swelling behavior for the same SAP sample through Stage 1 and 2.

The isotherm obtained by the study of the interaction between polymers and a solution with lower concentration of alkali ions and lower pH values shows the highest peak for liquid uptake at 10 minutes of hydration. After that, desorption takes place up to the point in which a more stable behavior is reached. For the solution that recreates the extracted pore solution from Cem2, the highest absorption peak takes place at 15 minutes of hydration. Later on, desorption occurs and a more stable value for absorption capacity is maintained only up to 2 hours when an increased capacity occurs. For the study using the synthetic solution of Cem3, which has the highest pH and highest ion concentration, an initial peak occurs at 15 minutes of hydration. After this, the slope of the plot changes.

4.5.2 Effect of pH and Ion Concentration

To investigate the way in which the absorption isotherm (Figure 48) changes when pH level, sodium, potassium, and calcium content are varied, various solutions were prepared, and tea bag method was conducted. This section compliments the statement just presented about the stages that take place during the swelling behavior of the superabsorbent polymers. Three groups of synthetic solutions were created, each one representing a solution previously studied (SPS-1, SPS-2, and SPS-3).

It is important to clarify that it was assumed that the concentration of alkalis remained constant during the tea bag experiment even though changes in pH and calcium content may occur due to carbonation; in addition, the measured pH of the solution differs from that calculated from the chemistry. See Table 15, in which the ionic concentration was used to calculate the expected pH of the solution compared to the pH measured.

In Figure 48, the first group considered the evaluation of absorption capacity of SAP in two solutions, the SPS-1 Cem1 and the derived from SPS-1, in which the sodium and potassium content were increased. To confirm what was stated in previous sections, the highest water uptake for SAP A is achieved in the solution with the lowest sodium, potassium and calcium content (represented by the dark blue line). The results correspond to the average of the measurements for SAP A when they are exposed to the synthetic solution SPS-1 Cem1. This solution, which has a pH of 12.73, and a concentration of ions as follows $[\text{Na}^+=46 \text{ mmol/L}]$, $[\text{K}^+=196 \text{ mmol/L}]$, and $[\text{Ca}^{2+}=11$

mmol/L], was compared to that of AVG SAP A_Cem1_2. The latter was found to show lower initial water uptake due to larger Na⁺ and K⁺ content, which corresponds to 90 mmol/L and 214 mmol/L, respectively. However, even at lower level of absorption capacity, the shape of the isotherm for the derived solution is very similar to that of SPS-1 Cem1. In both cases, a more stable behavior is observed after 30 minutes of hydration.

In the second group, two solutions, SPS-2 Cem2 and the derived from SPS-2, were compared. In this case, the derived solution had almost twice the sodium concentration and higher potassium content. As expected, a considerably lower absorption level is obtained during the first stage of water uptake due to the presence of a higher concentration of alkali metals, which once again confirms the effect of alkali metals in the early stage of absorption. During the second stage; however, the swelling behavior of the polymer in the derived solution changed by raising the plot after 60 minutes of hydration. At this point, when potassium significantly leads the concentration of ions in the solution, the shape of the plot starts to show the increasing behavior developed by the polymer tested in SPS-3 Cem3. Consequently, the hypothesis about the increase absorption capacity of the superabsorbent polymer studied at high potassium content is recalled.

In the third group, a set of four synthetic solutions derived from SPS-3 (Avg SAP A_Cem3) and the SPS-3 as well, were prepared and used to investigate the combined effect of potassium at different pH levels. This set of solutions was broken down into two

categories, one to test the combined effect of large potassium content at pH above 13.00, and the second, to investigate the effect of high potassium concentration and pH levels below 13.00. All of them are plotted in Figure 48. In general, it was found that the presence of sodium only contributes significantly to the first stage of absorption.

For the first category, which includes Avg SAP A_Cem3, Avg SAP A_Cem3_2, and Avg SAP A_Cem3_3, it was observed again that the concentration of alkali metals affects the swelling rate in the initial stage. The high concentration of alkalis in these solutions lowers the absorption capacity and slows down the swelling rate of the superabsorbent polymers studied. However, during the second stage, the absorption capacity of the polymer tested increases over time.

For the second category, which includes Avg SAP A_Cem3_4, Avg SAP A_Cem3_5, the polymers tested in these solutions show faster swelling ratio during the first stage. When the same type of hydrogel is tested in both solutions, a steeper swelling rate is observed in the Avg SAP A_Cem3_4 (pH=12.90 and $\Sigma[\text{Na}^+, \text{K}^+] = 508$ mmol/L), and the maximum absorption capacity for the polymer occurred at 3 minutes of hydration. On the other hand, for the solution Avg SAP A_Cem3_5 (pH=12.81 and $\Sigma[\text{Na}^+, \text{K}^+] = 605$ mmol/L), the maximum absorption capacity for SAP A occurs at 15 minutes of hydration. During the second stage, the isotherm illustrates lower values for absorption capacity. The overall capacity of the polymer to swell was lower than that obtained for polymers

tested in the first category. Then, it is again hypothesized that the large concentration of potassium motivates an increased absorption capacity behavior during the second stage. To sum up the experimental results, data obtained proved that there is an impact of potassium, calcium and pH on the development of the second stage and final absorption capacity for polymers tested in high alkalinity solutions. However, further research is recommended to clarify this phenomenon.

Table 15 - Concentration of ions and pH values (Calculated and measured) for synthetic solutions

Syntehtic Solution	Concentration of ions measured in (mMol/L)						pH calculated	pH measured
	Na ⁺	K ⁺	Ca ²⁺	Σ (Na + K + Ca)	SO ₄ ²⁻	OH ⁻		
Avg SAP A_Cem1	46	196	11	253	105	148	13,17	12.73
Avg SAP A_Cem1_2	90	214	11	315	105	210	13,32	12.67
Avg SAP A_Cem2	74	279	11	364	157	207	13,32	12.67
Avg SAP A_Cem2_2	130	349	11	490	157	333	13,52	12.77
Avg SAP A_Cem3	217	373	13	603	214	389	13,59	13.01
Avg SAP A_Cem3_2	221	435	14	670	214	456	13,66	13.41
Avg SAP A_Cem3_3	220	288	19	527	214	313	13,50	13.25
Avg SAP A_Cem3_4	215	390	19	624	216	408	13,61	12.90
Avg SAP A_Cem3_5	213	435	21	669	271	398	13,60	12.81

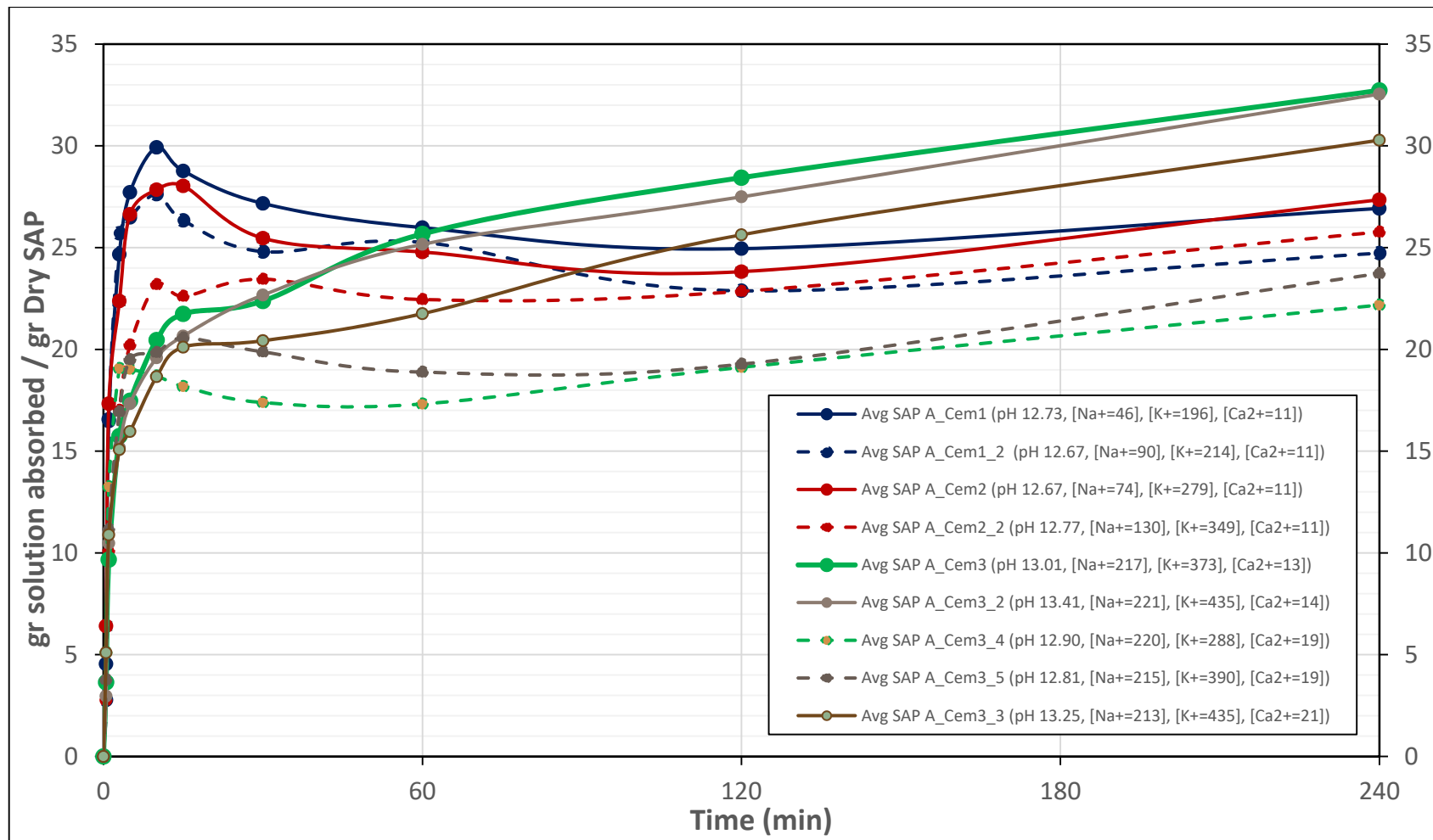


Figure 48 - Swelling behavior of SAP A for different pH and concentration of ions in synthetic pore solution. All the concentrations are in units of mmol/L

4.5.3 Statistical Analysis

In order to back up previous statements about the effect of solution chemistry on absorption capacity, statistical models were run in SAS statistical software comparing the correlation between various combinations of pH level and ion concentration with absorption capacity. The results from the most significant tests are shown in Table 16. An initial set of models was run based on the individual contribution of each ion studied. The strongest correlation was found for potassium, followed by calcium and sodium, respectively, although all were found to be significant. Next, interaction effects were tested for the sum of each combination of the ions. The highest correlation factor was found for those in which potassium was included. Similarly, the interaction between pH and each ion was evaluated. As seen in the Table 16, the r^2 was 0.77 for pH lower than 13 and potassium greater than 350 mmol; however, the adjusted r^2 was significantly lower and the significance test proved it was not significant. Additionally, the interaction effects of potassium and calcium along with pH were stronger than that of sodium and pH, again suggesting they may be more influential ions. All three of these models proved that pH higher than 13 was a strong predictor for increased absorption capacity. Similarly, the effect of pH greater than 13 was found to overshadow the effect of the ions when they were summed in various combinations, as the adjusted r^2 value was the same, independent of the ion predictors. Finally, high concentration of potassium and calcium ions were each tested with high and low values for sodium concentration. It was found that scenarios in which sodium is low show the highest coefficient of determination.

Table 17 presents experimental results obtained in this research and some data from the literature review (TC225-SAP, 2012) (Miller, 2014) (Luis Pedro Esteves, 2014). Different authors presented their results for absorption capacity of superabsorbent polymers tested in synthetic solutions with concentrations of alkali ions higher than that of the synthetic pore solutions used in this research work. Absorption capacities reported by these authors are not always higher than that obtained for the hydrogels tested in this study. Differences may be attributed to variations in the duration of the test, nature and properties of the polymer, and more importantly, the combined effect of pH and ion concentration of the synthetic solution, including calcium. For instance, in (TC225-SAP, 2012), a solution with a calculated pH of 13.86, which differs from the pH of the solutions studied, was used to test the absorption capacity of a crushed irregular SAP particles. For this, an absorption capacity of the hydrogel of about 37 grams of pore fluid per gram of polymer in 10 minutes is stated. A similar cement composition was studied by (Miller, 2014), following same test procedures. Comparable results were reported for absorption capacity, and lower absorption capacity was also observed for finer SAP.

Table 16 - Most significant models

			Significance test
Model (Concentration in mmol/L)	r²	Adjusted r²	p-value<0.05
Na ⁺ >215 mmol	0.6955	0.6549	OK
K ⁺ >350 mmol	0.7801	0.7581	OK
Ca ²⁺ >12 mmol	0.6986	0.6745	OK
Sum of Na ⁺ and K ⁺ > 580 mmol	0.7801	0.7581	OK
Sum of Na ⁺ and Ca ²⁺ > 90 mmol	0.6986	0.6745	OK
Sum of K ⁺ and Ca ²⁺ > 350 mmol	0.7801	0.7581	OK
Sum of Na ⁺ , K ⁺ and Ca ²⁺ > 600 mmol	0.7801	0.7581	OK
pH>13 and Na ⁺ >215 mmol	0.8549	0.8258	OK
pH>13 and K ⁺ > 350 mmol	0.8708	0.8536	OK
pH<13 and K ⁺ > 350 mmol	0.7714	0.5885	Not significant
pH>13 and Ca ²⁺ > 12 mmol	0.8708	0.8536	OK
pH>13 and sum of Na ⁺ and K ⁺ > 580 mmol	0.8708	0.8536	OK
pH<13 and sum of Na ⁺ and K ⁺ > 580 mmol	0.7714	0.5885	Not significant
pH>13 and sum of Na ⁺ and Ca ²⁺ > 90 mmol	0.8708	0.8536	OK
pH>13 and sum of K ⁺ and Ca ²⁺ > 350 mmol	0.8708	0.8536	OK
pH>13 and sum of Na ⁺ , K ⁺ and Ca ²⁺ > 600 mmol	0.8708	0.8536	OK
Na ⁺ >215 mmol and K ⁺ > 350 mmol	0.8549	0.8258	OK
Na ⁺ <215 mmol and K ⁺ > 350 mmol	0.9691	0.9444	OK
Na ⁺ >215 mmol and Ca ²⁺ > 12 mmol	0.6955	0.6549	OK
Na ⁺ <215 mmol and Ca ²⁺ > 12 mmol	0.9691	0.9444	OK

Table 17 - Determined absorption capacity of SAP based on the synthetic solutions

Information Provided by:	This research - Experiments			Literature review				
Solution tested / Author	SPS1 - Cem1	SPS2 - Cem2	SPS3 - Cem3	1. Jensen and Hansen	1. Jensen and Hansen	2. Miller	2. Miller	3. Estevez
Absorption Capacity of SAP (g _{Pore solution} /g _{Dry SAP})	26.93	27.35	32.73	20.00	37.00	18.30	23.50	From 10 to 16
pH of the solution	12.73	12.67	13.01	Not reported	Not reported	12.86	12.86	Not reported
K⁺ (mmol/L)	196	279	373	400	400	401	401	500
Na⁺ (mmol/L)	46	74	217	400	400	229	229	200
Ca²⁺ (mmol/L)	11	11	13	1	1	7	7	1
[K+Na (mmol/L)]	242	353	590	800	800	630	630	700
Type of SAP	Acrylic Acid - BASF	Acrylic Acid - BASF	Acrylic Acid - BASF	Covalently Crosslinked acrylamide/acrylic acid copolymers	Covalently Crosslinked acrylamide/acrylic acid copolymers	Not reported	Not reported	Covalently Crosslinked acrylamide/acrylic acid copolymers
Details about SAP	Not reported	Not reported	Not reported	Suspension-Polymerized SAP	Solution-polymerized SAP	Bulk solution polymerization	Bulk solution polymerization	Suspension polymerized SAP
Reference/Source	Material Data Sheet Provided by BASF	Material Data Sheet Provided by BASF	Material Data Sheet Provided by BASF	Appication of SAP in concrete construction	Appication of SAP in concrete construction	Using a centrifuge for quality control	Using a centrifuge for quality control	Superabsorbent polymers: On their interaction with water and pore fluid
Particle Shape and size	Irregular	Irregular	Irregular	Round particles, average 200 microns	Crushed irregular particles, 125-250 microns	Particle size between 50 and 125 microns	Particle size below 100 microns	Spherical particles, Particle size 50-500 microns
Time at which Absorption is calculated (Min)	240	240	240	60	10	30	30	≈ 20 min

1. (TC225-SAP, 2012)
2. (Miller, 2014)
3. (Luís Pedro Esteves, 2011a).

CHAPTER 5. INFLUENCE OF SUPERABSORBENT POLYMERS IN THE INTERNAL CURING MECHANISM IN CEMENT PASTE

5.1 Introduction

Chapter 5 presents the response of an ordinary Portland cement-based system to the addition of SAP as an internal curing mechanism. The experimental approach uses the variables studied in previous chapters to contribute to the understanding of the impact of hydrogels on the hydration process and volumetric change. Cement pastes were prepared with and without the addition of SAP A and B. Calorimetry and autogenous shrinkage tests were used to evaluate the extent of hydration at 7 days and the potential shrinkage due to self-desiccation, respectively.

5.2 Experimental Methods

5.2.1 Cement Paste

For this research, a reference cement paste is defined as a mixture of plain cement and water, without the addition of superabsorbent polymers. Reference cement pastes were prepared using cement from Cem1, Cem2 and Cem3. Similarly, internally cured cement pastes containing SAP A and B were made to evaluate the effect of their inclusion in an ordinary Portland cement-based system.

For all mixes, deionized water was used as the mixing water. Table 18 presents the mix designs implemented for cement paste preparation. For reference pastes, equal amounts of cement and water were mixed regardless of the cement source. In contrast, differences in mix proportioning were used when SAP was added due to variation in absorption capacity of the polymer for each cement.

Table 18 - Mix designs used for reference and internally cured cement pastes

Mixture Proportions		Reference	Internally cured cement pastes		
Materials	Description	REF 0.30	IC-Cem1 (kg/m ³)	IC-Cem2 (kg/m ³)	IC-Cem3 (kg/m ³)
Cement	Cem1, Cem2, Cem3	1618	1484	1484	1484
SAP	A or B	0	2.99	2.95	2.46
Water	Designed w/c water	485	445	445	445
	IC water	0	81	81	81
Total water	Designed w/c water + IC water	485	526	526	526
w/c	Based on designed w/c water	0.30	0.30	0.30	0.30
W _{ic}	W _{ic}	0	0.05	0.05	0.05
Overall w/c	Actual w/c	0.30	0.35	0.35	0.35
SAP	% SAP added (bwc)	0%	0.20%	0.20%	0.17%

The mass of SAP required was calculated by equating the water demand of the cementitious system and the expected supply provided by the hydrogels using Equation 1 (B. Y. D. P. Bentz, Lura, & Roberts, 2005) (D. P. Bentz & Snyder, 1999) (Dale P Bentz & Weiss, 2010). Mix proportioning calculations were developed following (B. Y. D. P. Bentz et al., 2005), which is the concept typically used for mix design of internal curing concrete.

$$M_{SAP} = \frac{C_f \times CS \times \alpha}{\Phi_{SAP}} \quad (1)$$

Where,

M_{SAP} = Mass of SAP (Kg of dry SAP per m^3 of concrete)

ϕ_{SAP} = Absorption capacity of the SAP in kg of solution absorbed per kg of dry SAP.

C_f = Cement content in kg/m^3 - Taken from mix design

CS= Chemical shrinkage of cement in gram of water per gram of cement.

α = Maximum expected degree of hydration of cement (DOH).

The absorption capacity of the polymers, also called ϕ_{SAP} , was determined using the tea bag method. Table 13 and Table 14, presented in Chapter 4, list the values used for mix design. Chemical shrinkage, CS, and the maximum degree of hydration (DOH), also called α , were calculated based on Power's model. For w/c of 0.30 in sealed condition, the DOH was found to be 0.73. Table 19 shows the distribution of volume based on Power's model.

Figure 49 illustrates the expected volume distribution based on Power's model when a cement paste is prepared at w/c=0.30 and cured under sealed condition. In this figure, the point at which maximum degree of hydration (DOH) is reached corresponds to the intersection between the orange line and the royal blue line. The former line denotes the evolution of chemical shrinkage, whereas the latter line corresponds to the increasing values for capillary water.

Table 19 - Volumetric distribution based on DOH of a sealed cement paste of w/c=0.30

w/c	0,3	
density of water	1000	
density of cement	3150	
Initial Porosity (p)	0,49	max DOH
Calculations		Sealed
Degree of Hydration (0 to1)	0	0,73
Volume of Chemical Shrinkage	0,00	0,07
Volume of Gel Water	0,00	0,22
Volume of Hydrated Solid (Gel Solid)	0,00	0,56
Volume of Capillary Water	0,49	0,00
Volume of Cement	0,51	0,14
Total Volume	1,00	1,00
Plot Values		
Degree of Hydration (0 to1)	0	0,73
Volume of Cement	0,51	0,14
Volume of Hydrated Solid (Gel Solid)	0,51	0,70
Volume of Gel Water	0,51	0,93
Volume of Chemical Shrinkage	1,00	0,93

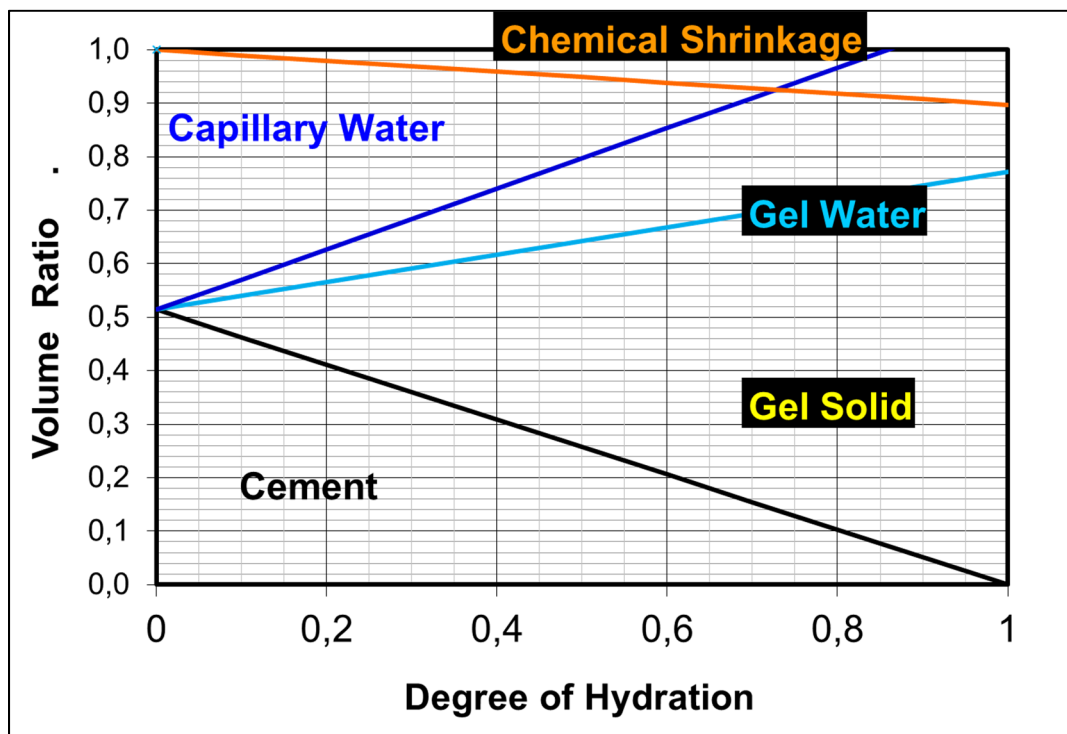


Figure 49 - Power's model for a cement paste at w/c 0.30 (cured in sealed condition)

A FlackTek Speedmixer™ DAC 400.1 FVZ, a dual asymmetric centrifuge that combines forces in different planes for fast mixing, is used to mix the cement and SAP in dry state. The mixing mechanism of the equipment allows the uniform distribution of SAP particles throughout the volume of cement. An alternating sequence of three mixing and two cooling stages is executed in the following fashion: 1-minute mixing at 1,000 rpm followed by a 30-second cooling stage. After removing the container with the sample from the mixer, the sample is allowed to cool at room temperature for approximately 5 minutes. After this, the material is mixed with water, and cement pastes are prepared following the ASTM C305-14 – “Standard Practice for Mechanical Mixing of Hydraulic Cement Pastes and Mortars of Plastic Consistency”.

5.2.2 Isothermal Calorimetry

The hydration process of cement is comprised of five reaction stages: initial hydrolysis, dormant period, acceleration, deceleration and steady state (Mindess & Young, 1981). These stages begin to occur as soon as cement, a hydraulic binder, is exposed to water. Isothermal calorimetry has previously been presented as the best way to monitor the evolution and extent of the hydration process (TA Instruments, 1985).

Due to the quick transition from the initial hydrolysis to the dormant period, cement and water must be mixed inside the calorimeter by means of an admix ampoule. However, in this research, all mixes were prepared outside the calorimeter due to the low w/c investigated. Cement pastes were made with and without the addition of SAP in

order to compare the consequences of including polymers in the evolution of the reactions and degree of hydration. Samples without hydrogels were labeled as reference whereas samples containing polymers were categorized as internally cured pastes. To prepare the samples, the ASTM C305-14, "Standard Practice for Mechanical Mixing of Hydraulic Cement Pastes and Mortars of Plastic Consistency" was followed.

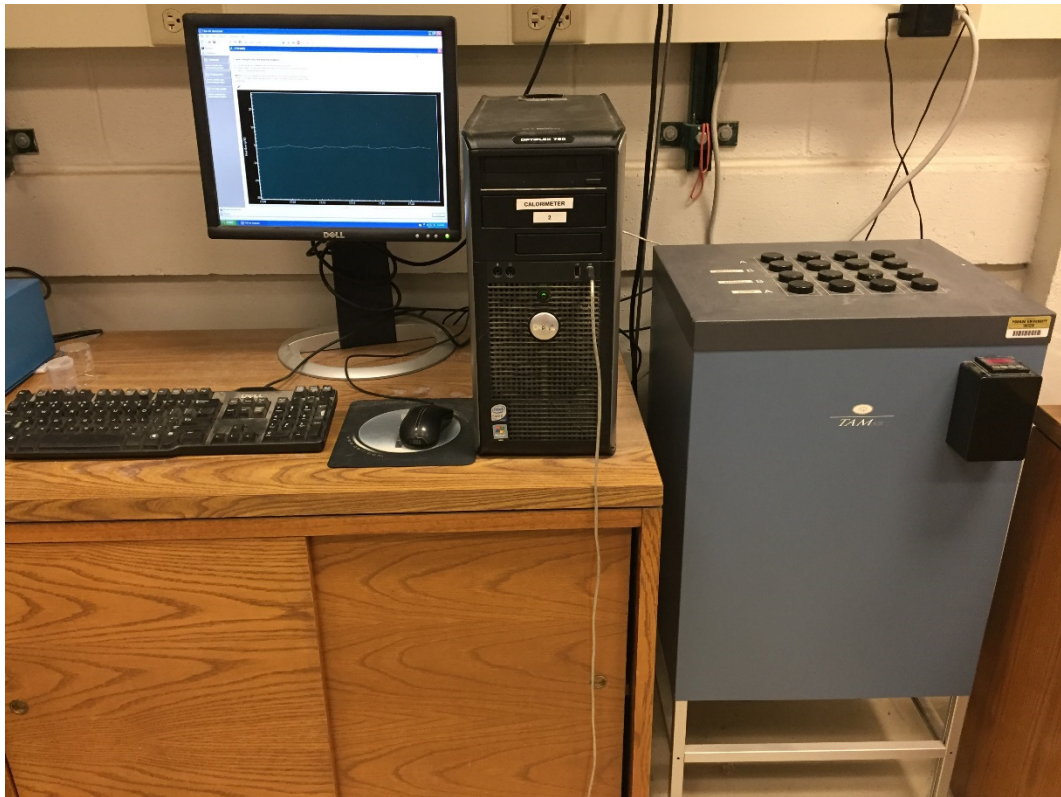


Figure 50 - TAM Air Isothermal Calorimeter used for calorimetry studies of cement pastes with and without inclusion of superabsorbent polymers (SAP)

An 8-channel TAM Air isothermal calorimeter manufactured by TAM Instruments and the TAM Air Assistant V1.0.116.50 were used to assess the extent of cement reaction for

reference and internally cured samples. Figure 50 presents the setup for the calorimeter and the computer unit connected to the equipment. For calorimetry results samples are labeled as follows: reference pastes are identified as Cem1, Cem2, and Cem3, whereas; for instance, internally cured systems (labeled IC-Cem1, IC-Cem2, and IC-Cem3 in Table 18) are identified as Cem1+SAP A, which corresponds to IC-Cem1 with addition of SAP A. Likewise, all the cement pastes are labeled.

5.2.3 Autogenous Strain of Cement Paste

According to (Japan Concrete Institute, 1999), the apparent volume or external volume of a cementitious system corresponds to the sum of the solid, liquid and gaseous components present in the system. Autogenous shrinkage is a reduction in the apparent volume of the cement paste, which is also related to self-desiccation. Before setting, a bulk contraction of the cement paste due to hydration of cement results in equivalent chemical and autogenous shrinkage (Lura, Winnefeld, & Klemm, 2010) (Gagné, Aouad, Shen, & Poulin, 1999). After setting, formation of solid hydration products creates a solid skeleton that avoids further external deformation of the cement paste (Gagné et al., 1999); therefore, the extent of autogenous shrinkage developed is less than that of chemical shrinkage. Figure 51 illustrates the shrinkage evolution on time, denoting differences between chemical and autogenous shrinkage. In addition, contrary to chemical shrinkage, empty and filled internal voids are taken into account as part of the apparent volume that describes autogenous shrinkage.

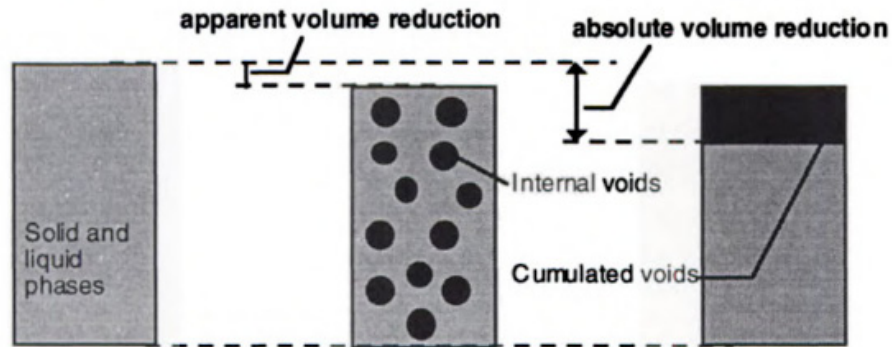


Figure 51 - Comparison of Autogenous and Chemical Shrinkage (Japan Concrete Institute, 1999)

The autogenous strain of cement pastes with and without the addition of SAP is measured in specimens prepared following the ASTM C1698 – 09 (Reapproved 2014), “Standard Test Method for Autogenous Strain of Cement Paste and Mortar”. Approximately 200 cm³ of cement paste is casted into standardized corrugated tubes of 420 ± 5 mm in length and 29 ± 0.5 mm in outer diameter (ASTM Standard C1698, 2014). Plastic end plugs are used to seal the molds. After weighing out the specimens, a sample is positioned horizontally on a stainless-steel dilatometer bench for 7 days. Calibrated linear variable displacement transformers (LVDTs) monitor the length change of the specimens and an automated system records the measurements taken at a rate of one measurement every 5 minutes. According to the standard, “three replicate specimens shall be tested for each cement paste”. Figure 52 shows the setup of the test while three samples are monitored.



Figure 52 –Autogenous shrinkage test of cement paste - ASTM C1698 – 09 (Reapproved 2014), “Standard Test Method for Autogenous Strain of Cement Paste and Mortar”.

5.3 Experimental Results

5.3.1 Isothermal Calorimetry

As expected, isothermal calorimetry showed differences in the hydration process between reference and internally cured ordinary cement pastes. Differences were primarily identified at early age (within the first 24 hours) and at 7 days. For the former, changes in the dormant period and heat flow rate at the acceleration period were identified. At 7 days, variation in cumulative heat of hydration was obtained for all the systems. The common shift obtained between the isothermal calorimetry plots of cement pastes with and without addition of SAP is attributed to changes in

concentration of alkali ions and water-to-cement ratio available throughout the hydration process.

Figure 54 presents the results of isothermal calorimetry for reference cement pastes prepared at $w/c=0.30$ and using cement from Cem1, Cem2 and Cem3 for 7 days. Figure 53 is a close-up of the same reference systems during the first 24 hours of hydration. In the short-term, cement pastes prepared with Cem1 have the shortest dormant period and the lowest heat flow rate (mW/gcement). The latest beginning of the acceleration period is developed by samples prepared with Cem3 as well as the steepest main hydration peak; consequently, it has the largest heat flow rate followed by Cem2 and Cem1, respectively.

The behavior shown in Figure 53 and Figure 54 relates to the chemical composition presented in the mill certificate (Table 2). In this, both Cem2 and Cem3 have larger C_3S content than that of Cem1, which along with the alkalis content (mainly potassium ions (Odler, 2003)) contributes to the high intensity of the main peak in the acceleration period. Cem1 contains lower C_3S yet the largest C_2S content, which over time reacts and overlaps with the contribution of C_3S to the hydration reaction of Portland cement. On the other hand, Cem2 experiences a hump before the main peak that may be related to low sulfate content (not enough to control C_3A hydration).

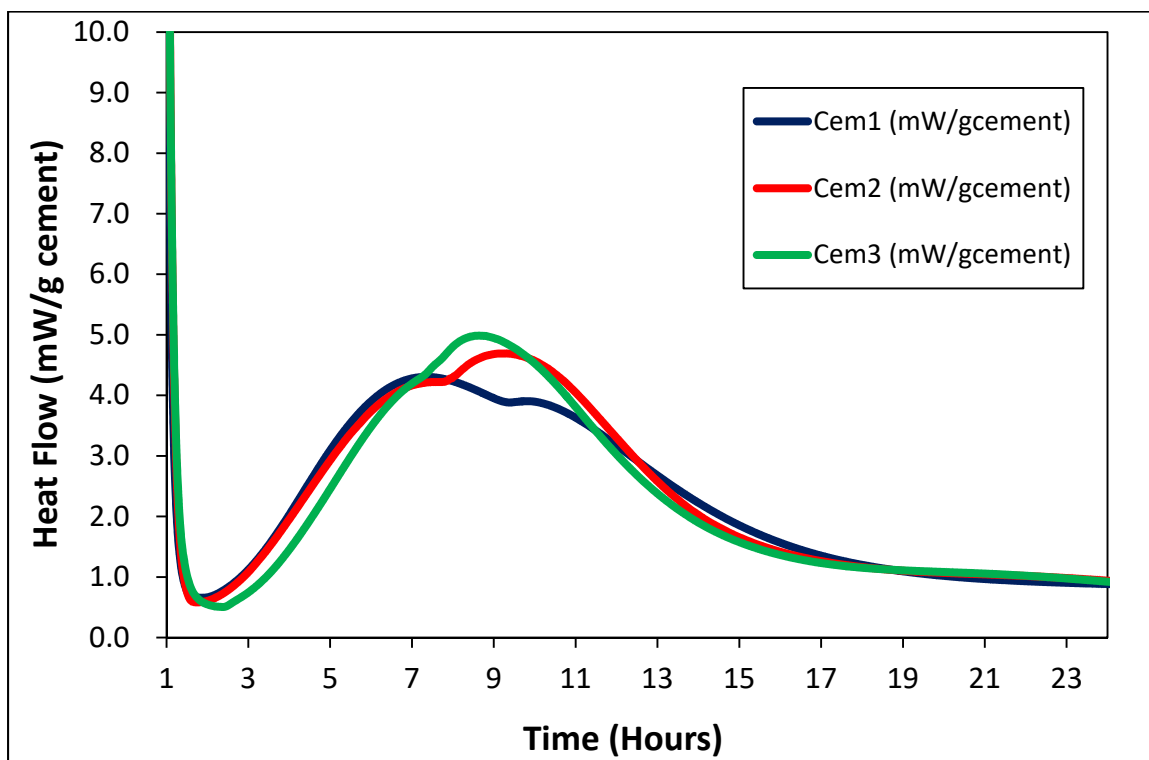


Figure 53 - Isothermal Calorimetry of reference cement pastes at w/c=0.30 (First 24 h)

Figure 53 also evidences the effect of alkalis content in the regulation of set time of cement. Cem3 and Cem2, which have the highest and second highest alkalis content, 0.72% and 0.62%, respectively, present the largest and second largest heat release during hydration.

To evaluate the evolution of hydration, in Figure 54, the cumulative heat (in units of Joule per gram of cement, J/g_{cement}) is plotted also on the secondary vertical axis (right hand side of the plot). The reference paste prepared using Cem1 develops the largest cumulative heat released compared to those of the other two cement pastes. The cement paste prepared using Cem2 develops the second largest cumulative heat. At 7 days, the cement paste prepared with Cem1 released approximately $275 J/g_{\text{cement}}$ while Cem2 released around $266 J/g_{\text{cement}}$, followed by Cem3 paste with an approximate cumulative heat release of $258 J/g_{\text{cement}}$.

During the hydration of Cem1, two small peaks were detected after the main peak or deceleration stage. The first hump is related to the renewed AFt formation whereas the second one is due to the AFt-AFm conversion (Odler, 2003). The latter peak was common for all the cements studied.

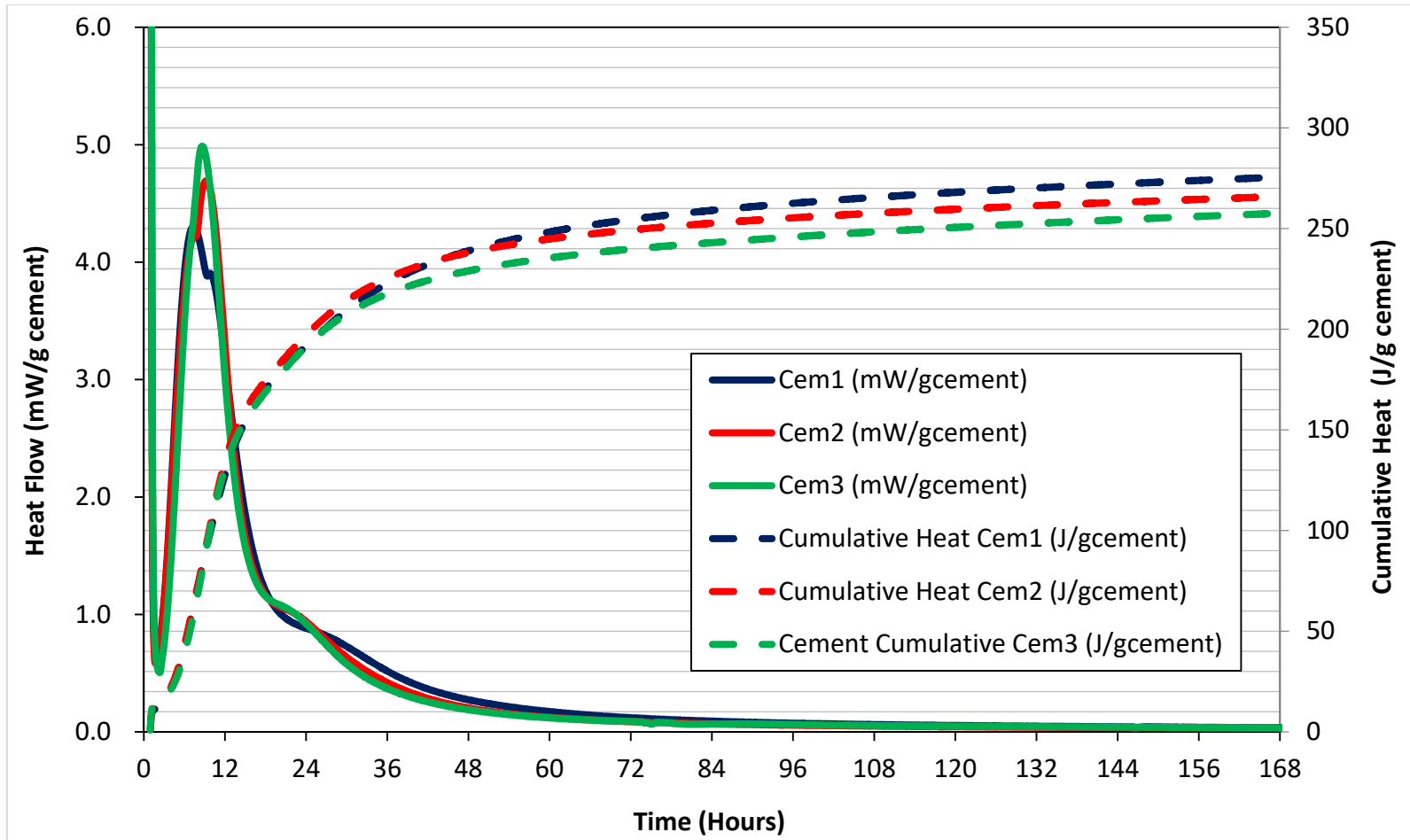


Figure 54 - Isothermal Calorimetry of reference cement pastes prepared with Cem1, Cem2 and Cem3 at free w/c=0.30

Isothermal calorimetry was also conducted for cement pastes in which SAP was added for internal curing purposes. The first cementitious system investigated corresponds to pastes prepared with Cem1. Both reference and internally cured pastes are compared in Figure 55 and Figure 56. An overall lower heat flow rate is observed for cement samples that are internally cured. Even though a retardation effect is observed, no significant differences are obtained for systems in which the polymer size was modified. In the case of IC-Cem1-SAP B (labeled Cem1+SAP B), the rate of heat flow was slightly higher than that of IC-Cem1-SAP A (Cem1+SAP A). This is perhaps related to a better SAP distribution throughout the volume of cement, which promotes hydration of more cement particles.

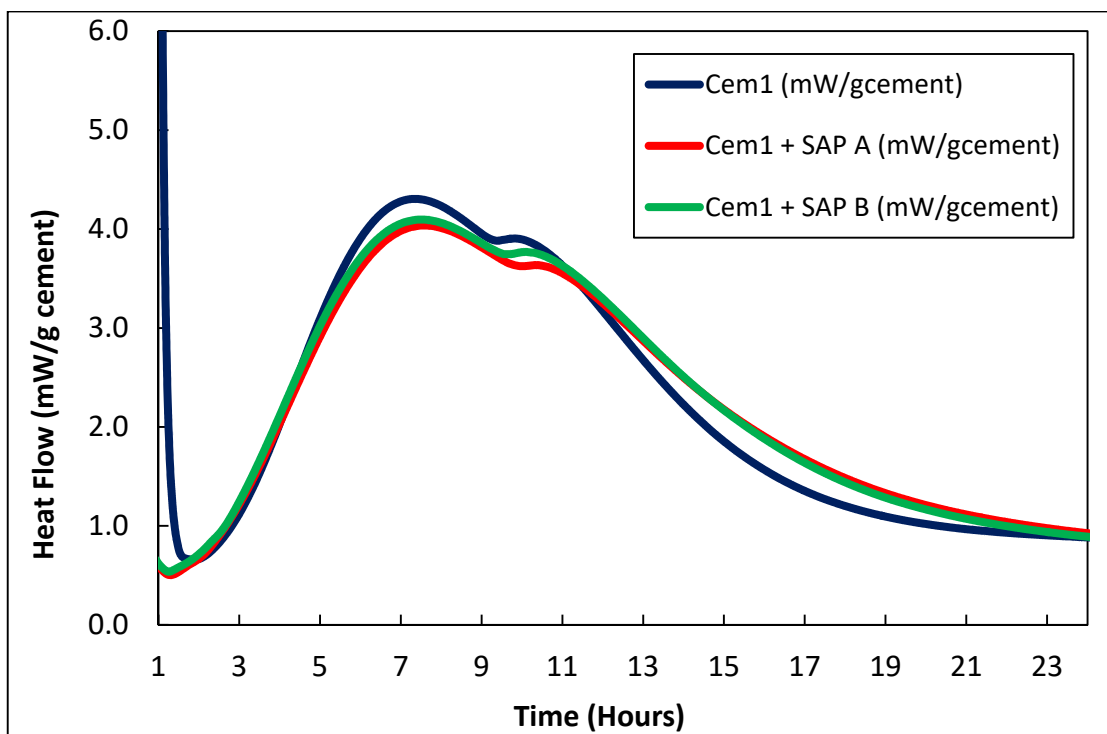


Figure 55 - Rate of heat Flow for cement pastes prepared with Cem1 at $w/c=0.30$ and SAP A and B

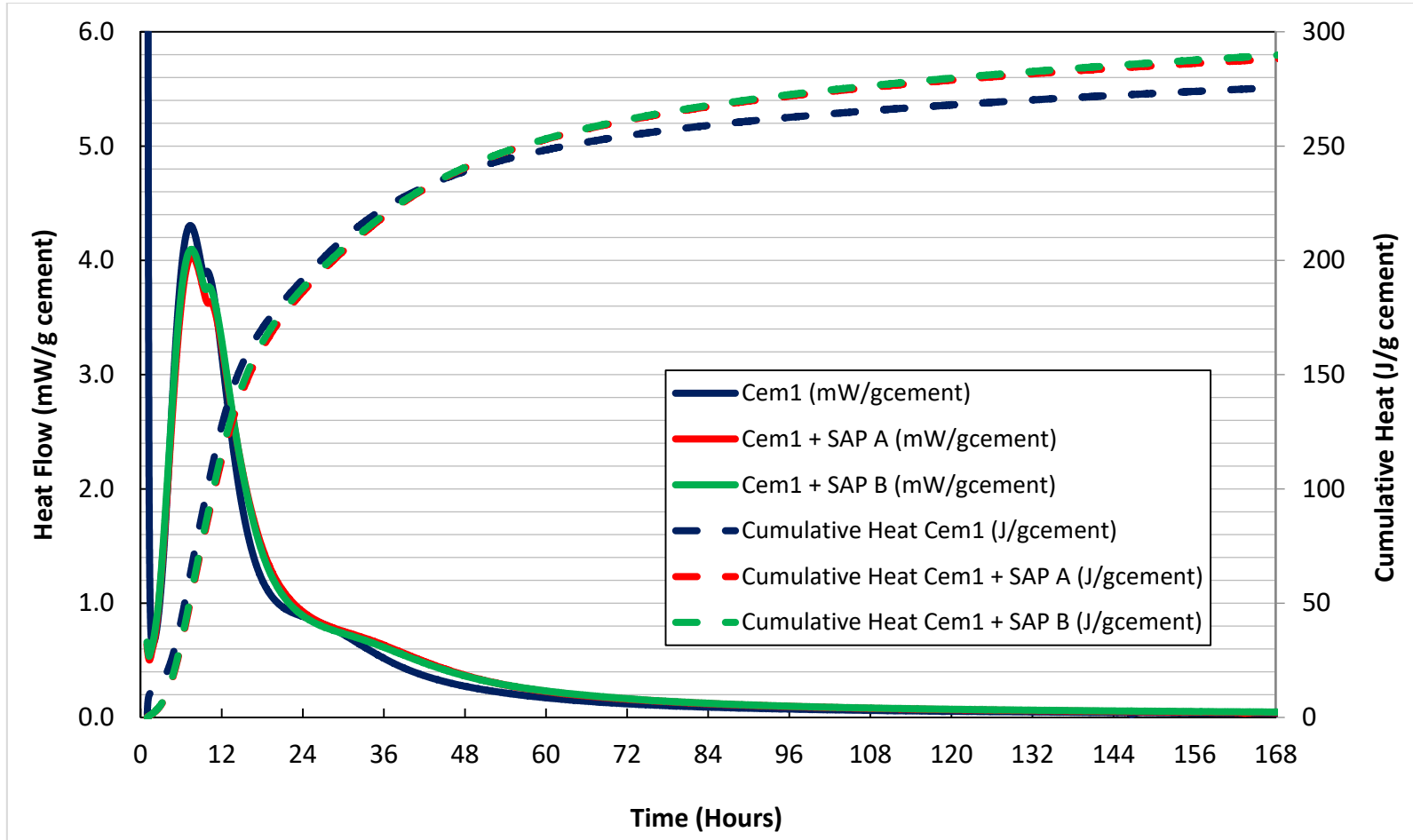


Figure 56 - Isothermal Calorimetry of cement pastes with and without SAP prepared with Cem1 at free w/c=0.30

The retardation of the main peak along with a slower rate of heat liberation are attributed to less concentration of alkalis due to the absorption developed by the SAP, in which cations are fixed to the carboxylic groups of the hydrogels, and higher water-to-cement ratio, also called dilution effect (Janis Justs et al., 2014) (J. Justs et al., 2015). Concentration of alkalis drives the pH of the pore solution, which catalyzes or delays cement hydration (Janis Justs et al., 2014). For Cem2, similar behavior to that of Cem1 was observed (see Figure 57 and Figure 58). As observed in ICS prepared with Cem1 and Cem2, larger w/c slows down the rate of heat flow in the main calorimetric peak. In low to medium alkalinity cements, this effect is more notorious (Janis Justs et al., 2014).

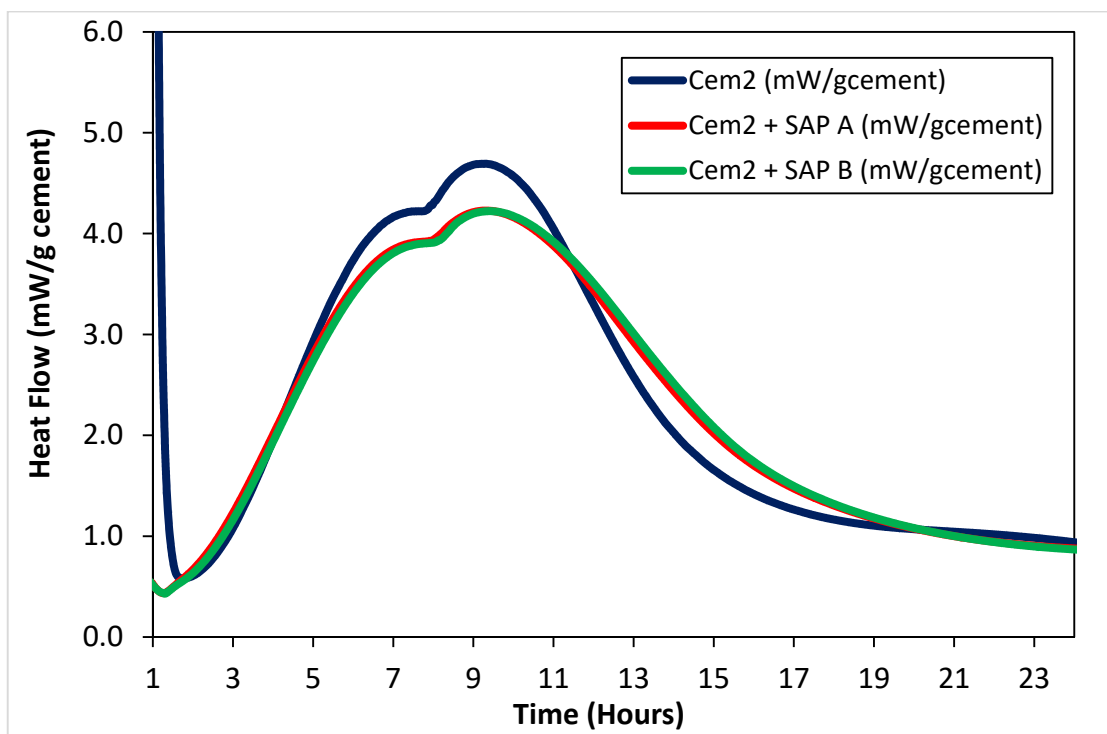


Figure 57 - Rate of heat Flow for cement pastes prepared with Cem2 at w/c=0.30 and SAP A and B

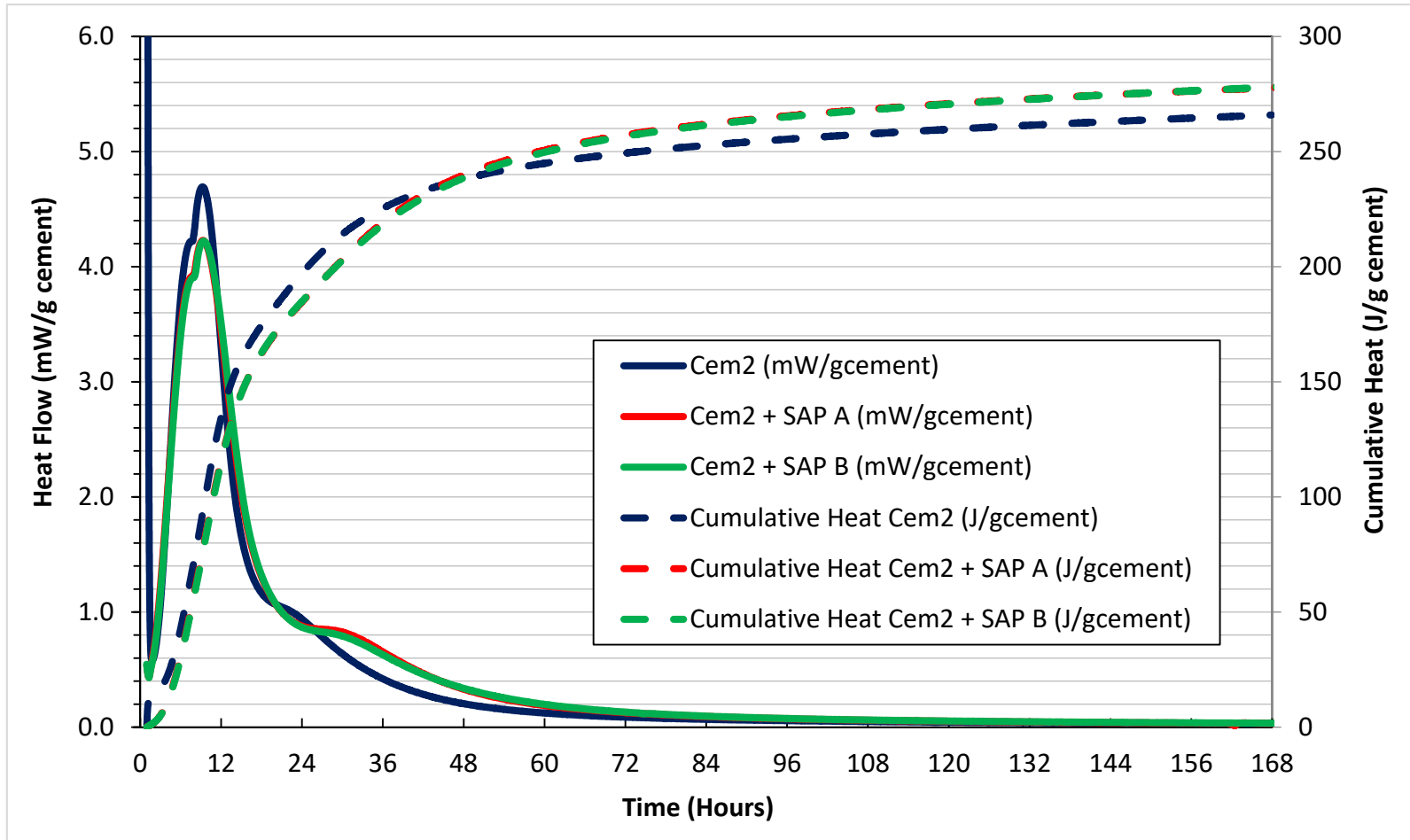


Figure 58 - Isothermal Calorimetry of cement pastes with and without SAP prepared with Cem2 at free w/c=0.30

Figure 59 and Figure 60 show the isothermal calorimetry results obtained for Cem3 with and without the addition of SAP at 24 hours and 7 days, respectively. If all the calorimetry results are to be analyzed at the same time, it is observed that as the alkalinity increases, the acceleration period shifts to the left showing earlier development yet lower heat flow rate (as it is common for all the ICS). As it was observed in the absorption capacity test for SAP in high alkalinity pore solution, lower absorption capacity is developed at the beginning but the same property increases over time, which results in more alkalis released back to the system during desorption. It is hypothesized that during absorption or polymer swelling, more deprotonation takes place, more alkalis get fixed to the carboxylic acid group, and some additional water molecules are formed. However, deprotonation effects might be considered negligible due to the low density of carboxylic groups contained in a swollen polymer particle. It is suggested that monitoring the change in mass for longer periods of time using the tea bag method would represent better the balanced reached by the polymer after the osmotic pressure developed by the high ionic concentration of the solution is reduced.

In terms of cumulative heat, changes are observed after 12 hours when the hydration rate changes, and the secondary hump is delayed in ICS. However, the cumulative heat plots for ICS surpass the reference samples after 60 hours due to further extent of hydration promoted by the internal curing agents. The usage of lower amount of SAP in ICS prepared with Cem3 results in a small difference between the overall cumulative heats released obtained at 7 days for reference samples and that of ICS.

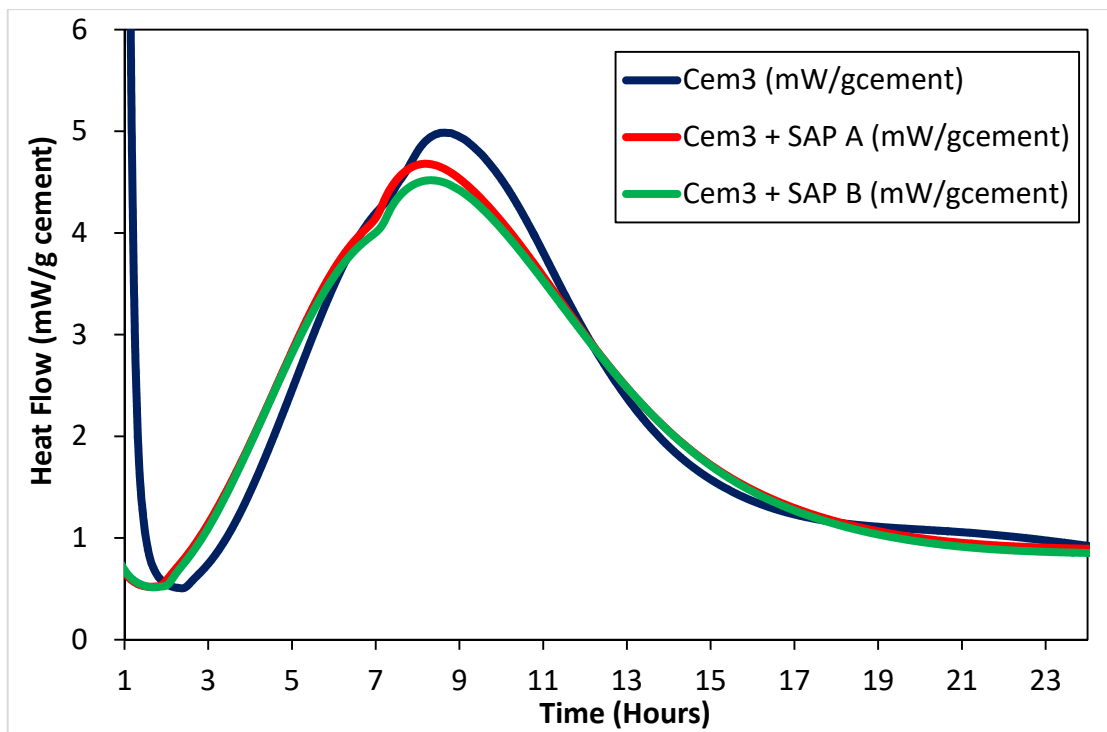


Figure 59 - Rate of heat Flow at 24 h for cement pastes prepared with Cem3 at $w/c=0.30$ with and without SAP. Samples with SAP inclusion are considered Internally Cured Systems (ICS)

To separate the effect of SAP addition from that caused by larger w/c ratio on calorimetry, reference mixes were prepared at the designed water to cement ratio of 0.30 and 0.35. These were compared to internally cured systems, in which the internal curing water corresponds to $w_{IC}/c=0.05$, for a total $w/c=0.35$. Table 20 contains the mix proportions used. For reference samples, Cem3 was run at $w/c=0.35$. For internally cured systems (IC-0.20SAP), Cem1 and Cem3 were tested with the same amount of SAP B to investigate the effect of the same amount of SAP in different alkalinity cements. The results for isothermal calorimetry for the first 24 hours, presented in Figure 61, show a slight retardation effect for all the internally cured systems as well as the

reference cement paste with $w/c=0.35$. In the case of Cem1, the reasons were already covered in previous sections. Since the isothermal for the ICS of Cem3 shows very similar behavior to that of reference Cem3, the ICS sample indicates that most of the SAP desorption occurs within the first 24 hours, and the water absorbed is available for hydration purposes. A very slight difference in the acceleration period between the latter two samples may be attributed to the fact that the pore solution released contains alkali ions that accelerate the hydration of the cementitious system. Although the isothermal results (see Figure 62) for the same water-to-cement ratio are similar, there exists a difference that becomes an advantage for durability purposes. It is that in systems in which SAP are added, there is better control over the internal curing water as well as over the porosity formed by the hydrogels' inclusions. In contrast, for the reference paste with $w/c=0.35$, randomly distributed and connected voids are developed. Then, the permeability level of the cementitious matrix may reach higher values, which influences the service life of reinforced concrete structures.

Table 20 - Mix proportions for reference samples at different w/c ratios and internally cured samples

Mixture Proportions - Isothermal Calorimetry		Reference $w/c=0.30$	Reference $w/c=0.30$	IC Cement Pastes
Materials	Description	REF 0.30	REF 0.35	IC-0.20SAP
Cement	Cem1, Cem3	1618	1618	1484
SAP	SAP B	0	0	2.99
Water	Designed w/c water	485	566	445
	IC water	0	0	81
Total water	Designed w/c water + IC water	485	566	526
w/c	Based on designed w/c water	0.30	0.35	0.30
SAP	% SAP added (bwc)	0%	0%	0.20%

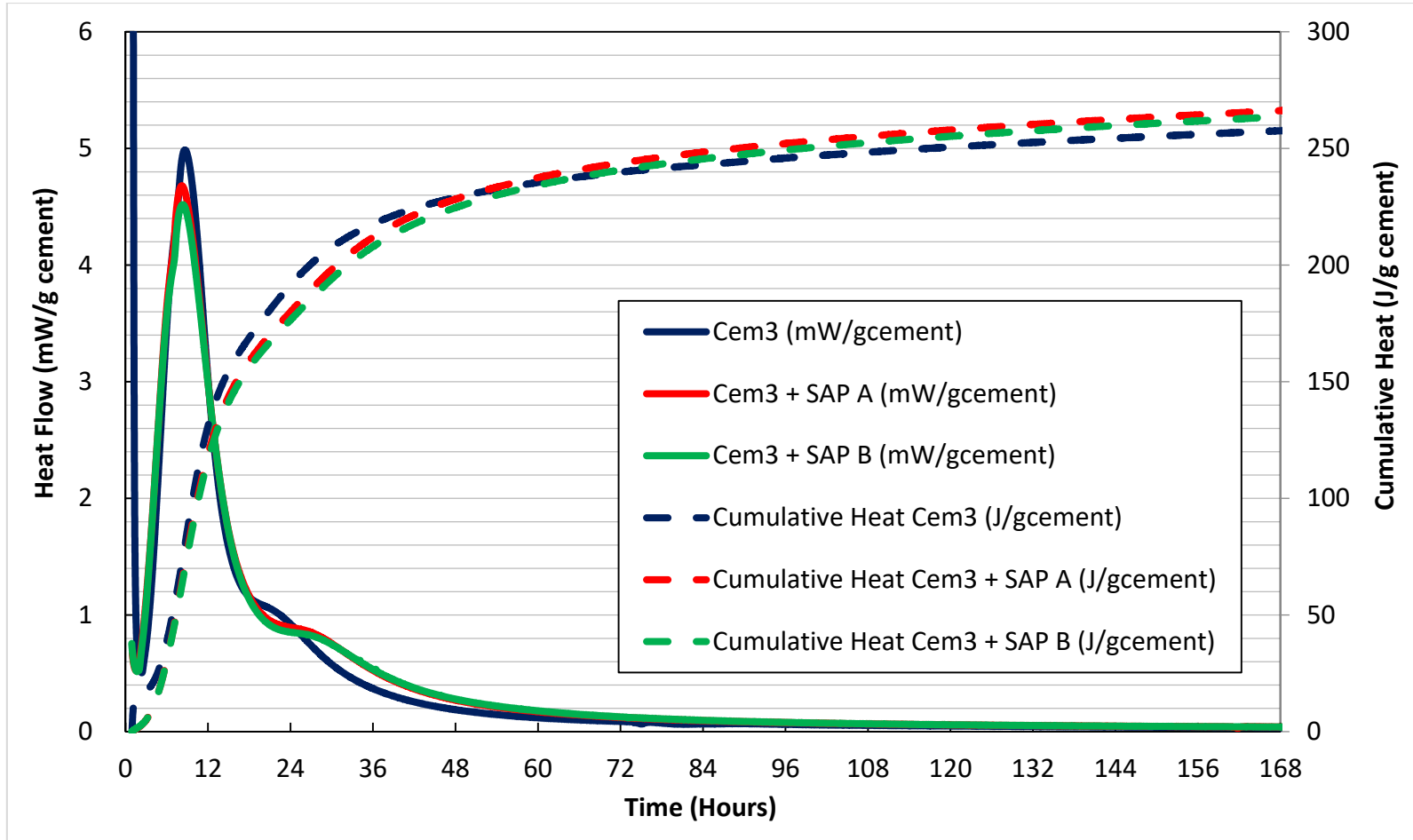


Figure 60 - Isothermal Calorimetry of cement pastes with and without SAP prepared with Cem3 at free w/c=0.30

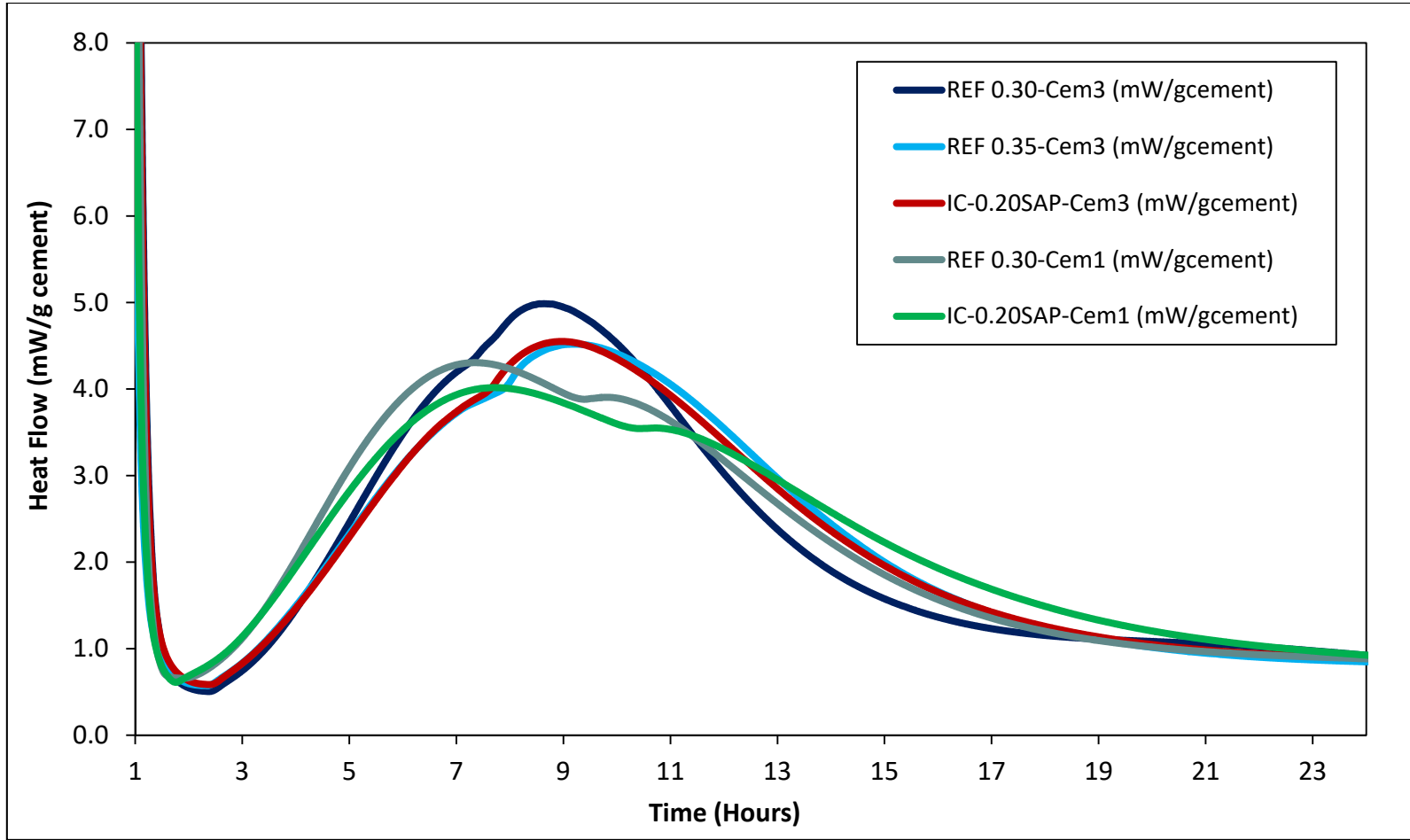


Figure 61 - Rate of heat Flow at 24 h for reference cement pastes and IC-0.20SAP cement pastes

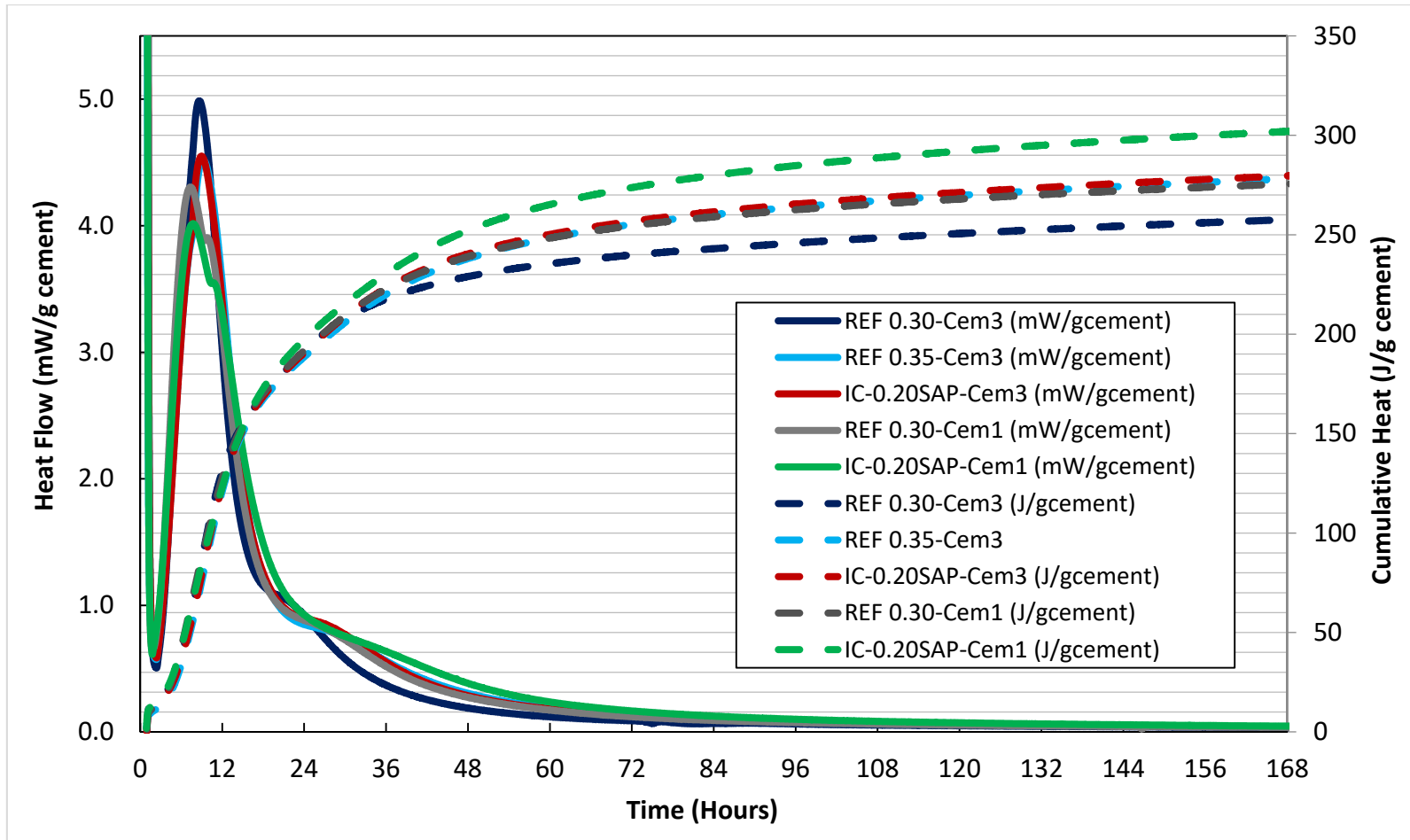


Figure 62 - Isothermal Calorimetry of cement pastes with and without SAP B prepared with Cem1 and Cem3

5.3.2 Autogenous Shrinkage

According to Figure 63, the levels of autogenous shrinkage developed for reference cement pastes are considerably high. However, in good agreement with similar studies (Jensen, 2013), the addition of SAP (according to the absorption capacity of SAP in synthetic pore solution-SPS) reduces the magnitude of shrinkage significantly. When an internal curing agent is added, it is expected to reduce the autogenous shrinkage to almost zero micro-strains or even above zero (showing expansion). In this case, for all the systems, this expectation was not met. This happens because the expected absorption capacity of the polymer (tested in SPS) was not reached in the hydrating cementitious system, and more SAP needs to be considered in mix proportioning.

For internally cured cement pastes prepared with Cem1 (see Figure 64), a reduction in autogenous shrinkage from -687 to -275 micro-strain (more than 410 micro-strain) is experienced. In this case, more pore solution was absorbed by SAP during the first minutes of hydration due to the low concentration of alkalis in pore solution. Since more pore solution was absorbed, more solution is expected to be released back to the system as soon as the system starts to run out of water. Then, the internal relative humidity (IRH) of the hydrating cement paste is conserved and less shrinkage due to self-desiccation is experienced. However, in order to fully reduce the autogenous shrinkage, the amount of SAP proportioned (0.20% by mass of cement) has to be increased. With regard to polymer size, negligible differences are observed. Therefore,

the polymer size, in this case, does not play a significant role in autogenous shrinkage mitigation.

For internally cured cement pastes prepared with Cem3 (see Figure 65), a reduction in autogenous shrinkage from -886 to -510 micro-strain (around 376 micro-strain) is experienced. In this case, this cement has the highest alkalinity (represented by the largest sodium equivalent content (0.72%)); consequently, lower than expected absorption of SAP would occur and; as a result, SAP would not provide enough internal curing water to maintain IRH and reduce autogenous shrinkage. More C₃S content as well as larger concentration of alkalis make this cement more reactive at early ages; therefore, it reaches faster strength development. As seen in Figure 63 and Figure 65; however, this becomes a drawback in terms of autogenous shrinkage. To eliminate shrinkage in high-alkalinity cementitious systems, it is recommended to increase the SAP content and evaluate mechanical and durability properties. Similar to what was observed for Cem1, the contribution of polymer size to mitigate autogenous shrinkage seems to be negligible as well.

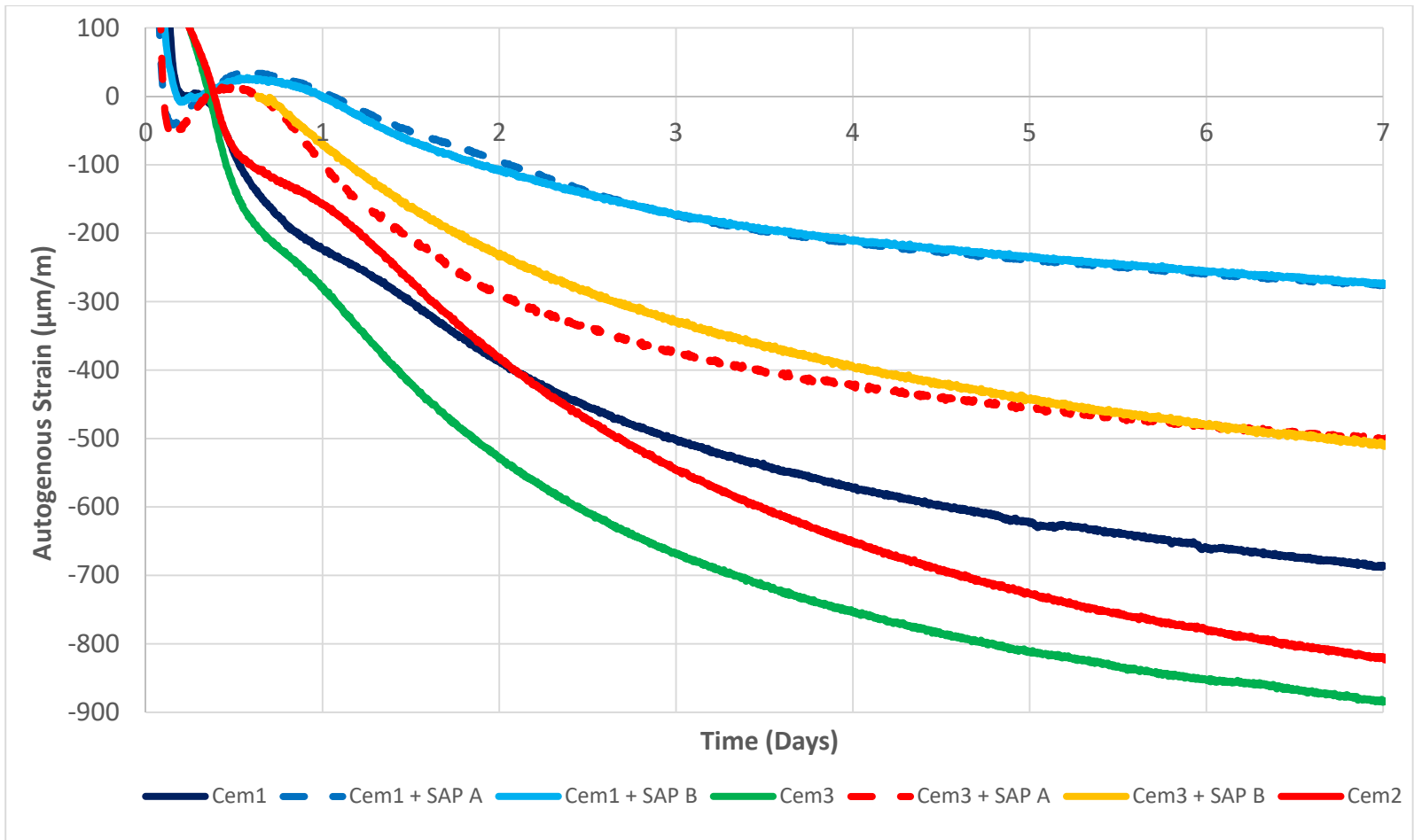


Figure 63 - Autogenous Shrinkage of cement Pastes with and without SAP - Following ASTM C1698 – 09 (Reapproved 2014)

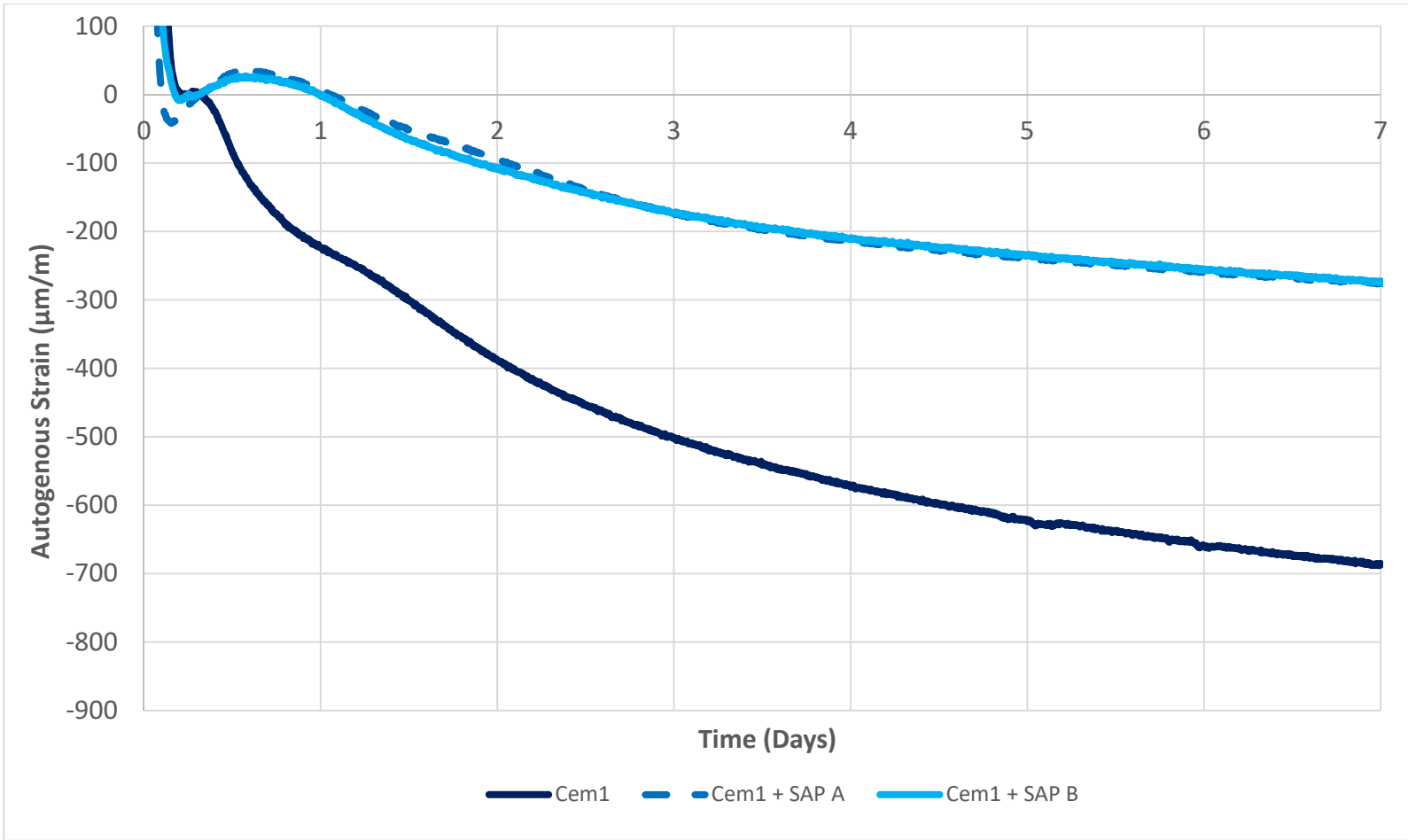


Figure 64 - Autogenous Shrinkage of Cem1 with and without SAP - Following ASTM C1698 – 09 (Reapproved 2014)

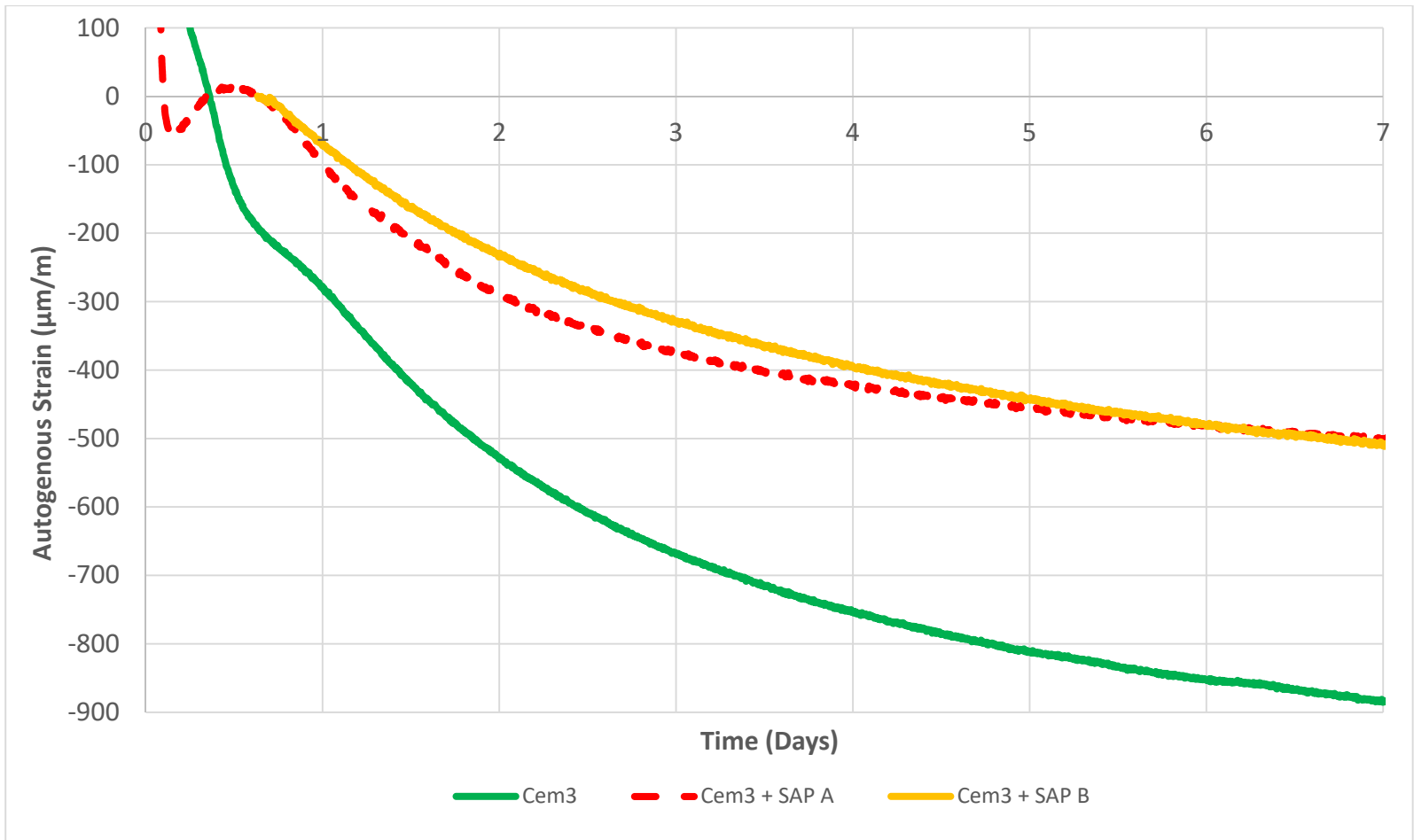


Figure 65 - Autogenous Shrinkage of Cem3 with and without SAP - Following ASTM C1698 – 09 (Reapproved 2014)

CHAPTER 6. CONCLUSIONS

Internal curing (IC) of cementitious systems by means of superabsorbent polymers (SAP) promotes additional (compared to traditionally cured systems) cement hydration, and mitigates autogenous shrinkage (potentially due to availability of internal curing water that helps preserve the internal relative humidity of the cementitious system), which reduces the risk of early-age cracking. However, the effectiveness of SAP as the internal curing agent was found to be a function of the alkalinity of the pore solution. Specifically, this research confirmed the hypotheses that the overall level of alkalinity (represented by the pH of the pore solution) as well as the type and concentration of alkali metal ions (Na^+ , K^+ , and Ca^{2+}) present in the solution influenced the absorption capacity of superabsorbent polymers and their absorption kinetics. In turn, the absorption capacity was found to influence the effectiveness of SAP as the internal curing agent.

In terms of the kinetics of the absorption process, the swelling behavior of SAPs was found to follow a two-stage process:

- During Stage 1 (the first 30 minutes of hydration), the high concentration of alkali ions in pore solution reduces the absorption efficiency of SAP.

- At later ages (Stage 2), the amount of solution absorbed by SAP increases (or stabilizes) depending (predominantly) on the pH, and K^+ , and Ca^{2+} contents.

Isothermal calorimetry indicated that the addition of SAP possibly increases the extent of cement hydration. This was indirectly confirmed by conducting the isothermal calorimetry study of hydrating pastes with comparable w/c ratios with and without the addition of SAP. However, more direct method, e.g. the loss on ignition (LOI) or thermogravimetric analysis (TGA), should be conducted to determine the actual degree of hydration.

The following comments (presented in the order of increasing cement alkalinity) summarize the overall results of this study:

Among the three cements utilized in this study, the use of low alkalinity ($Na_2O_{eq}=0.37\%$) cement resulted in the fastest (and the largest) initial (i.e. observed during the first 10 minutes of hydration (stage 1)) absorption of the pore solution by SAP. This was followed by a very stable absorption isotherm observed during the second stage (monitored up to 240 minutes). For this cement, the level of absorption reached by the polymer during stage 1 was $30 \text{ g}_{\text{pore solution}}/\text{g}_{\text{Dry SAP}}$. This is not unexpected since, as stated previously, SAP's ability to absorb fluids is strongly influenced by the ionic concentration of the aqueous solution, and the low alkalinity cement will, naturally, produce solutions with lower (compared to other cements) ionic concentrations. In the early part of stage

2, the absorption levels dropped to $27 \text{ g}_{\text{pore solution}}/\text{g}_{\text{Dry SAP}}$ and plateaued over time. This stability (in terms of the ability to absorb/release pore solution) of the system was indirectly confirmed by lack of any significant changes in parameters related to hydration kinetics (such as heat flow rate and development of cumulative heat) as observed from the results of internal calorimetry measurements.

In terms of shrinkage reduction, internal curing of low alkalinity cementitious systems presents the most significant reduction in autogenous strain. It is postulated that if the proportions of SAP were to be increased, the autogenous shrinkage may be fully mitigated. Furthermore, based on the results of this study, it appears that this particular SAP (made of predominantly acrylic acid) may be expected to be more efficient as an internal curing agent in cementitious systems with lower alkalinity compared to that with higher alkalinities.

In medium alkalinity cements ($\text{Na}_2\text{O}_{\text{eq}}=0.62\%$), slight changes are observed in the absorption isotherm when compared to that of low alkalinity cement. In stage 1, around $28 \text{ g}_{\text{pore solution}}/\text{g}_{\text{Dry SAP}}$ are absorbed by SAP whereas in stage 2, around $27 \text{ g}_{\text{pore solution}}/\text{g}_{\text{Dry SAP}}$ are absorbed. After 2 hours of free solution absorption, a slight tendency to start increasing the absorption capacity is attributed to the high potassium content. In terms of isothermal calorimetry and autogenous shrinkage, lower heat flow rate and less autogenous shrinkage at 7 days were observed for internally cured systems. In addition,

when compared to the reference cement paste, more cumulative heat was obtained at 7 days for internally cured cement pastes.

In cements with medium to high alkalinity ($\text{Na}_2\text{O}_{\text{eq}}=0.72\%$), the concentration of alkalis provides a different isotherm. In stage 1, due to the high concentration of alkalis, lower pore solution is absorbed within the first 10 minutes ($20 \text{ g}_{\text{pore solution}}/\text{g}_{\text{Dry SAP}}$). In stage 2, it is hypothesized that due to pH and interaction effects between concentration of Ca^{2+} and K^+ with the functional groups of the hydrogel, the absorption of pore solution rises to $33 \text{ g}_{\text{pore solution}}/\text{g}_{\text{Dry SAP}}$ after 4 hours. This overall isotherm for absorption capacity of SAP is concluded to be less stable and more difficult to understand. With respect to the effect on hydration, changes in the isothermal calorimetry study are more notable due to the high concentration of ions during the solution desorption, which accelerates the main peak of hydration. Although autogenous shrinkage is diminished by the addition of SAP, larger proportions of the hydrogels should be considered in order to completely mitigate self-desiccation of the cement system.

It is recommended that for mix design purposes, the amount of pore solution absorbed within the first 10 minutes corresponds to the absorption capacity used in the Bentz equation for the determination of the mass of SAP to include in the internally cured mix. It is based on the observation that not all the expected (determined) absorption capacity of the SAP is reached during mixing and hydration.

LIST OF REFERENCES

LIST OF REFERENCES

- American Society of Civil Engineers. (2013). Released March 2013 About the American Society of Civil Engineers, (March), 1–119.
- Assmann, A. (2013). Physical properties of concrete modified with superabsorbent polymers.
- ASTM Standard C1698. (2014). Test Method for Autogenous Strain of Cement Paste and Mortar, *i*(2014), 1–8. <http://doi.org/10.1520/C1698-09.2>
- Bentz, B. Y. D. P., Lura, P., & Roberts, J. W. (2005). Mixture Proportioning for Internal Curing, (February), 35–41.
- Bentz, D. P., & Snyder, K. A. (1999). Protected paste volume in concrete: Extension to internal curing using saturated lightweight fine aggregate. *Cement and Concrete Research*, 29(11), 1863–1867. [http://doi.org/10.1016/S0008-8846\(99\)00178-7](http://doi.org/10.1016/S0008-8846(99)00178-7)
- Bentz, D. P., & Weiss, W. J. (2010). Internal Curing : A 2010 State-of-the- Art Review.
- Brouwers, H. J. H., & Eijk, R. J. Van. (2003). Alkali concentrations of pore solution in hydrating OPC, 33(October 2002), 191–196.
- Buchholz, F. (1994). Preparation Methods of Superabsorbent Polyacrylates. *Superabsorbent Polymers*, 27–38.
- Bye, G. (2011). Introduction and composition of Portland cement. In *Portland Cement* (pp. 13–26). <http://doi.org/10.1680/pc.36116.001>
- Castro, J., Keiser, L., Golias, M., & Weiss, J. (2011). Absorption and desorption properties of fine lightweight aggregate for application to internally cured concrete mixtures. *Cement and Concrete Composites*, 33(10), 1001–1008. <http://doi.org/10.1016/j.cemconcomp.2011.07.006>

- Craeye, B., Geirnaert, M., & Schutter, G. De. (2011). Super absorbing polymers as an internal curing agent for mitigation of early-age cracking of high-performance concrete bridge decks. *Construction and Building Materials*, 25(1), 1–13.
<http://doi.org/10.1016/j.conbuildmat.2010.06.063>
- Diamond, S. (1981). EFFECTS OF TWO DANISH FLYASHES ON. *Cement and Concrete Research*, 11(c), 383–394.
- Elliott, J. E., MacDonald, M., Nie, J., & Bowman, C. N. (2004). Structure and swelling of poly(acrylic acid) hydrogels: Effect of pH, ionic strength, and dilution on the crosslinked polymer structure. *Polymer*, 45(5), 1503–1510.
<http://doi.org/10.1016/j.polymer.2003.12.040>
- Esteves, L. P. (2011a). Superabsorbent polymers: On their interaction with water and pore fluid. *Cement and Concrete Composites*, 33, 717–724.
<http://doi.org/10.1016/j.cemconcomp.2011.04.006>
- Esteves, L. P. (2011b). Superabsorbent polymers: On their interaction with water and pore fluid. *Cement and Concrete Composites*, 33(7), 717–724.
<http://doi.org/10.1016/j.cemconcomp.2011.04.006>
- Esteves, L. P. (2014). Recommended method for measurement of absorbency of superabsorbent polymers in cement-based materials.
<http://doi.org/10.1617/s11527-014-0324-5>
- Esteves, L. P., Lukosiute, I., & Cesniene, J. (2014). Hydration of cement with superabsorbent polymers, 1385–1393. <http://doi.org/10.1007/s10973-014-4133-4>
- Gagné, R., Aouad, I., Shen, J., & Poulin, C. (1999). Development of a new experimental technique for the study of the autogenous shrinkage of cement paste. *Materials and Structures*, 32(9), 635–642. <http://doi.org/10.1007/BF02481701>
- Hasholt, M. T., & Jensen, O. M. (2015). Chloride migration in concrete with superabsorbent polymers. *Cement and Concrete Composites*, 55, 290–297.
<http://doi.org/10.1016/j.cemconcomp.2014.09.023>

- Herbert, N. (1994). Characterization of a New Superabsorbent Polymer Generation. *Superabsorbent Polymers*, 573(i), 99–111. <http://doi.org/doi:10.1021/bk-1994-0573.ch008>
- Ichikawa, M.; Komukai, Y. (1993). Effect of burning conditions and minor components on the color of Portland Cement clinker. *Cement and Concrete Research*, 23, 933–938.
- Jackson, P. J. (2003). *Portland Cement: Classification and Manufacture*. *Lea's Chemistry of Cement and Concrete* (Fourth Ed). Elsevier Ltd. <http://doi.org/10.1016/B978-075066256-7/50014-X>
- Jensen, O. M. (2013). Use of Superabsorbent Polymers in Concrete concrete admixtures. *Concrete International*, 48–52.
- Justs, J., Wyrzykowski, M., Bajare, D., & Lura, P. (2015). Internal curing by superabsorbent polymers in ultra-high performance concrete. *Cement and Concrete Research*, 76, 82–90. <http://doi.org/10.1016/j.cemconres.2015.05.005>
- Justs, J., Wyrzykowski, M., Winnefeld, F., Bajare, D., & Lura, P. (2014). Influence of superabsorbent polymers on hydration of cement pastes with low water-to-binder ratio, 425–432. <http://doi.org/10.1007/s10973-013-3359-x>
- Klemm, A. J., & Sikora, K. (2012). The effect of cement type on the performance of mortars modified by superabsorbent polymers, 210–216.
- Kurdowski, W. (2014). *Cement and Concrete Chemistry*. Springer.
- Lemay, L., & Lobo, C. (2011). Concrete Sustainability Report - CSR02. *Concrete Sustainability Report*, (September), 11–12.
- Lopez, M., Kahn, L. F., & Kurtis, K. E. (2010). High-strength self-curing low-shrinkage concrete for pavement applications. *International Journal of Pavement Engineering*, 11(February 2014), 333–342. <http://doi.org/10.1080/10298436.2010.488731>
- Lura, P., Winnefeld, F., & Klemm, S. (2010). Simultaneous measurements of heat of hydration and chemical shrinkage on hardening cement pastes. *Journal of Thermal Analysis and Calorimetry*, 101(3), 925–932. <http://doi.org/10.1007/s10973-009-0586-2>

- Macphee, D. E., & Lachowski, E. E. (2003). *Cement Components and Their Phase Relations*. *Lea's Chemistry of Cement and Concrete* (Fourth Ed). Elsevier Ltd. <http://doi.org/10.1016/B978-075066256-7/50015-1>
- Miller, A. E. (2014). *Using a centrifuge for quality control of pre-wetted lightweight aggregate in internally cured concrete*.
- Miller, A. E., Barrett, T. J., & Weiss, W. J. (2013). Evaluation of Superabsorbent Polymers for Use in Cementitious Systems for the Purpose of Mitigating Autogenous Shrinkage, c(SEPTEMBER 2014).
- Mönning, S. (2005). Water saturated super-absorbent polymers used in high strength concrete. *Otto-Graf-Journal*, 16(16), 193–202. [http://doi.org/10.1016/0144-8617\(87\)90041-5](http://doi.org/10.1016/0144-8617(87)90041-5)
- Moreno, E. I. (2006). Determinación del pH de la solución de los poros de concreto después de un proceso acelerado de carbonatación . pH determination of concrete pore solution after an accelerated carbonation process ., 3, 5–12.
- Odler, I. (2003). *Hydration, Setting and Hardening of Portland Cement*. *Lea's Chemistry of Cement and Concrete* (Fourth Ed). Elsevier Ltd. <http://doi.org/10.1016/B978-075066256-7/50018-7>
- Snoeck, D., Jensen, O. M., & De Belie, N. (2015). The influence of superabsorbent polymers on the autogenous shrinkage properties of cement pastes with supplementary cementitious materials. *Cement and Concrete Research*, 74, 59–67. <http://doi.org/10.1016/j.cemconres.2015.03.020>
- TA Instruments. (1985). *The Study of Cement Hydration by Isothermal Calorimetry*, 99–101.
- TC225-SAP, R. (2012). *Application of Superabsorbent Polymers (SAP) in Concrete Construction*. (V. Mechtcherine & H.-W. Reinhardt, Eds.).
- TC 260-RSC, T. committee 260-R. (2014). Recommendations for use of superabsorbent polymers in concrete construction.

Vollpracht, A., Lothenbach, B., Snellings, R., & Haufe, J. (2016). The pore solution of blended cements: a review. *Materials and Structures*, 49(8), 3341–3367.

<http://doi.org/10.1617/s11527-015-0724-1>

Wang, F., Zhou, Y., Peng, B., Liu, Z., & Hu, S. (2009). Autogenous shrinkage of concrete with super-absorbent polymer. *ACI Materials Journal*, 106(2), 123–127.

Zhu, Q. (2014). *Effect of multivalent ions on the swelling and mechanical behavior of superabsorbent polymers (saps) for mitigation of mortar autogenous shrinkage.*